2013

ASSESSMENT OF THE DRUG-DRUG INTERACTION POTENTIAL OF ANIONIC COMPONENTS IN THE DIET AND HERBAL MEDICINES ON ORGANIC ANION TRANSPORTERS (SLC22 FAMILY)

Li Wang
Virginia Commonwealth University

ASSESSMENT OF THE DRUG-DRUG INTERACTION POTENTIAL OF ANIONIC COMPONENTS IN THE DIET AND HERBAL MEDICINES ON ORGANIC ANION TRANSPORTERS (SLC22 FAMILY)

A Dissertation submitted in partially fulfillment of the requirements for the degree of Doctor of Philosophy at Virginia Commonwealth University

By

Li Wang
Master of Science, Shanghai Institute of Materia Medica, Chinese Academy of Sciences, China, 2007

Director: Douglas H. Sweet, Ph.D.
Associate Professor, Department of Pharmaceutics

Virginia Commonwealth University
Richmond, Virginia,
August, 2013

ACKNOWLEDGEMENTS

It is never easy to make a successful completion of Ph.D. Thanks to the help and support of the kind people around me, I eventually finish my doctoral training and make my dream come to life.

Foremost, I would like to express my sincere gratitude to my advisor Dr. Douglas H. Sweet, for the continuous support of my study and research, for his patience, motivation, and enthusiasm. Indeed, his passion in science would definitely encourage me to move forward in future.

I would also like to thank Dr. Jürgen Venitz for the consistent help in my research project. His valuable suggestions give me inspirations to enrich my research.

I would like to acknowledge Drs. Patricia W. Slattum, H Thomas Karnes, and Satjit S. Brar who serve in my advisory committee and provide me timely guidance and input.

A special gratitude I give to Dr. Matthew S. Halquist for his guidance in my bioanalytical work. In addition, many thanks go to all faculties in School of Pharmacy for their help in my coursework. I would also like to thank Ms. Keyetta Tate and Ms. Laura Georgiadis for their kindly help in ordering lab supplies, arranging departmental activities, and providing directions for living in Richmond. I would thank the VCU School of Pharmacy and Graduate School for the financial support.

I would like to thank my lab-mates Dr. Aditi Mulgaonkar, Raymond, Lai, and Christine A. Farthing for their help for my study. Thank you to all my fellow and senior Pharmaceutics graduate students for their help and advice. In addition, a special thank you to my roommates and good friends Kan Qian and Chenxiao Da for their support and encouragement.

Finally, I would like to thank my parents for their love and unconditional support, and my wife, Xiaolei Pan, who is always there to cheer me up and encourage me to overcome the problems emerged in my life.

TABLE OF CONTENTS

LIST OF TABLES

LIST OF FIGURES

LIST OF ABBREVIATIONS

AA	aristolochic acid
AAN	aristolochic acid nephropathy
ABC	ATP binding cassette
ACN	anthocyanin
AKI	acute kidney injury
ANOVA	analysis of variance
APCI	atmospheric pressure chemical ionization
ARF	acute renal failure
ATF1	activating transcription factor 1
BCL6	B-cell lymphoma 6 protein
BCRP	breast cancer resistance protein
BUN	blood urea nitrogen
C_{max}	maximum plasma concentration
CA	California
CAD	collision gas
CE	collision energy
CHO	Chinese hamster ovary
COX	cyclooxygenase
CRE	cAMP responsive element

CREB1	cAMP responsive element binding protein 1
CRF	chronic renal failure
CXP	collision exit potential
CUR	curtain gas
Da	Dalton(s)
DDI	drug-drug interaction
DP	declustering potential
EMSA	electrophoretic mobility shift assays
EP	entrance potential
ES	estrone sulfate
ESI	electrospray ionization
f_u,	fraction unbound in plasma
FDA	Food and Drug Administration
GFR	glomerular filtration rate
GS1	gas one
GS2	gas two
H_2O	water
HCl	hydrochloric acid
HEK	human embryonic kidney 293
HNF	hepatocyte nuclear factors
HPLC	high performance liquid chromatography
IC_{50}	half maximal inhibition concentration
IS	internal standard

K_i	inhibitory constant
K_m	Michaelis constant;
LC	liquid chromatography
LC-MS	liquid chromatography mass spectrometry
LC-MS/MS	liquid chromatography tandem mass spectrometry
LLOQ	lower limit of quantification
LSA	lithospermic acid
MA	Massachusetts
MDCK	Madin Darby canine kidney
MDR1	multidrug resistance transporter
MO	Missouri
MS	mass spectrometry
NSAIDs	non-steroidal anti-inflammatory drugs
OAT	organic anion transporter
OATP1B1	organic anion transporting polypeptide 1B1
OCT2	organic cation transporter 2
Q3	third quadrupole
QC	quality control
PAH	*para*-aminohippurate
PCA	protocatechuic acid
PGE_2	prostaglandin E_2
PKA	protein kinase A
RMA	rosmarinic acid

SAA	salvianolic acid A
SAB	salvianolic acid B
SAR	structure-activity relationship
SLC	solute carrier
SNPs	single nucleotide polymorphisms
SiRNA	small interfering RNA
SRM	selected reaction monitoring
TSL	tanshinol
TEM	temperature
UPLC	ultra pressure liquid chromatography

ABSTRACT

ASSESSMENT OF THE DRUG-DRUG INTERACTION POTENTIAL OF ANIONIC COMPONENTS IN THE DIET AND HERBAL MEDICINES ON ORGANIC ANION TRANSPORTERS (SLC22 FAMILY)

By Li Wang, M.S.

A dissertation submitted in partially fulfillment of the requirements for the degree of Doctor of Philosophy at Virginia Commonwealth University

Virginia Commonwealth University, 2013

Major Director: Douglas H. Sweet, Ph.D.
Associate Professor
Department of Pharmaceutics, School of Pharmacy

Numerous natural products are widely used as first-line/alternative therapeutics and dietary supplements in both western and eastern society. However, the safety and efficacy profiles for herbal products are still limited. Organic anion transporters (OATs; SLC22 family) are expressed in many barrier organs and mediate *in vivo* body disposition of a broad array of endogenous substances and clinically important drugs. As some dietary flavonoids and phenolic acids were previously demonstrated to interact with OATs, it is necessary to explore the potential interaction

of such components found in natural products in order to avoid potential OAT-mediated drug-drug interactions (DDIs).

The inhibitory effects of 23 natural products were assessed on the function of human (h) OATs, hOAT1 (SLC22A6), hOAT3 (SLC22A7), and hOAT4 (SLC22A11) and/or the murine (m) orthologs mOat1 and mOat3. For compounds exhibiting marked inhibition at initial screening, dose-response curves (IC_{50} values) and DDI indices were determined. At the initial screening concentrations, 14, 19, and 2 test compounds exhibited significant inhibition on hOAT1, hOAT3, and hOAT4, respectively. Additionally, all test Danshen (a Chinese herbal medicine) hydrophilic components significantly reduced mOat1- and mOat3-mediated substrate uptake at 1 mM. For selected compounds, the IC_{50} and K_i values were estimated to be in the micromolar or even nanomolar range. Considering the clinical plasma concentration and unbound fraction in plasma, DDI indices for gallic acid, gentisic acid, lithospermic acid, protocatechuic acid, rosmarinic acid, salvianolic acid B, and tanshinol indicated DDIs may occur *in vivo* in situations of co-administration of these compounds and clinical therapeutics known to be OAT substrates. Finally, a new, rapid, and sensitive liquid chromatography-tandem mass spectrometry (LC-MS/MS) method was developed and validated to quantify gallic acid and gentisic acid in cell lysates in order to measure cellular uptake of these compounds in mOat1- or mOat3-expressing cells. Significant cellular uptake of gallic acid was observed in mOat1-expressing cells, compared with background control cells. The absorptive uptake was completely blocked by probenecid (known OAT inhibitor) at 1 mM. These results indicate that gallic acid is a substrate for mOat1 and suggest that human OAT1 might be involved in the active renal secretion of gallic acid.

CHAPTER 1

RENAL ORGANIC ANION TRANSPORTERS (SLC22 FAMILY): EXPRESSION, REGULATION, ROLES IN TOXICITY, AND IMPACT ON INJURY AND DISEASE

Drawn from manuscript published in *AAPS J.* Jan 2013; 15(1): 53-69

1.A INTRODUCTION

Two vital functions performed by the kidney are the removal of substances from the blood followed by their elimination via urine and the reabsorption of specific compounds from the glomerular filtrate back into the systemic circulation. Much of the secretion and reabsorption of charged organic solutes occurs in the proximal tubule. However, the plasma membrane of the proximal tubule cells presents a barrier to the passive diffusion of such charged, hydrophilic molecules and renal transcellular solute flux is a complex process involving dozens of membrane bound transporter proteins. Two major superfamilies of transport proteins that have been identified are the ATP binding cassette (ABC) transporters, which can directly bind and hydrolyze ATP as a driving force for the unidirectional transport of substrates across cell membranes, and the solute carriers (SLC), transport proteins that are indirectly coupled to cellular energy and utilize the membrane potential difference and/or the stored energy of concentration gradients as driving forces (1-3). Currently, the human SLC superfamily has at

least 55 separate gene families encompassing a combination of 362 confirmed and putative transporter proteins (1). The SLC22 family is comprised of the organic cation/anion/zwitterion transporters with ~30 identified/putative members and includes the organic cation transporters (OCTs and OCTNs), which mainly interact with cationic and zwitterionic organic molecules, and the organic anion transporters (OATs), which predominantly interact with anionic and zwitterionic organic molecules (2-4).

In vitro characterization of cloned transporters has demonstrated that OAT function is impacted by an enormous variety of structurally diverse organic anions. Many drugs, including diuretics, antihypertensives, antibiotics, antivirals, and anticancer agents, are organic anions at physiological pH and, thus, subject to active tubular secretion which, in turn, impacts their pharmacokinetic, pharmacodynamic, and toxic properties. In addition, endogenous substances (*e.g.*, metabolic intermediates/byproducts and hormones) and environmental toxins and toxicants (*e.g.*, mycotoxins and pesticides) also exist as anionic species. Indeed, the attributes of known OAT substrates indicate that renal OAT function is central to organism homeostasis and the progression of certain disease states. Further, interindividual variation in therapeutic response within human populations may be linked to altered renal OAT affinity, expression level, and/or spatial distribution as a result of dietary or genetic factors. Clearly, a more thorough understanding of OAT function is necessary if we wish to accurately assess their impact on drug efficacy and the extent of exposure to endogenous and xenobiotic toxins/toxicants.

This review will focus on the OATs of the SLC22 transporter family and in particular on those OATs for which transport activity has been demonstrated and expression/function in kidney established (Table 1.1). Basic cloning, expression profile, and functional characterization information for each transporter has been summarized in great detail recently and will not be

repeated here (3, 4). Rather, evidence supporting the involvement of renally expressed OATs in drug clearance, food/drug-drug interactions, and renal pathology will be emphasized. Appendix I provides a listing of compounds demonstrated to interact with various OATs and reported kinetic parameters (K_m, K_i, or IC_{50} values), when available, that serves as an update (2010-2012) to the comprehensive table from reference (3). An update of the current information regarding the regulation of OAT expression is also provided. Throughout this review the convention of referring to human transporters with all capital letters (*i.e.*, OAT1) and non-human transporters with initial capital followed by lower case letters (*i.e.*, Oat1), is used.

Table 1.1. Functional SLC22 family organic anion transporters

Transporter (gene designation)	Organic anion transport demonstrated	mRNA expression detected in kidney	Protein expression confirmed in kidney
Human			
OAT1 (SLC22A6)	✓	✓	✓
OAT2 (SLC22A7)	✓	✓	✓
OAT3 (SLC22A8)	✓	✓	✓
OAT4 (SLC22A11)	✓	✓	✓
OAT5 (SLC22A10)[a]	--	--	--
OAT7 (SLC22A9)	✓	--	--
OAT10 (SLC22A13)	✓	✓	--
URAT1 (SLC22A12)	✓	✓	✓
Rodent			
Oat1 (Slc22a6)	✓	✓	✓
Oat2 (Slc22a7)	✓	✓	✓
Oat3 (Slc22a8)	✓	✓	✓
Oat5 (Slc22a19)[a]	✓	✓	✓
Oat6 (Slc22a20)	✓	--	--
Oat8 (Slc22a25)	✓	✓	✓
Oat9 (Slc22a27)	✓	✓	✓
Oat10 (Slc22a13)	--	✓	✓
Urat1 (Slc22a12)	✓	✓	✓

[a]Human OAT5 (SLC22A10) and rodent Oat5 (Slc22a19) are not orthologs, *i.e.*, are not coded for by the same gene and therefore do not represent the same transporter; rat and mouse Oat5 are paralogs, *i.e.*, represent the same gene across species and thus code for the same transporter

1.B ORGANIC ANION TRANSPORTERS IN RENAL PROXIMAL TUBULE

As indicated in Table 1.1, species differences in known OAT family members do exist, with OAT4 (SLC22A11), OAT5 (SLC22A10), and OAT7 (SLC22A9) being unique to humans and Oat5 (Slc22a19), Oat6 (Slc22a20), Oat8 (Slc22a25), and Oat9 (Slc22a27) being restricted to non-human species (most thoroughly explored in mice and rats). It is important to clarify that OAT5 (SLC22A10) and Oat5 (Slc22a19) are not orthologs. Of the 11 OATs for which transport activity has been demonstrated, OAT1 (SLC22A6), OAT2 (SLC22A7), OAT3 (SLC22A8), OAT4, and URAT1 (SLC22A12) proteins have been detected and localized in human kidney and Oat1 (Slc22a6), Oat2 (Slc22a7), Oat3 (Slc22a8), Oat5, Oat8, Oat9, Oat10 (Slc22a13), and Urat1 (Slc22a12) proteins have been detected and localized in rodent kidney (2-5). OAT1/Oat1, OAT2/Oat2, and OAT3/Oat3 are targeted to the basolateral membrane of renal proximal tubule cells (Figure 1.1) and mediate the movement of substrate molecules from the blood into the cells via dicarboxylate/organic anion exchange (2-4). In the apical membrane, OAT4 appears to mediate substrate reabsorption from urine through exchange with dicarboxylates or hydroxyl ions and URAT1/Urat1 mediates reabsorption of urate and other substrates by monocarboxylate exchange (Figure 1.1). In rodent proximal tubules, Oat5 may mediate substrate reabsorption via dicarboxylate exchange, however no information is available regarding the driving forces and directionality of Oat9 (2-5). While Oat8 was identified as a dicarboxylate/organic anion exchanger, immunohistochemistry localized this transporter to the apical membrane of intercalated cells in the collecting ducts, with no signal in proximal tubule. Finally, organic anion transport by OAT10 (SLC22A13) was reported to be driven by exchange with dicarboxylates or hydroxyl ions, similar to OAT4, however localization information is restricted to brush border membrane vesicles prepared from rat kidney (2-4).

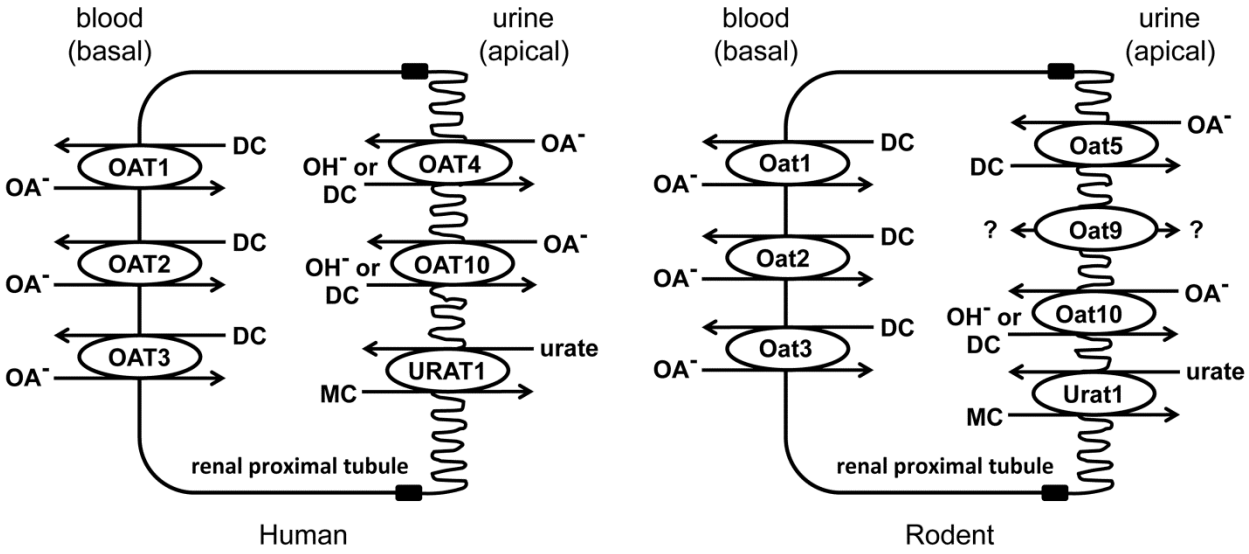

Figure 1.1. Organic anion transporters of the SLC22 family in human and rodent renal proximal tubule cells

As illustrated, human and rodent orthologs of OAT1/Oat1, OAT2/Oat2, OAT3/Oat3, OAT10/Oat10, and URAT1/Urat1 have been identified. Notable species differences are OAT4 having no identified rodent ortholog and Oat5 and Oat9 having no known human orthologs. Oat8 mRNA has been detected in rodent kidney, however it is expressed in cortical collecting ducts, not in the proximal tubule; its membrane targeting is not known. The driving forces governing Oat9 function have not been elucidated.

1.C REGULATION OF OAT EXPRESSION

Mounting evidence suggests that OAT expression can be regulated at both the mRNA and protein level. Examination of the promoter regions of the *hOAT1, hOAT2, hOAT3, hOAT4,* and *hURAT1* genes identified putative binding sequences for several transcription factors including activating transcription factor 1 (ATF1), cAMP responsive element binding protein 1 (CREB1), hepatocyte nuclear factors 1α, 1β, and 4α (HNF1α, HNF1β, HNF4α), paired box protein Pax-1, B-cell lymphoma 6 protein, and Wilm's tumor protein 1 (6-9). The presence of DNA binding sequence motifs for known transcription factors suggest they might be involved in the regulation of OATs and a number of recent studies have investigated this possibility.

Deletion analysis of the *hOAT3* promoter indicated the sequence from -214 to -77 basepairs was required for basal level transcriptional activity and this region was found to contain a cAMP-response element (CRE) (8). Mutation of this sequence resulted in reduced *hOAT3* promoter activity. Both ATF1 and CREB1 are known to bind to CRE, and subsequent electrophoretic mobility shift assays (EMSA) confirmed binding of these transcription factors to the *hOAT3* promoter (8). Further, phosphorylation of CREB1 and ATF1 in response to activation of protein kinase A (PKA) appeared to induce increased hOAT3 expression, suggesting stimulatory effects of PKA on hOAT3 activity might be explained through increased transcriptional activity (8).

The transcription factors HNF1α and HNF1β are expressed in the epithelia of many organs including liver, kidney, and intestine (10-12). When explored in Hnf1α knockout mice, it was observed that renal mRNA expression of mOat1, mOat2, mOat3, and mUrat1 was reduced (13, 14). Examination of the *mOat1* and *hOAT1* promoter regions revealed a HNF1 binding motif at -56 to -44 basepairs (15). Forced expression of HNF1α and HNF1β increased activity of both

promoters, with HNF1α producing the greatest increase, followed by co-expression of HNF1α and HNF1β, and expression of HNF1β alone producing little to no effect. EMSA analysis detected binding of HNF1α homodimers and HNF1α/HNF1β heterodimers to the *hOAT1* promoter (15). The promoter sequence of *hOAT3* (-308 to +6 basepairs) also contains a HNF1α motif, as do the rat and mouse orthologs (16). Mutation of the HNF1α motif reduced basal *hOAT3* promoter activity. Similar to *hOAT1,* expression of HNF1α increased *hOAT3* and *mOat3* promoter activity more than co-expression of HNF1α and HNF1β, however, in contrast, expression of HNF1β alone also increased activity, although to a lesser extent (16). EMSA analysis confirmed binding of HNF1α homodimers and HNF1α/HNF1β heterodimers to the *hOAT3* promoter (16). Repression of endogenous HNF1α expression in a human-derived liver cell line (Huh7) with a small interfering RNA (siRNA) construct significantly decreased expression of hOAT5 and hOAT7 message, but was without effect on hOAT2 mRNA expression level (17). Binding and upregulation of *hOAT5* and *hOAT7* promoter activity by HNF1α was also demonstrated, but as mentioned previously, these OATs are not expressed in kidney (17). The *hURAT1* (-253 to +83 basepairs) and *mUrat1* (-261 to +80 basepairs) minimal promoter regions were found to contain a HNF1 motif and mutation of the sequence in *hURAT1* abolished promoter activity (14). Both *hURAT1* and *mUrat1* responded to forced HNF1α and HNF1β expression like *hOAT3* and *mOat3*, suggesting HNF1α homodimers, HNF1α/HNF1β heterodimers, and HNF1β homodimers all stimulate promoter activity with the same respective order of potency as on *hOAT3/mOat3* (14). In contrast to the other OATs, EMSA analysis confirmed that HNF1β homodimers, in addition to HNF1α homodimers and HNF1α/HNF1β heterodimers, could bind to the promoter region of *hURAT1* (14). Lastly, two HNF1 motifs (at -97 to -85 and -41 to -29) were located in the *hOAT4* promoter (18). Overexpression of either

HNF1α or HNF1β alone, or in combination, enhanced *hOAT4* promoter activity, and this enhanced activity was blunted by mutation of either motif and abolished when both motifs were mutated (18). When examined under conditions of endogenous HNF1α expression level (HepG2 cells), or endogenous HNF1α and HNF1β levels in combination (Caco-2 cells), promoter activity was only responsive to the HNF1 motif at the -97 to -85 positions (18). Like *hURAT1*, EMSA analysis demonstrated that HNF1β and HNF1α homodimers, as well as HNF1α/HNF1β heterodimers, could bind this HNF1 motif; binding to the -41 to -29 motif was reported as barely detectable (18). Since it has been determined that, in renal proximal tubules, HNF1α/HNF1β heterodimers and HNF1β/HNF1β homodimers predominate, one or both of these complexes likely influences OAT expression *in vivo* (12).

Another HNF family member, HNF4α, was observed to enhance the activity of both *hOAT1* (-2747 to +88 basepairs) and *hOAT2* (-679 to +54 basepairs) promoter constructs (19, 20). HNF4α is known to have several potential sequence motifs; a direct repeat of hexamers separated by one (DR-1) or two (DR-2) nucleotides, or an inverted repeat of hexamers separated by 8 nucleotides (IR-8). For *hOAT1*, promoter scanning revealed the presence of a DR-2 motif (at -875 to -862 basepairs) and an IR-8 motif (at -123 to -104 basepairs) (19). Co-expression of HNF4α with constructs containing either one or both of these motifs resulted in increased *hOAT1* promoter activity, which was diminished by mutation (19). Subsequent EMSA experiments confirmed binding of HNF4α homodimers to each of these motifs in the *hOAT1* promoter (19). The promoter region of *hOAT2* was found to contain a DR-1 type HNF4α consensus motif at position -329 to -317 that is conserved in the rat ortholog (20). Presence of the wildtype sequence correlated with HNF4α activated *hOAT2* promoter activity and sequence mutation resulted in loss of HNF4α activation (20). EMSA analysis demonstrated HNF4α binding to

hOAT2 promoter fragments containing the motif and introduction of HNF4α siRNA constructs markedly reduced endogenous hOAT2 mRNA expression in Huh7 cells (20).

Recently, microarray analysis identified B-cell lymphoma 6 protein (BCL6) as a transcription factor exhibiting male dominant expression in rats (9). Since rOat1 and rOat3 had previously been reported to exhibit male dominant expression that is modulated by steroid hormones (21), the investigators examined the promoter regions for BCL6 consensus binding motifs. Five putative BCL6 sequence motifs were identified in the promoter region of *rOat1* and six in the promoter of *rOat3*, no mention of whether these sites are found in the promoters of *hOAT1* and/or *hOAT3* was made (9). Expression activity of a construct corresponding to -2,252 to +113 basepairs of the *rOat1* promoter, which contained 4 of the identified BCL6 sites, was increased when BCL6 was co-expressed. Activity of a truncated construct (-1,266 to +113 basepairs) containing only 2 of the sites showed a similar level of activity, suggesting that either not all of the potential binding sites are functional or that response to binding of BCL6 is "all or none", and interaction with multiple sites does not further modulate expression level (9). A similar effect was observed for *rOat3*, with a clear increase in promoter activity upon co-expression of BCL6, but with no difference in the magnitude of effect between constructs containing six (-2,567 to +12 basepairs), three (-752 to +12 basepairs), or two (-444 to +12 basepairs) BCL6 binding motifs (9).

In addition to transcriptional regulation, there is evidence supporting post-translational regulation of OATs by protein kinases. As recently reviewed (3), there appeared to be a general trend for decreased OAT1/Oat1 and OAT3/Oat3 activity via non-specific protein kinase C (PKC) activation. However, a reported exception to this was stimulation of rat and mouse Oat1- and rat and mouse Oat3-mediated transport upon activation of the atypical isoform PKCζ (22). Increased

transport of para-aminohippurate (PAH), estrone sulfate, and adefovir was observed in renal cortical slices in response to PKCζ activation (22). The effect on estrone sulfate transport was not observed in slices prepared from Oat3 knockout mice. Direct binding of PKCζ to hOAT3 was demonstrated in a yeast two-hybrid system and binding to rOat3 was demonstrated by immunoprecipitation and immunoblotting (22). Recently, another study confirmed the binding and stimulatory effects of PKCζ on hOAT3 (23). In addition, the isoforms PKCδ and PKCε, were observed to bind to hOAT3 (23). This was associated with increased hOAT3 at the cell surface, with no effect on total cellular hOAT3, suggesting redistribution of hOAT3 from intracellular compartments as the mechanism behind upregulation of transport activity (23). In contrast, activation of the PKCα isoform by angiotensin II has been demonstrated to decrease transport activity of hOAT1 and hOAT3 in concert with decreased cell surface expression (24). Therefore, it appears as though the effects of PKC activation on OAT activity are PKC isoform dependent, and can lead to either upregulation or downregulation of OAT activity depending upon the specificity of PKC isoform activation. Thus, rapid short-term modulation of OAT activity appears possible through changes in transporter cell surface expression via cycling in and out of the membrane from a cytoplasmic pool of transporters under the control of kinases, whereas long-term changes might involve alteration of gene transcriptional activity and, presumably, protein synthesis.

1.D OATs IN RENAL INJURY AND PROTECTION

Many clinical therapeutics, endogenous metabolic toxins, and xenobiotic toxins/toxicants accumulate in renal proximal tubules cells and induce renal injury. Cellular damage can take a variety of forms including oxidative stress, protein acylation, DNA-adduct formation, mitochondrial dysfunction (impaired ATP synthesis), lipid peroxidation, and necrosis. In opposition, a number of molecules purported to exert protective effects, such as antioxidant, anti-inflammatory and anti-proliferative activities, also enter renal proximal tubule cells. There is growing evidence from both *in vitro* and *in vivo* systems implicating OATs in the renal targeting of these substances.

Inorganic mercury (Hg^{2+}) accumulates preferentially in the kidneys and can result in acute renal failure. Typical manifestations of mercury intoxication include renal vasoconstriction, reduced glomerular filtration rate (GFR), enzymuria, tubular dilatation, and formation of epithelial cell casts. Early *in vitro* and *in vivo* studies indicated that entry of mercury from the systemic circulation into proximal tubule cells occurred via the same transport pathway as PAH (recently reviewed in (2, 4). Subsequent studies using Madin Darby canine kidney (MDCK) cells stably expressing hOAT1 indicated a direct correlation between hOAT1 expression and uptake and toxicity of mercury-thiol conjugates (25, 26). Recently, direct *in vivo* evidence supporting the role of OAT1/Oat1 in mediating mercury nephrotoxicity was obtained in studies utilizing Oat1 knockout mice (27). Renal function and histopathology were examined in wildtype and Oat1 knockout mice 18 hours post-intraperitoneal injection with $HgCl_2$ (4 mg/kg). Wildtype mice treated with $HgCl_2$ exhibited significantly increased kidney:body weight ratio (indicative of edema) and blood urea nitrogen (BUN) levels, as compared to saline injected wildtype animals (27). These indicators of renal injury and renal insufficiency were significantly blunted in Oat1

knockout mice treated with $HgCl_2$ (27). Furthermore, histopathological markers of nephrotoxicity observed in mercury treated wildtype mice, including tubular dilatation and necrosis, and sloughing of the brush border membrane, were virtually undetectable in kidneys from Oat1 knockout mice (27). These findings strongly support a major role for OAT1/Oat1 in the pathology of renal mercury toxicity.

Renewed interest in complementary and alternative therapies, particularly in Western cultures, has led to the increased use of herbal therapies. Often these are complex mixtures of dried plants or plant extracts with poorly defined active components and unregulated manufacturing processes. As they are marketed for their beneficial health effects, such therapies are frequently viewed as being safe, however, a number of herbal medicines have produced unwanted toxicities and drug interactions (28, 29). For example, *Aristolochia* plants, used in herbal remedies for thousands of years in both Eastern and Western countries, contain the nephrotoxic agent aristolochic acid (AA), identified as the causative agent in what is now referred to as aristolochic acid nephropathy (AAN) (30-33). The proximal tubule has been identified as the main target site for AAN in both humans and rodent models (34, 35). AA collectively refers to a complex mixture of carboxylic acids, the major components of which are AA-I and AA-II. The only structural difference between the two compounds is the presence of an *O*-methoxy group at the 8-position of AA-I (36). Both AA-I and AA-II have metabolic intermediates capable of forming DNA adducts that produce carcinogenic effects, however this property is not linked to their toxicity, as only AA-I is nephrotoxic (37, 38). When examined directly in overexpressing HEK-293 cell lines, AA-I was demonstrated to be a competitive inhibitor of hOAT1, hOAT3, and hOAT4 with K_i values of 0.63 ± 0.15, 0.50 ± 0.10 and 20.63 ± 1.7 µM, respectively (39). Significantly increased AA-I DNA adducts were observed in all three

transporter expressing cell lines as compared to non-transporter expressing cells, and this increase was reversed in the presence of probenecid, supporting hOAT-mediated accumulation of AA-I (39). In another *in vitro* study, both AA-I and AA-II were shown to inhibit hOAT1, hOAT3, and hOAT4, but produced no effect on hOAT2 activity (40). Reported IC_{50} values indicated that AA-I was a slightly better inhibitor than AA-II on all three transporters, although the differences were not great; (in µM) 0.44 ± 0.08 and 1.06 ± 0.09 (hOAT1), 0.65 ± 0.08 and 1.28 ± 0.18 (hOAT3), and 61.3 ± 8.35 and 72.0 ± 9.32 (hOAT4), for AA-I and AA-II, respectively (40). Recently, direct uptake of AA-I and AA-II was demonstrated for mOat1, mOat2, and mOat3 indicating both compounds are high affinity substrates for these transporters (36). Michaelis constants (K_m values) correlated well with inhibitory values reported for the human orthologs; (in µM) 0.791 ± 0.007 and 1.498 ± 0.371 (mOat1), 0.356 ± 0.050 and 0.673 ± 0.1192 (mOat2), and 0.514 ± 0.057 and 1.047 ± 0.360 (mOat3), for AA-I and AA-II, respectively (36). Discrepancy of the results for mOat2 and hOAT2 in cellular uptake of AA-I and AA-II may represent species differences.

Analysis of structural determinant effects on uptake indicated that the carboxyl group of AA-I is key to high-affinity interaction with mOat1, mOat2, and mOat3, whereas the nitro group only impacted interactions with mOat1 (36). Accumulation of AA-I in mouse renal cortical slices was found to be probenecid-, PAH-, and estrone sulfate-sensitive, correlating with an OAT-mediated transport process (36). Furthermore, this accumulation in slices resulted in AA-I DNA adduct formation that was reversed by probenecid (36). In agreement with these findings, a recent *in vivo* study in mice demonstrated that probenecid reduced the urinary excretion of AA-I and protected the kidney from AA-I induced nephrotoxicity (41). Results in mOat1 and mOat3 knockout mice indicated that loss of function of either transporter was associated with decreased

renal accumulation of AA-I and lessened the severity of renal injury as compared to wildtype animals (41). Significant downregulation of rOat3, but not rOat1, protein also was observed after long-term (7 days) administration of an AA mixture (42). Taken together, these findings strongly suggest an OAT-mediated mechanism in the pathology of AAN and suggest inhibition of renal OAT activity might serve as a potential therapeutic strategy following AA exposure.

Phenolic acids represent a growing class of OAT substrates/inhibitors. They are common dietary constituents as they are produced from the amino acids phenylalanine and tyrosine in plants (43). Many phenolic acids are also metabolically derived from anthocyanidins and anthocyanins after consumption (44). They are purported to have beneficial health effects in chronic diseases, *e.g.*, diabetes, cardiovascular disorders, and cancer, through free radical scavenging, anti-proliferative, and anti-inflammatory activities (43, 45-47), hence their growing popularity as alternative medicines/dietary supplements. Interaction of the related dietary polyphenols and human OATs was being investigated as many as seven years ago, when ellagic acid was identified as a substrate for hOAT1 (IC_{50} = 207 nM), rOat1, and hOAT4, but not mOat2, hOAT3, or mOat5 (48). More recently, the phenolic acids, lithospermic acid, protocatechuic acid, rosmarinic acid, salvianolic acid A, salvianolic acid B, and tanshinol, identified as active components of the traditional Chinese medicine Danshen (*Salvia miltiorrhiza*) which is utilized in cardiovascular disease, were shown to inhibit mOat1- and mOat3-mediated transport (49). Lithospermic acid, rosmarinic acid, and salvianolic acid A were found to be potent competitive inhibitors; K_i constants were 14.9 ± 4.9 vs. 31.1 ± 7.0 for lithospermic acid, 5.5 ± 2.2 vs. 4.3 ± 0.2 µM for rosmarinic acid, and 4.9 ± 2.2 µM vs. 21.3 ± 7.7 µM for salvianolic acid A, on mOat1 and mOat3, respectively (49). An extensive study showed the phenolic acids caffeic acid, dihydrocaffeic acid, dihydroferulic acid, and ferulic acid were substrates of hOAT1 and/or

hOAT3, while a number of their glucuronide- and sulfate-conjugated metabolites were effective inhibitors (50). An independent study identified caffeic acid as a competitive inhibitor of both hOAT1 and hOAT3 (IC_{50} = 16.6 and 5.4 µM, respectively) and demonstrated the potential for food-drug interactions via inhibition of hOAT1 and hOAT3-mediated transport of antifolates and antivirals (51). Inhibition of hOAT1 by gallic acid, protocatechuic acid, sinapinic acid, and vanillic acid, and of hOAT3, by ferulic acid, gallic acid, gentisic acid, protocatechuic acid, and sinapinic acid has been observed (52). IC_{50} values ranged from 1.24-18.08 µM on hOAT1 and from 7.53-87.36 µM on hOAT3 (Appendix I) (52). Inhibition of hOAT1 by gallic acid, and of hOAT3 by gallic or gentisic acid, was identified as having potential for clinically significant food/drug-drug interactions. Human OAT4 activity was not affected by any of these compounds (52). Whether or not any dietary polyphenols/phenolic acids actually promote human health or improve disease outcomes remains unresolved. However, these studies provide clear evidence for the potential of phenolic acids to interact with OATs and to produce food-drug interactions, emphasizing the need to better understand the impact of transport processes on the distribution and elimination of these compounds. Regardless of any health benefits through anti-oxidant or anti-inflammatory-type activities, these compounds might provide an alternative treatment in the management of OAT-mediated nephrotoxicity, without producing significant side effects.

1.E OAT FUNCTION AND EXPRESSION IN MODELS OF RENAL INJURY AND DISEASE

Renal function plays a vital role in the clearance of drugs and endogenous/exogenous toxins and toxicants. The overall renal clearance of substances is determined by the net effect of glomerular filtration, tubular secretion, and reabsorption processes. Renal disease states that result in dysfunction or loss of function can greatly influence the rate of elimination and tissue level of transporter substrates (53, 54). OATs, which are known to mediate the accumulation of organic anions from the blood and urine into proximal tubule cells, can be affected by renal failure and disease in terms of mRNA and protein expression level, transport activity, and membrane cycling, showing altered renal clearance of their substrates (53-55).

Progression of chronic renal failure (CRF) leads to impaired activity and function of the proximal tubule. In the laboratory, this pathological condition is mimicked with the 5/6 nephrectomy model, which replicates the onset of uremia and chronic kidney disease-related complications observed in humans (56). More recently this model has been used to examine changes in OAT protein levels in response to CRF (57-59). When examined 14 days post-surgery, Ji *et al.* found a 50% decrease in the renal clearance of unbound PAH, but no significant changes in rOat1 or rOat3 protein levels by Western blot (57). In agreement, Torres and co-workers reported significant decreases in filtered, secreted, and excreted PAH at 168 days post-surgery in 5/6 nephrectomized animals vs. sham-operated controls (59). However, in this study changes in renal PAH handling correlated with an ~40% decrease in rOat1 protein expression in kidney homogenates and basolateral membrane preparations from CRF rats. Rat Oat3 protein levels were also significantly reduced in kidney homogenates, but not in the basolateral membranes (59). Finally, Naud, *et al.* detected reduced rOat1 (~40%), rOat2 (~40%), rOat3

(~87%), and rUrat1 (~38%) proteins in CRF vs. control animals 42 days after surgery, but renal clearance was not examined in these animals (58).

While this model has the potential to yield much information on the effects of CRF on renal OAT expression and function, several important differences between these studies need to be noted (57-59). First, while described generically as 5/6 nephrectomized animals, the methodologies used to establish the model varied considerably, with one study removing the right kidney and ligating the posterior and anterior segmental branches of the left renal artery in a single operation (57), and the others utilizing a "two-stage 5/6 nephrectomy" procedure wherein the two poles of the left kidney were removed in one operation, followed by removal of the right kidney during a second operation one week later (58, 59). Second, as indicated, the interval post-surgery when the observations were made varied widely between the studies. Third, the origins of the antibodies used to visualize the OATs via immunoblotting, and the predicted weights of the protein bands detected, differed. Ji *et al.*, developed custom antibodies that detected ~77 kD and ~72 kD bands for rOat1 and rOat3, respectively. These bands are bigger than the predicted molecular weights of ~61 kD for rOat1 and ~59 kD for rOat3, however there is evidence supporting post-translational glycosylation of OATs *in vivo*. Their findings are in good agreement with published results with a polyclonal antibody directed against hOAT1 which recognized an ~80 kD band in crude renal cortex homogenate that was reduced to ~60 kD upon treatment with glycosidase, and matched an ~60 kD band corresponding to an unglycosylated hOAT1 *in vitro* transcription/translation reaction product (60). The study by Torres, *et al.* used a commercial rOat1 antibody (Alpha Diagnostics, Inc.) and reported an ~57 kD rOat1 band, and a custom rOat3 antibody and reported an ~130 kD band for rOat3 (59). As indicated above, the result for rOat1 would correspond nicely with its unglycosylated form, however, these were

native kidney homogenates and no glycosidase treatment was performed. Since the protein samples were reduced (boiled in the presence of mercaptoethanol and sodium dodecyl sulfate) the reported rOat3 signal seems unexpectedly large. Naud, *et al.* used all commercial antibodies, with anti-rOat1 and anti-rUrat1 from Abbiotec and anti-rOat2 and anti-rOat3 from Alpha Diagnostics, Inc., and did not report the predicted molecular weight for any of the detected bands (58). To aid interpretation of future studies it may be useful to standardize the 5/6 nephrectomy surgical techniques used, optimize/standardize the time post-surgery experiments are conducted, and perform more rigorous antibody characterizations prior to use, *e.g.*, comparison of signal across preparations from transporter expressing cell lines and/or transporter knockout mouse tissues to confirm specificity/lack of cross-reactivity and predicted molecular weight of detected protein(s).

In contrast to CRF, even a small reduction in renal blood flow can lead to hypoxic injury and/or acute renal failure (ARF). ARF is commonly seen in critically ill patients and exhibits a mortality rate exceeding 50% (61). Ischemia/reperfusion injury associated with disease or physical injury is a common trigger for ARF, and once induced, ARF can lead to a systemic build up of uremic toxins via a combination of reduced GFR and impaired tubular transport. Ischemia/reperfusion injury is also observed in kidneys utilized for transplant and can result in marked impairment of PAH extraction (62). This observation led to immunohistochemical studies examining the cellular distribution of hOAT1 in biopsies obtained from cadaveric renal allografts 1 hour post-reperfusion (63). While most allografts were seen to maintain some degree of basolaterally targeted hOAT1, it appeared to be greatly reduced as compared to control tissues and was accompanied by the appearance of fine and coarse ‘cytoplasmic aggregates’ positive for hOAT1 (63). This correlated with depressed net tubular secretion of PAH in 15 out of 18 patients

examined 3-7 days post-transplant (63). No clear association between total ischemic time, which varied from 13-32 hours, could be made and it should be noted that patients were taking a number of drugs known to interact with hOAT1 and hOAT3 when PAH secretion was measured. None-the-less, these data support the contention that renal organic anion transport impairment observed in some instances of disease, injury, or transplant induced ARF might be due to loss of OATs in the proximal tubule cell membranes.

Experimentally induced ARF, achieved via clamping of the renal arteries, is a common approach used to model this type of renal injury in the laboratory. When this same group examined localization of rOat1 in the induced ARF model, redistribution of rOat1 was observable with as little as 5 minutes of ischemia, but the amount of rOat1 protein did not diminish until 1 hour post-reperfusion, and was still not fully recovered after 10 days (64). A similar study examined rOat1 and rOat3 expression for 14 days following ischemia induced ARF (65). Both transporter proteins showed a similar response to ARF, exhibiting a significant reduction (~50%) from 6 hours to 3 days post-ischemia, returning to control levels by 7 days post-injury (65). This loss and recovery of transporter protein levels correlated with effects on the net renal secretion of PAH (a measure insulated from changes in GFR), which was significantly reduced from 6 hours to 3 days post-reperfusion as compared to sham-operated animals, returning to control levels by 7 days (65). Matsuzaki *et al*. also reported down-regulation of rOat1 and rOat3 protein expression level in rat kidney 48 hours after ischemia (66). Significant decline in accumulation of PAH and estrone sulfate in renal slices from ARF animals suggested reduced transport capacity mediated by rOat1 and rOat3 (66). Interestingly, administration of cobalt, a treatment proposed to stabilize hypoxia inducible factor 1, an oxygen-sensitive transcription factor which serves to upregulate certain genes under low oxygen

conditions, significantly blunted the downregulation of rOat3 protein, partially restoring estrone sulfate accumulation in renal slices (66). The treatment was without effect on rOat1 or PAH accumulation (66).

The apical transporter rOat5 also has been demonstrated to be downregulated in response to ischemia induced ARF (67). When examined 1 hour post-reperfusion after 5 minutes of ischemia, no change in rOat5 protein level was detected in renal homogenates or apical membrane preparations. However, if ischemia was maintained for 1 hour, a significant reduction (~40%) in rOat5 was observed (67). Regardless, rOat5 protein levels detected in urine (relative to urinary creatinine) were significantly elevated 1 hour after either 5 or 60 minutes of ischemia, leading the authors to suggest that urinary excretion of rOat5 protein may serve as a sensitive, non-invasive measure of renal functional and structural integrity following renal injury or during renal dysfunction (67). Since there is no identified human ortholog of rodent Oat5, the clinical utility of this finding is unclear. However, urinary hOAT1, hOAT3, and hOAT4 protein levels were recently examined in patients diagnosed with acute kidney injury (AKI) (68). Two AKI patient groups were identified, those who recovered without intervention ("early reversible proximal tubular damage") and those who required intervention in the form of dialysis ("severe AKI"). Patients who suffered "early reversible proximal tubular damage" exhibited increased urinary levels of hOAT1 and hOAT3, but decreased levels of hOAT4, as compared to controls, and patients experiencing "severe AKI" exhibited increased urinary levels of all three transporters (68). The authors speculated that in patients with "early reversible proximal tubular damage" the transporters became mistargeted, with basolateral hOAT1 and hOAT3 translocating to the apical membrane and sloughing into the urine with apical hOAT4 moving 'inward',

whereas “severe AKI” resulted in proximal tubule cell apoptosis. Whether such a profound mechanism is the underlying cause of the observed patterns is unclear at this time.

There is clear evidence that prostaglandin E_2 (PGE_2) plays a role in the downregulation of OAT1/Oat1 and OAT3/Oat3 in response to ARF and CRF. Dose-dependent downregulation of both rOat1 and rOat3 protein expression by PGE_2 (IC_{50} ~25 nM) was demonstrated in NRK-52E cells, which are a rat renal proximal tubular cell model (69). Cortical PGE_2 levels are elevated in response to ARF and CRF and inhibition of the cyclooxygenase (COX) cascade was shown to exert protective effects (70-72). Since COX-1 and COX-2 mediate prostaglandin synthesis from arachidonic acid, it is thought that COX inhibitors work by preventing generation of cortical PEG_2 in response to injury. Accordingly, in the ischemia/reperfusion rat model, administration of the nonselective COX inhibitor indomethacin (1 mg/kg) immediately post-ischemia completely reversed ARF-induced downregulation of rOat1 and rOat3 protein expression levels within 24 hours (73). Moreover, renal PAH net secretion was also recovered (73). In a different study, the COX-2 specific inhibitor, parecoxib, was found to produce similar effects when administered 1 hour (20 mg/kg intraperitoneally) prior to the start of ischemia (74). When examined 12 hours post-reperfusion both rOat1 and rOat3 protein levels were significantly higher than in ARF animals that did not receive parecoxib, however the levels were still significantly reduced as compared to sham control animals (74). Similarly, PAH secretion was markedly restored in parecoxib animals, but still blunted as compared to sham controls (74). Whether this difference is due to the shorter duration post-reperfusion that the animals were examined (12 vs. 24 hours) or to the more selective action of parecoxib vs. indomethacin is not known. Together, these data strongly implicate induced PGE_2 as being responsible for the downreguation of OATs observed in CRF, ARF, and human renal allografts.

1.F OATs AND DRUG-DRUG INTERACTIONS

Following the development of probenecid as an agent to block the renal elimination of penicillin almost 70 years ago, clinical reports of probenecid-mediated DDIs resulting in altered distribution and renal elimination of a variety of drugs, including other β-lactams, cephalosporin antibiotics, fluoroquinolone antimicrobials, diuretics, and chemotherapeutic agents, began to appear (75-78). Modern studies using cloned transporters and knockout mouse lines have demonstrated a clear role for OATs in mediating, at least in part, a number of these DDIs (3, 79-85). Recently, a clinical study using healthy volunteers demonstrated that when probenecid was administered concomitantly with mesna, a cancer chemotherapy adjuvant used to decrease the renal toxicity of some chemotherapeutic agents, the fraction of mesna secreted was reduced by 67% and total mesna renal clearance was decreased by 55% (86). Moreover, hOAT1, hOAT3, and hOAT4 were demonstrated to mediate the probenecid-sensitive transport of mesna and dimensa *in vitro*, with inhibitory constants (K_i) in the ~15-30 µM range, values below their clinical concentrations, strongly implicating OATs in this DDI as well as having a vital role in the effectiveness of this therapy (86).

Patients taking paravastatin and gemfibrozil in combination to control their cholesterol and triglyceride levels have experienced alterations in pravastatin pharmacokinetics (increased plasma levels and decreased renal clearance) and been reported to suffer from increased pravastatin-associated adverse events (87). Subsequent work indicated this DDI might be the result of gemfibrozil inhibition of hOAT3-mediated paravastatin transport in these patients (88). Another lipid altering agent, gemcabene, has been implicated in exacerbating blood pressure reduction when co-administered with the angiotensin converting enzyme inhibitor, quinapril, in hypertensive patients (89). When examined *in vitro*, gemcabene was found to inhibit hOAT3

transport of quinaprilat**,** the pharmacologically active quinapril metabolite, in a dose-dependent manner, suggesting a DDI involving hOAT3 as the molecular basis for the observed increase in pharmacological activity (89).

Clearly, renally expressed OATs are poised to make great contributions to the pharmacokinetic profiles of many clinical therapeutics, having significant impact on their dosing regimens, pharmacodynamics, efficacy, and toxicity. OATs have great potential to be the sites for many clinically relevant DDIs, and the conclusive identification of their contributions to such interactions is expanding. In recognition of these facts, a recent whitepaper by the "International Transporter Consortium" (90), in conjunction with guidance documents issued by the United States Food and Drug Administration (FDA) (http://www.fda.gov/downloads/Drugs/GuidanceComplianceRegulatoryInformation/Guidances/UCM292362.pdf) and by the European Medicines Agency (http://www.ema.europa.eu/ema/index.jsp?curl=pages/includes/document/document_detail.jsp?webContentId=WC500090112&murl=menus/document_library/document_library.jsp&mid=WC0b01ac058009a3dc&jsenabled=true), have provided recommendations concerning which transporters are thought to have sufficient evidence regarding their impact on drug disposition and pharmacokinetics (*e.g.*, hOAT1, hOAT2, and hOAT3) to warrant investigation of new molecular entities for interactions, as a substrate or inhibitor, during the drug development process. In the whitepaper, it was recommended that *in vitro* studies with transporter expressing cell lines should be conducted to determine if the compound is a substrate, if the renal clearance is greater than or equal to 50% of the total clearance (considered to be substantial and clinically important) and greater than 1.5 times the unbound fraction times the GFR (90). The FDA guidance recommends that greater than 2 fold accumulation over background in transporter

expressing cells is necessary to regard the compound as a substrate. If these conditions are met, clinical DDI studies should be considered. For compounds found to be inhibitors of these transporters, if the ratio of the unbound maximum serum level (C_{max} or C_{ss}) divided by the compound-specific inhibition potency (K_i or IC_{50}) is greater than or equal to 0.1, clinical DDI studies are recommended. In 2010, VanWert *et al.* provided a comprehensive table on OATs summarizing the orthologs studied, compounds reported to interact with each of the OATs, whether they were confirmed substrates or only examined as inhibitors, and their affinities (reported K_m, K_i, or IC_{50} values) that is a useful reference tool when exploring such assessments (3). In Appendix I of this work we provide an update to the 2010 table, focusing on recent publications (2010-2012) in this area.

1.G CONCLUSIONS

Over the last fifteen years great progress has been made in identifying the biological properties, physiological roles, and biopharmaceutical significance of OATs. However, more effort is required to better define the role of OATs in 'normal' physiology, their changing function across an organism's lifespan, and their response to toxic exposure, whether environmental or as part of disease progression. While single nucleotide polymorphisms (SNPs) have been identified in both coding and regulatory regions of hOAT1, hOAT3, hOAT4, and hURAT1, most identified SNPs have failed to significantly impact OAT expression and function (91-96). Thus, modulations in OAT expression and transport activity through transcriptional and post-translational mechanisms might exert greater influence on the individual variations in pharmacokinetics and drug efficacy observed in clinical investigations, at different developmental stages (*e.g.*, pediatric vs. geriatric), and during progression of certain diseases (97-99). A more thorough understanding of these processes, in addition to OAT substrate specificity, might lead to new approaches for protecting renal function after injury or toxic insult, or for manipulating renal secretory or reabsorptive pathways to more effectively remove or reclaim endogenous metabolites and xenobiotics. Greater insight to the pathophysiogical changes to normal renal proximal tubule cell functions vital to OAT activity, *e.g.*, production of the intracellular mono- and dicarboxylates utilized as counterions by exchangers, would also be invaluable. As we move forward in our study of renal OAT function and make determinations as to the likely significance of DDIs involving OATs we need to remember that, while we have come a long way, there is still much we do not know and this changing context (*e.g.*, developmental stage, long-term polypharmacy, disease) might transcend a previously trivial interaction to one of great significance.

CHAPTER 2

RESEARCH HYPOTHESES AND SPECIFIC AIMS

2.A HYPOTHESES:

2.A.1 Flavonoids, phenolic acids, and other organic acid components of natural products exhibit significant inhibitory effects on human OATs (*e.g.*, hOAT1, hOAT3, and hOAT4) and their murine orthologs (*e.g.*, mOat1 and mOat3).

2.A.2 Compounds identified as strong OAT inhibitors have the potential to perpetrate transporter-mediated drug-drug interactions based on their affinity (K_i and IC_{50}) and clinical unbound plasma concentration.

2.A.3 Compounds identified as strong OAT inhibitors and undergone active tubular secretion have the potential to be substrates for OATs.

2.B SPECIFIC AIMS TO ADDRESS THE ABOVE HYPOTHESES:

2.B.1 SPECIFIC AIM 1

To characterize the inhibitory effects of components of natural products on transport activity mediated by human (h) OATs, hOAT1, hOAT3, and hOAT4 and the murine orthologs mOat1 and mOat3 using stably-expressing cell lines and radiolabeled prototypical substrates and known OAT inhibitors.

2.B.2 SPECIFIC AIM 2

1. To determine initial rates of cellular transport of prototypical substrates in OAT expressing cells and estimate the K_m values for individual transporters.
2. To estimate IC_{50} and K_i values for the selected compounds for individual transporters.
3. To collect clinical literature values for unbound plasma concentrations of the selected compounds and calculate the DDI index (ratio of unbound C_{max}/ IC_{50} (or K_i) based on "Guidance for Industry: Drug Interaction Studies" recently issued by the FDA.

2.B.3 SPECIFIC AIM 3

1. To develop a robust, specific, and sensitive liquid chromatography tandem mass spectrometry (LC-MS/MS)-based method for quantification of gallic acid and gentisic acid in cell lysate. A complete method validation, required by "Guidance for Industry: Bioanalytical Method Validation" issued by the FDA, will be conducted to evaluate sensitivity, selectivity, within-run and between-run precision and accuracy, recovery, stability, and matrix effects.
2. To apply the developed assay on the measurement of the cellular uptake of gallic acid and gentisic acid in stably transfected mOat1- and mOat3-expressing cells.

CHAPTER 3

ACTIVE HYDROPHILIC COMPONENTS OF THE MEDICINAL HERB SALVIA MILTIORRHIZA (DANSHEN) POTENTLY INHIBIT ORGANIC ANION TRANSPORTERS 1 (SLC22A6) and 3 (SLC22A8)

Drawn from manuscript published in *Evid Based Complement Alternat Med*. vol.2012, Article ID 872458, 8 pages, 2012.

3.A INTRODUCTION

The Chinese herbal medicine, Danshen (*Salvia miltiorrhiza*), has been employed for thousands of years in the relief of symptoms of cardiovascular disease (100-102). Despite this long history of medicinal use, the issue of which component(s) is(are) responsible for its therapeutic effects, and the precise biochemical mechanisms underlying their absorption, distribution and elimination, remain largely unknown. Increasingly, six hydrophilic compounds, lithospermic acid (LSA), protocatechuic acid (PCA), rosmarinic acid (RMA), salvianolic acid A (SAA), salvianolic acid B (SAB), and tanshinol (TSL), are gaining favor as the Danshen components responsible for the beneficial effects on heart disease (103-105). Since these compounds are organic, small in size (154-718 Da), and exist as anions at physiological pH, it is possible that they are substrates and/or inhibitors of the organic anion transport pathway that exists in organs such as the kidney, liver, intestine, and choroid plexus (3).

We now know that this organic anion transport pathway is actually a complex system of transport proteins that belong to a variety of gene families. Members of the solute carrier (SLC) superfamily, composed of ~55 gene families containing almost 400 identified transporters, are an important component of this pathway (2, 3, 106). Of particular interest for the Danshen components examined in this work is the SLC22 (organic cation/anion/zwitterion transporters) family, which includes both the organic cation transporters and the organic anion transporters (OATs). Members of the OAT family are found in virtually every barrier tissue in the body and mediate the transepithelial flux (absorption, distribution and elimination) of a multitude of endogenous and xenobiotic compounds (2, 3, 106). Typical endogenous OAT substrates include sulfated steroid conjugates, indoxyl sulfate, uric acid, and acidic metabolites of monoamine neurotransmitters. Xenobiotic substrates include clinically important therapeutics such as antibiotic (benzylpenicillin), antiviral (adefovir, cidofovir) and anticancer (methotrexate) agents, statins, and angiotensin-converting enzyme inhibitors, as well as environmental toxins such as ochratoxin A and aristolochic acid (2, 3, 36)

Currently, there are 29 putative SLC22 family members, 18 of which are believed to be OATs. Of those, transport activity has been demonstrated for eleven, OAT1-10 and URAT1 (2, 3). OATs expressed in the proximal tubule cells of the kidney mediate the blood to urine secretory flux and urine to blood reabsorptive flux of substrate compounds (2, 3, 106). Since these compounds are negatively charged, OATs provide a passageway through which they can readily cross the lipid bilayer of cells. Substrate entry into proximal tubule cells from the blood across the basolateral membrane is energized by exchange for intracellular α-ketoglutarate (*i.e.*, organic anion/dicarboxylate exchange). In humans and rodents this process involves the basolateral exchangers, organic anion transporter 1 (Oat1; Slc22a6) and 3 (Oat3; Slc22a8) (107,

108). OAT-mediated exit of organic anions from the cell into the urine is accomplished via facilitated diffusion using the electrochemical gradient. There appears to be distinct species differences between rodents and humans in terms of OATs targeted to the apical membrane of proximal tubule cells. For example, while both species express Urat1 (Slc22a12), humans also have OAT4 (SLC22A9; no current rodent ortholog), whereas rodents have Oat5 (Slc22a19; no human ortholog identified) (2, 3).

The basolateral uptake transporters Oat1 and Oat3 share a high degree of amino acid sequence identity (mOat1 vs. mOat3 = 48% and hOAT1 vs. hOAT3 = 50%). This protein homology likely contributes to the greatly overlapping substrate profiles exhibited by these two transporters. However, despite this general similarity, the individual affinities for the same substrate often differ greatly between Oat1 and Oat3 (3). Further, unique substrates that interact with Oat1, but not with Oat3 (and vice-versa) have been identified (3). Preclinical *in vivo* studies utilizing knockout mouse lines have also demonstrated that, in terms of renal transport function, expression of Oat1 does not fully compensate for loss of Oat3 (and vice-versa) (80-82, 85). For example, Oat1 knockout mice exhibited complete loss of active tubular *para*-aminohippuric acid (PAH) secretion and decreased renal clearance of the diuretic, furosemide, which was accompanied by significantly decreased efficacy (monitored as decreased natriuresis and increased ED_{50}) (85). Pharmacokinetic studies performed in Oat3 knockout mice detected reduced clearance and increased plasma half-life of benzylpenicillin, ciprofloxacin, and methotrexate (80-82). However, PAH clearance was unaffected in these animals (81).

To more fully understand the therapeutic efficacy (and/or adverse effects) of herbal products and optimize their clinical use, a more thorough identification of the active components they contain and greater knowledge of the mechanisms determining their pharmacokinetic and

pharmacodynamic properties, *e.g.*, transporter interactions, need to be elucidated. The aim of the present study was to characterize the effects of six active hydrophilic Danshen components on the transport activity of mOat1 and mOat3. Danshen components producing the greatest inhibition were examined further in studies designed to elucidate the mechanism of inhibition (competitive vs. non-competitive vs. uncompetitive). Combining this information with dose response data we derived inhibitory constants (K_i values). Evidence was gathered showing that LSA, RMA, and SAA serve as potent competitive inhibitors of mOat1 and mOat3 and indicating the potential for marked herb-drug interactions, such as altered pharmacokinetics and pharmacodynamics of co-administered clinical therapeutics that are OAT substrates.

3.B MATERIALS AND METHODS

3.B.1 Purified chemicals

The Danshen components LSA, PCA, RMA, SAA, SAB, and TSI96 (≥ 96% purity) were obtained from Tauto Biotech (Shanghai, China). Their chemical structures are illustrated in Figure 3.1. Tritiated PAH ([^{3}H]PAH) and estrone sulfate ([^{3}H]ES) were purchased from PerkinElmer Life and Analytical Sciences (Waltham, MA) and unlabeled PAH, ES, and probenecid were purchased from Sigma-Aldrich (St. Louis, MO).

3.B.2 Tissue culture

Derivation of the stably transfected Chinese hamster ovary (CHO) cell lines expressing mOat1 (CHO-mOat1), mOat3 (CHO-mOat3), and the empty vector (FRT) transfected control cell line (CHO-FRT), was described previously (80, 82). Cell lines were maintained at 37°C with 5% CO_2 in DMEM F-12 media (Mediatech, Inc., Herndon, VA) containing 10% serum, 1% Pen/Strep and 125 µg/ml hygromycin B.

3.B.3 Cell accumulation assays

Cell transport assay procedures were adapted from those previously published (82, 109). In brief, 2×10^5 cells/well were seeded in 24-well tissue culture plates and grown in the absence of antibiotics for 48 hr. On the day of the experiment cells were equilibrated with transport buffer for 10 min [500 µL of Hanks' balanced salt solution containing 10 mM HEPES, pH 7.4]. Equilibration buffer was replaced with 500 µL of fresh transport buffer containing 5 µM [^{3}H]PAH or 1 µM [^{3}H]ES (0.25 µCi/mL) with or without inhibitors. After incubation, cells were immediately rinsed three times with ice-cold transport buffer, lysed, and analyzed via liquid scintillation counting. Uptake values were normalized to corresponding total protein content in cell lysates as determined by the Bradford method. Substrate accumulation is reported as

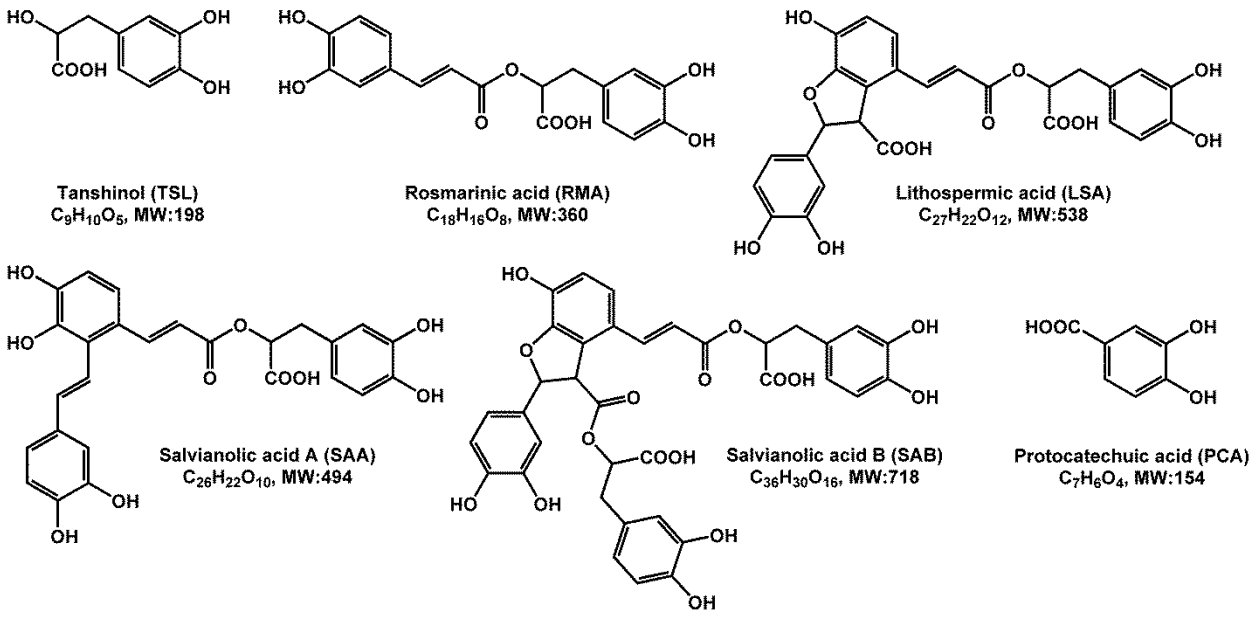

Figure 3.1. Chemical structures of six active hydrophilic Danshen components.

MW, molecular weight.

picomoles of substrate per milligram protein. Substrate concentration and accumulation time used for kinetic analysis of mOat3 (1 µM ES for 1 min, K_m = 12.2 ± 4.8 µM) were determined previously (82). Substrate concentration (Figure 3.3) and accumulation time (data not shown) for mOat1 kinetic analysis (5 µM PAH for 2 min, K_m = 13.0 ± 3.3 µM) were determined in this study. Kinetic calculations were performed using GraphPad Prism Software version 5.0 (GraphPad Software Inc., San Diego, CA). Michaelis constant (K_m) values were calculated by nonlinear regression using the Michaelis-Menten model. Mode of inhibition was identified by using mixed model inhibition analysis (110):

$$V_{\max\,Apparent} = \frac{V_{\max}}{(1+[I]/(\alpha \times K_i))}$$

$$K_{\mathrm{m}\,Apparent} = K_m \frac{1+[I]/K_i}{(1+[I]/(\alpha \times K_i))}$$

$$Y = \frac{V_{\max\,Apparent} \times x}{K_{\mathrm{m}\,Apparent} + x}$$

where V_{max}, K_i, and I represent the maximum transport velocity without inhibitor, the inhibition constant generated from the data set under analysis, and the concentration of inhibitor, respectively. In this study, three curves were constructed (no inhibitor, plus two selected inhibitor concentrations) with uptake of substrate plotted as a function of its concentration for each condition. These untransformed data were fit to the equations shown above using nonlinear regression to estimate the α values summarized in Table 3.1. The parameter, α, can then be used to determine the mode of inhibition. When α is very large (α > 1), it indicates competitive inhibition. Otherwise, it indicates noncompetitive inhibition (α = 1) or uncompetitive inhibition (0 < α < 1). To estimate K_i values, IC_{50} values were calculated using nonlinear regression and inserted into the Cheng-Prusoff equation: $K_i = IC_{50}/(1 + [Substrate]/K_m)$ (111). Results were

confirmed by repeating all experiments at least three times with triplicate wells for each data point in every experiment.

3.B.4 Statistics

Data are reported as mean ± S.D. or mean ± S.E.M. as indicated. Statistical differences were assessed using one-way ANOVA followed by post-hoc analysis with Dunnett's t-test or using Student's unpaired t-test, as indicated ($\alpha = 0.05$).

3.C RESULTS

3.C.1 Inhibition of mOat1 and mOat3 by hydrophilic Danshen components

Accumulation of PAH in the CHO-mOat1 cell line (98.5 ± 14.6 pmol/mg protein/10 min) was ~30 fold greater than that in the background control CHO-FRT cells (3.3 ± 0.7 pmol/mg protein/10 min; Figure 3.2A). Initially, an uptake assay with excess (1 mM) Danshen components was performed to identify which, if any, of the compounds might interact with mOat1 (Figure 3.2A). Each of the Danshen components, LSA, PCA, RMA, SAA, SAB, and TSL, significantly inhibited PAH uptake in CHO-mOat1 cells ($P < 0.001$) under these conditions. LSA, SAB, and TSL produced approximately 70-85% inhibition, whereas PCA, RMA, and SAA, each reduced PAH accumulation to the background level (> 95% inhibition), similar to the prototypical OAT inhibitor, probenecid. Further, addition of these compounds (1 mM) did not significantly influence the low, probenecid-insensitive (*i.e.*, non-specific) PAH uptake in the CHO-FRT cells (data not shown), indicating that the reduction in uptake of PAH in the CHO-mOat1 cells is attributable to inhibition of mOat1 activity and that CHO-FRT PAH level serves as an appropriate background correction factor.

Stably transfected mOat3-expressing (CHO-mOat3) cells showed significantly greater accumulation of ES (~20 fold) relative to control CHO-FRT cells (5.02 ± 0.19 vs. 0.25 ± 0.04 pmol/mg protein/10 min, respectively; Figure 3.2B). Similar to mOat1, all of the Danshen components (1 mM) significantly inhibited mOAT3-mediated ES uptake ($P < 0.001$). SAB and TSL produced approximately 53% and 55% inhibition, respectively. LSA, PCA, RMA, and SAA, like probenecid, blocked virtually all (> 91%) mOat3-mediated ES transport (Figure 3.2B). As with PAH, these compounds (1 mM) failed to consistently or significantly influence non-specific ES uptake in CHO-FRT cells (data not shown), indicating that the reduction in uptake of ES in

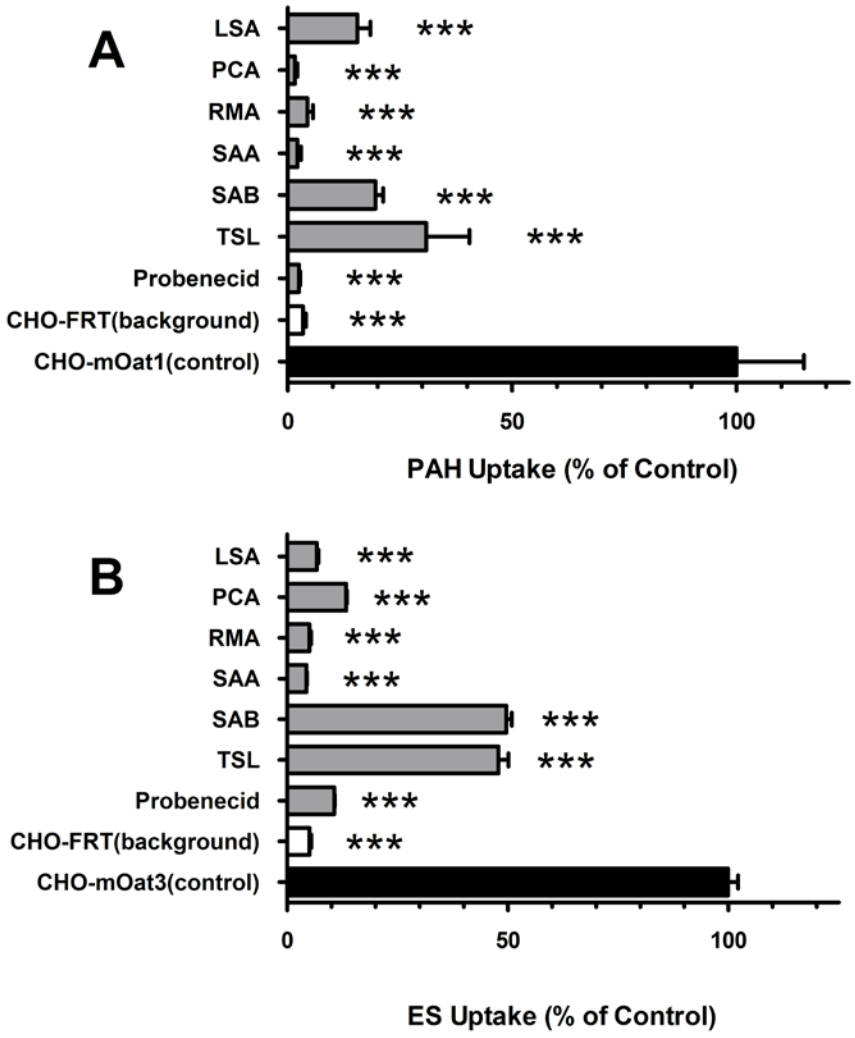

Figure 3.2. Inhibition profile of mOat1 and mOat3

A: Inhibition of mOat1-mediated uptake of [^{3}H]PAH (5 µM) by LSA, PCA, RMA, SAA, SAB, TSL, and probenecid (1000 µM) was measured in the CHO-mOat1 cells (10 min). Background PAH accumulation was measured in CHO-FRT cells in the absence of inhibitor and is shown to provide a clear gauge of the low background in the experimental system. B: Inhibition of mOat3-mediated uptake of [^{3}H]ES (1 µM) by LSA, PCA, RMA, SAA, SAB, TSL, and probenecid (1000 µM) was measured in the CHO-mOat3 cells (10 min). Background ES accumulation was measured in CHO-FRT cells in the absence of inhibitor and is shown to provide a clear gauge of the low background in the experimental system. Values are mean ± S.D. of triplicate values. *** denotes $p < 0.001$ as determined by one-way ANOVA followed by Dunnett's t-test.

the CHO-mOat3 cells is attributable to inhibition of mOat3 activity and that CHO-FRT ES level serves as an appropriate background correction factor.

3.C.2 Determination of the type of inhibition induced by Danshen components on mOat1 and mOat3

Although PCA exhibited as potent inhibition as LSA, RMA, and SAA, it is not a major component in Danshen preparations. Therefore, the mechanism of inhibition of mOat1/mOat3-mediated transport of PAH/ES was investigated for LSA, RMA, and SAA (Table 3.1). Our previous work with CHO-mOat3 cells showed that ES accumulation was linear through the first 5 min and that ES exhibited a K_m of 12.2 ± 4.8 μM (82). In this study, time course evaluations in CHO-mOat1 cells indicated PAH accumulation was linear through at least the first 5 min and K_m was estimated as 13.0 ± 3.3 μM (Figure 3.3). Using these parameter estimates as guidelines, kinetic experiment conditions were set to 1 μM ES for 1 min and 5 μM PAH for 2 min. The background corrected untransformed data for LSA, RMA, and SAA on mOat1 or mOat3 were fit to the mixed inhibition model, which incorporates competitive, non-competitive, and uncompetitive inhibition modes. The estimated α values were found to be much larger than 1, indicating that inhibition of mOat1- and mOat3-mediated transport by LSA, RMA, and SAA was competitive in nature (Table 3.1).

3.C.3 Inhibition potencies of LSA, RMA, and SAA

To allow direct comparison of inhibition potencies of LSA, RMA, and SAA for mOat1 and mOat3, experiments were conducted to determine the inhibition constant (K_i) values (Figures 3.4 and 3.5 and Table 3.2). Since LSA, RMA, and SAA were found to be competitive inhibitors of mOat1- and mOat3-mediated transport, subsequent K_i analysis was performed using competitive inhibition. Applying increasing concentrations of unlabeled test compounds (10^{-7} to 5×10^{-4} M),

inhibition of mOat1- or mOat3-mediated transport was measured (Figures 3.4 and 3.5). Inhibition constants were estimated as 14.9 ± 4.9 µM for LSA, 5.5 ± 2.2 µM for RMA, and 4.9 ± 2.2 µM for SAA on mOat1-mediated transport (Table 3.2). Values determined in the CHO-mOat3 cell line were 31.1 ± 7.0 µM for LSA, 4.3 ± 0.2 µM for RMA, and 21.3 ± 7.7 µM for SAA (Table 3.2). For all of these analyses the coefficient of determination (r^2) was > 0.9. No significant differences between K_i values for mOat1 and mOat3 were detected as determined by a Student's unpaired t-test.

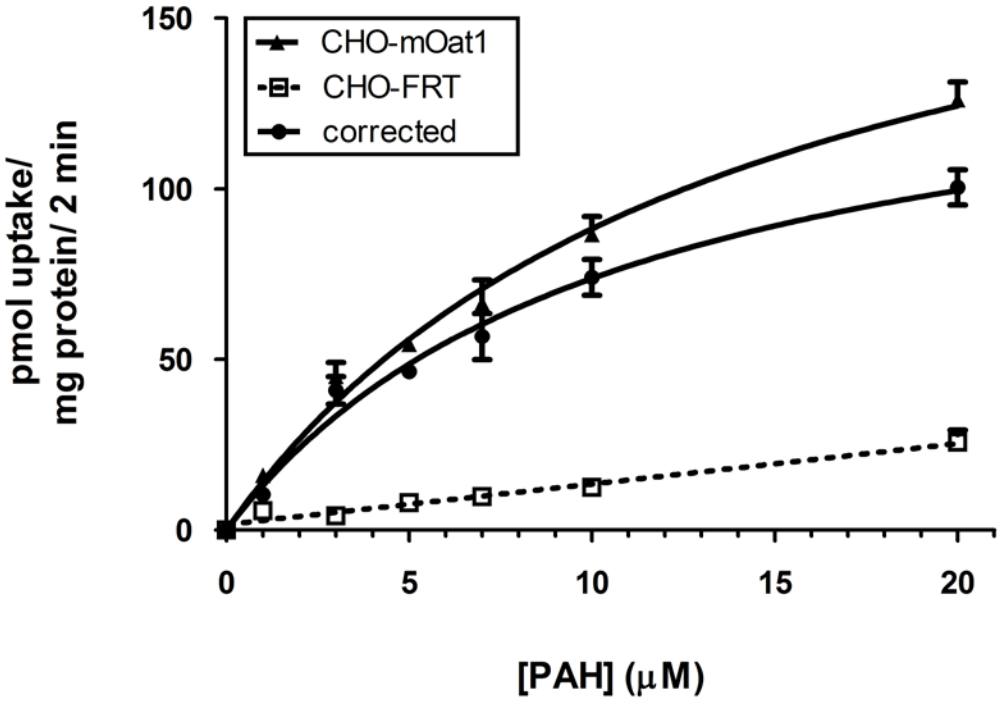

Figure 3.3. Michaelis-Menten kinetics of PAH transport in CHO-mOat1 cells

In order to calculate K_i values for mOat1, the K_m value for PAH needed to be determined in the CHO-mOat1 cell system. Uptake of [^{3}H]PAH was measured for 2 min at room temperature in CHO-mOat1 (closed triangles) and CHO-FRT (open squares) cells in order to construct a saturation curve. The corrected curve (closed circles) was obtained by subtracting the non-specific background uptake as measured in the CHO-FRT cells from CHO-mOat1 accumulation to allow analysis of mOat1-mediated activity. Experiments were repeated three times in triplicate and Michaelis constant (K_m) values were calculated by nonlinear regression using the Michaelis-Menten model. The K_m for PAH on mOat1 was estimated as 13.0 ± 3.3 μM (mean ± S.E.M.). Graph shown is from a representative experiment with values plotted as mean ± S.D. (n=3).

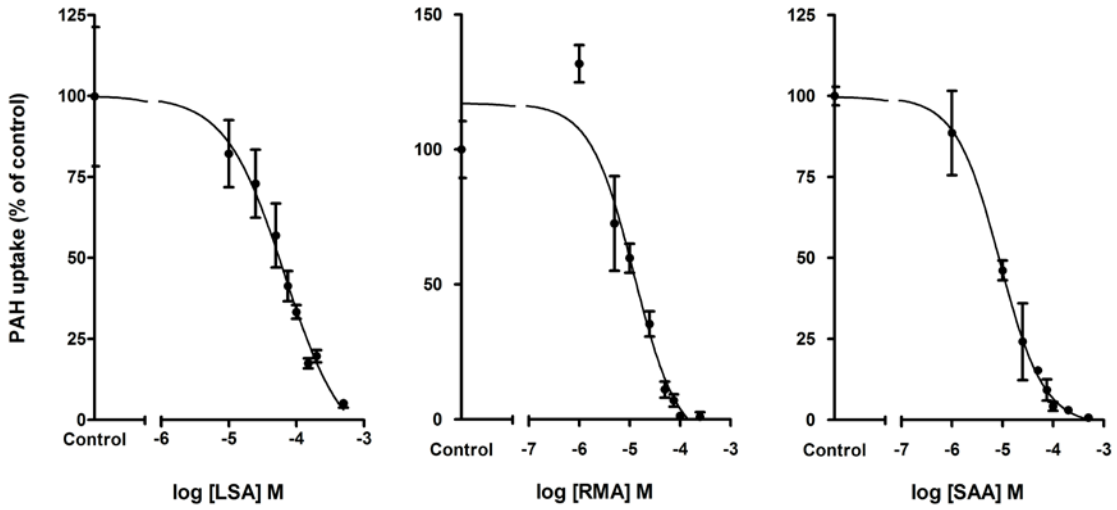

Figure 3.4. K_i determination for LSA, RMA, and SAA in the CHO-mOat1 cell line

Two minute uptake of [^{3}H]PAH (5 µM) in CHO-mOat1 cells was measured in the presence of increasing concentrations (10^{-7} to 5×10^{-4} M) of LSA, RMA, and SAA. Data were corrected for non-specific background measured in the CHO-FRT cells prior to kinetic analysis. K_i values were determined with non-linear regression and the "one-site competition" model using GraphPad Prism software. Experiments were repeated three times in triplicate with the mean K_i ± S.E.M. reported in Table 3.2. Graphs shown are from representative experiments with values plotted as mean ± S.D. (n=3).

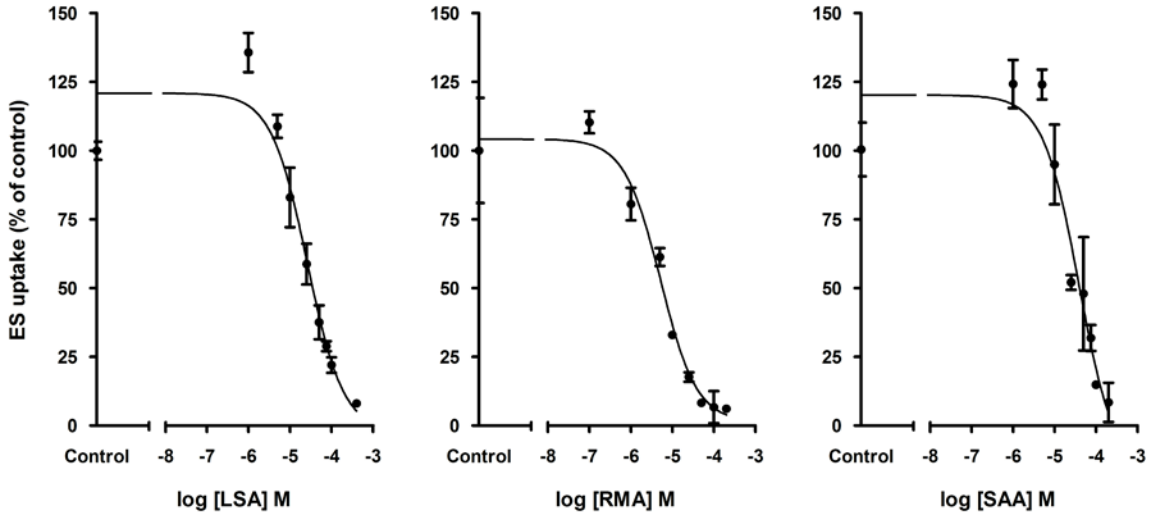

Figure 3.5. K_i determination for LSA, RMA, and SAA in the CHO-mOat3 cell line

One minute uptake of [^{3}H]ES (1 µM) in CHO-mOat3 cells was measured in the presence of increasing concentrations (10^{-7} to 4×10^{-4} M) of LSA, RMA, and SAA. Data were corrected for non-specific background measured in the CHO-FRT cells prior to kinetic analysis. K_i values were determined with non-linear regression and the "one-site competition" model using GraphPad Prism software. Experiments were repeated three times in triplicate with the mean K_i ± S.E.M. reported in Table 3.2. Graphs shown are from representative experiments with values plotted as mean ± S.D. (n=3).

Table 3.1. Estimated α values from a mixed inhibition model analysis for LSA, RMA, and SAA

Compound	mOat1	mOat3
LSA	6.7×10^{11}	1.9×10^{15}
RMA	1.3×10^{12}	2.5×10^{19}
SAA	2.6×10^{14}	3.4×10^{14}

Values are reported as mean. The S.E.M. is not applicable in this analysis.

Table 3.2. Estimated K_i (μM) values for mOat1- and mOat3-mediated transport

Compound	mOat1	mOat3	K_i Ratio (mOat1/ mOat3)
LSA	14.9 ± 4.9	31.1 ± 7.0	0.48
RMA	5.5 ± 2.2	4.3 ± 0.2	1.29
SAA	4.9 ± 2.2	21.3 ± 7.7	0.23

Values are reported as mean ± S.E.M. (n=3). No significant differences between K_i values for mOat1 and mOat3 were detected ($P < 0.05$) as determined by Student's unpaired t-test.

3.D DISCUSSION

Many natural products, which are extracted from living organisms, have beneficial biological or pharmacological activities and have been used as medicines throughout the world for more than 1,000 years. Today, they are often used as first-line therapeutics, dietary supplements, or complementary/alternative medicines and it is reported that ~20% of adults in the United States are taking an herbal product (112). Over the last decade a number of studies have identified transporter proteins, including OATs, as sites of drug-drug and natural product-drug interactions. For example, the dietary polyphenol, ellagic acid, which exhibits beneficial antioxidant and anticancer properties, was demonstrated to be one of the most potent inhibitors of hOAT1 (IC_{50} = 207 nM) identified to date (48). Recently, the nephrotoxin aristolochic acid, which is produced by *Aristolochia sp.* plants, was identified as the causative agent for "Chinese herbs nephropathy" (now referred to as aristolochic acid nephropathy). When investigated, aristolochic acid was found to be a high affinity substrate for both mOat1 (K_m = 790 nM) and mOat3 (K_m = 514 nM), suggesting these transporters may be key mediators in the renal proximal tubule cell accumulation of this toxicant (36, 113). Thus, this interaction likely explains the biochemical mechanism underlying the acutely targeted, proximal tubule specific nature of aristolochic acid toxicity. Clearly, OATs expressed in the renal proximal tubule represent highly probable sites of natural product-drug (or natural product-endogenous substrate) interactions. Further studies such as these are needed in order to establish informed safety and efficacy profiles for herbal products.

Danshen, a traditional herbal medicine, continues to be used in the treatment of angina, myocardial ischemia, and other cardiovascular diseases throughout the world including Asia, Europe, and North America (100). In 2010, the Danshen pharmaceutical product, Fufang Danshen Dripping Pill, successfully completed Phase II clinical trials in the United States

(http://clinicaltrial.gov/ct2/show/NCT00797953?term=tasly&rank=1). To date, however, no formal studies examining the interaction between OATs and hydrophilic Danshen compounds, which are small organic acids and known to be major components in its pharmaceutical products, have been reported. Therefore, in the present study we investigated whether any of the six purported active Danshen components, LSA, PCA, RMA, SAA, SAB, and TSL, interacted with the transporters mOat1 and/or mOat3 (Figures 3.1 and 3.2).

A major advantage of this study is that, while Danshen preparations (and indeed the majority of herbal medicines) include multiple active components, purified preparations of individual Danshen extract components were used. Thus, the strength of interaction of each compound could be quantified independently vs. the merged effects of a mixture containing all of the compounds. Similarly, since the transporters were expressed in isolation, the interaction of each individual compound with each individual transporter could be specifically assessed vs. the *in vivo* situation where multiple transporter proteins are expressed simultaneously in a tissue and the measured response is possibly an amalgamation of the activities of multiple transporter proteins. While under certain conditions all six compounds significantly inhibited mOat1- and mOat3-mediated transport, LSA, RMA, and SAA emerged as potent competitive inhibitors, (Figures 3.4 and 3.5 and Tables 3.1 and 3.2). The rank order of their potencies was different between the two transporters with RMA≈ SAA > LSA for mOat1 and RMA > SAA≈ LSA for mOat3. While statistically not different, the K_i ratio (Table 3.2) suggests that mOat1 may have a slightly higher affinity (lower K_i) for LSA and SAA than mOat3. However, in general all of the values are quite similar and exhibit well below an order of magnitude in difference. The estimates are comparable to those reported for the strong OAT inhibitor, probenecid, K_i = 6.4 and 4.6 µM for mOat1 and mOat3, respectively (114, 115). Thus, LSA, RMA, and SAA may

affect the disposition and elimination of co-administered drugs that are also mOat1 and mOat3 substrates. This may be particularly relevant in patients suffering from coronary disease where Danshen pharmaceutical products could be combined with drugs such as angiotensin converting enzyme inhibitors and studies with the human orthologs of these transporters need to be conducted.

In vivo pharmacokinetic studies have indicated that elimination of hydrophilic Danshen components involves active renal secretory pathways. In rats, the unbound renal clearance of TSL was ~5X greater than the glomerular filtration rate (116). A separate study in rats found that spiking additional SAA into Danshen preparations increased the AUC of SAB (82.4%) and TSL (26.7%), and markedly reduced their clearances (46.8% and 32.9% for SAB and TSL, respectively) (117). As we determined SAA was a potent competitive mOat1/mOat3 inhibitor, and SAB and TSL can interact with mOat1 and mOat3, our data suggest that these *in vivo* results may be explained by competition for transport on Oat1/Oat3. An *in vivo* pilot study conducted in healthy humans reported C_{max} values for LSA and RMA of 2.1 μM and 6.7 μM after *i.v.* dosing of a Danshen product (104). These C_{max} values are ~0.07-1.56 fold higher than the K_i values for mOat1 and mOat3 determined in the present study (Table 3.2). As recommended by the FDA Guidance for Drug Interaction Studies, when *unbound* C_{max}/IC_{50}(or K_i) ≥ 0.1, it indicates that drug-drug interactions may occur *in vivo* (118). Unfortunately, the plasma protein binding for LSA and RMA have not been reported, while TSL showed 25% plasma protein binding in rat plasma (116). However, if we assume RMA to be highly protein bound (90%), the unbound C_{max}/K_i ratio for RMA would be 0.12 and 0.16 on mOat1 and mOat3, respectively, indicating potential for herb-drug interactions. Naturally, if human OAT orthologs show similar (or higher) affinities, possible herb-drug interactions should be considered.

A recent investigation indicated that flavonoid and hydroxycinnamic acid aglycones and their phase II metabolites (*e.g.*, sulfate and glucuronide conjugates) significantly inhibit hOAT1 and hOAT3 transport activity (50, 119). It is known that after oral administration in healthy volunteers, the majority of RMA exists as such conjugated forms, as well (120, 121). Currently, there are no reports on characterization of LSA and SAA metabolites in human plasma, while SAA might undergo methylation and glucuronidation in rats (122). Therefore, studies elucidating the metabolic pathways of these compounds are needed such that potential interactions of their metabolites with Oat1 and/or Oat3 can be examined.

In addition, there are other transporter families known to interact with small organic anions, *e.g.*, the multidrug resistance associated proteins (MRPs, ABCC family) and the organic anion transporting polypeptides (OATPs, SLCO family). For the most part these latter two transporter families and the OATs have fairly distinct substrate interactions, however, the possibility that they also may contribute to the overall clinical pharmacokinetic profile of Danshen components *in vivo* needs to be considered until investigated directly. For example, it was recently suggested that SAB might be an OATP substrate based upon inhibition of total and biliary clearance of SAB by rifampicin, an OATP inhibitor, in rats (123).

Finally, the amount of each active component in Danshen preparations varies with different cultivation regions and manufacturing processes (103). The variation of RMA in raw plant material was observed to be ~16 fold between different growing regions and the dose of RMA ranged from 4.1-160 mg (~40 fold) in injectable dosage forms produced by different manufacturers (103, 104). In a clinical study, the C_{max} of RMA after *i.v.* infusion of a 160 mg dose was 1.2-1.6 fold higher than the K_i values for mOat1 and mOat3 (104). These data suggest that, clinically, patients either would or would not have the potential for significant herb-drug

interactions solely depending upon which manufacturer's product they were administered. Thus, although tanshinone II A, SAB, and protocatechuic aldehyde have been used as quality control markers in the manufacture of Danshen pharmaceutical dosage forms, the work presented here indicates that perhaps the content of LSA, RMA, and SAA, should be monitored and controlled as well.

CHAPTER 4

COMPETITIVE INHIBITION OF HUMAN ORGANIC ANION TRANSPORTERS 1 (SLC22A6) AND 3 (SLC22A8) BY MAJOR COMPONENTS OF THE MEDICINAL HERB SALVIA MILTIORRHIZA (DANSHEN)

Drawn from manuscript published in *Drug Metab Pharmacokinet* 2012; 28(3):220-8

4.A INTRODUCTION

Danshen, the dried root of *Salvia miltiorrhiza*, has been used as a traditional Chinese medicine for thousands of years in the treatment of angina, myocardial ischemia, and other cardiovascular diseases (100-102). *In vitro* and *in vivo* studies demonstrated that Danshen could improve microcirculation, facilitate coronary vasodilatation, and increase blood flow (124-127). Danshen products are readily available throughout the world including Asia, Europe, and North America, and annual sales volume is in the hundreds of millions of dollars (100). According to the China State Food and Drug Administration database of drug manufacturing certificates, there are currently more than 980 commercial Danshen preparations, 289 of which are injectable dosage forms (http://www.sda.gov.cn/WS01/CL0001/). The oral dosage form, Fufang Danshen Dripping Pill, was approved for Phase II and Phase III clinical trials by the United States Food and Drug Administration in 1997 (IND No. 56956). In 2010, the Phase II clinical trials were successfully completed (http://clinicaltrial.gov/ct2/show/NCT00797953?term=tasly&rank=1),

but no formal clinical trials for any injectable Danshen formulations have been reported. Use of the injectable products is of particular concern, as the spectra and amounts of the compounds they contain are not well standardized. More than 70 lipophilic and hydrophilic compounds have been separated and identified from Danshen extract (128). However, which component(s) is/are responsible for the beneficial pharmacological effects of Danshen is virtually unknown. Among hundreds of Danshen pharmaceutical products, lithospermic acid (LSA), rosmarinic acid (RMA), salvianolic acid A (SAA), salvianolic acid B (SAB), and tanshinol (TSL) exhibited markedly high content and were considered as major components (103-105).

Currently, the clinical pharmacokinetic literature on Danshen is extremely limited. One study assayed LSA, RMA, SAA, SAB, and TSL in human urine and plasma samples obtained after oral dosing and found TSL was the only compound detectable (116). However, this study examined just a single formulation and dose. In contrast, LSA, RMA, SAA, SAB, and TSL were all detected after administration of an injectable Danshen preparation (104). To improve the clinical safety of Danshen herbal therapies (especially injectables), better estimation of the composition and dose of active components, as well as a greater knowledge of the processes affecting their pharmacokinetic and pharmacodynamic properties, including potential transporter-mediated herb-drug interactions, is required.

Since these Danshen components are relatively small (198-718 Da) and exist as anions at physiological pH, it is possible that they are organic anion transporter (OAT; SLC22) family substrates or inhibitors. OATs are key mediators in the distribution and elimination of a multitude of endogenous compounds and xenobiotics, which include clinically important therapeutics such as antibiotics, antiviral and anticancer agents, statins, and angiotensin-converting enzyme inhibitors (2, 3, 106). A number of clinical and pre-clinical studies have

demonstrated that concomitant administration of drugs that are eliminated from the body by renally expressed OATs may result in longer plasma half-life and reduced renal clearance.

For example, co-administration of probenecid, a known OAT inhibitor, has been demonstrated to diminish the renal clearance of benzylpenicillin and ciprofloxacin (77, 129). In accord with these clinical findings, *in vivo* pharmacokinetic studies using organic anion transporter 3 (Oat3) knockout mice demonstrated that loss of murine Oat3 (mOat3) activity increased the plasma half-life and reduced the clearance of benzylpenicillin, ciprofloxacin, and methotrexate (80-82). Further, cephalosporin antibiotics, including cephaloridine, cephalothin, cefadroxil, cefamandole, cefazolin, cefoperazone, cefotaxime, and ceftriaxone, exhibited low inhibition constant (K_i) values for hOAT1 (0.03-6.14 µM), indicating the potential for drug-drug interactions during combined therapy with other therapeutics that are hOAT1 substrates (84). Recent work with the cancer chemotherapy adjuvants, mesna and dimesna, demonstrated *in vitro* that hOAT1 and hOAT3 transport these compounds and *in vivo* that concomitant probenecid administration reduced their renal elimination in healthy human volunteers (86). In addition, concomitant gemfibrozil administration was found to influence the pharmacokinetic properties of pravastatin in patients, increasing pravastatin-related adverse effects, and it has been proposed that the mechanism may be due to competition for hOAT3-mediated tubular secretion (87, 88). Similarly, co-administration of the lipid altering compound, gemcabene, with the angiotensin converting enzyme inhibitor, quinapril, resulted in a reduction in blood pressure in hypertensive humans and rats (89). In rats, co-dosing of gemcabene and quinapril resulted in significantly elevated plasma levels of quinaprilat, the pharmacologically active metabolite of quinapril (89). Further, *in vitro* experiments demonstrated dose-dependent inhibition of hOAT3- and rat Oat3-mediated quinaprilat transport by gemcabene, at clinically relevant levels, implicating drug-drug

interaction on hOAT3 as the mechanism for elevated circulating levels of quinaprilat and greater pharmacological activity (89). In response to the increase in known transporter-mediated drug-drug interactions such as these the United States Food and Drug Administration and the European Medicines Agency have issued guidance documents regarding circumstances under which drug interactions with specified transporters (including hOAT1 and hOAT3) need to be investigated

(http://www.fda.gov/downloads/Drugs/GuidanceComplianceRegulatoryInformation/Guidances/UCM292362.pdf

and http://www.ema.europa.eu/ema/index.jsp?curl=pages/includes/document/document_detail.jsp?webContentId=WC500090112&murl=menus/document_library/document_library.jsp&mid=WC0b01ac058009a3dc&jsenabled=true).

Our recent study investigating the inhibition profiles of LSA, RMA, SAA, SAB, and TSL on murine Oat1 and Oat3 (mOat1 and mOat3)-mediated substrate uptake demonstrated that LSA, RMA, and SAA exerted markedly stronger inhibitory effects compared to SAB and TSL (49). Kinetic analysis revealed that LSA, RMA, SAA were potent competitive inhibitors of both transporters, exhibiting K_i values ranging from 4.9-14.9 μM for mOat1 and from 4.3-31.1 μM for mOat3. However, the affinities of Danshen compounds with human OATs remained unknown, and the potential for marked species differences between transporter orthologs has been well documented (3). Therefore, the aim of the present study was to characterize the inhibitory effects of LSA, RMA, and SAA on *para*-aminohippuric acid (PAH) transport mediated by hOAT1 or estrone sulfate (ES) transport mediated by hOAT3. Further, studies designed to elucidate the mechanism of inhibition (competitive vs. non-competitive vs. uncompetitive) were also conducted. Using this information we derived inhibitory constants (K_i

values) for each compound to allow direct comparison of their potencies between transporter paralogs and orthologs. Finally, using published human pharmacokinetic values, unbound C_{max}/K_i (recommended by FDA Guidance for Drug Interaction Studies) were calculated as an indicator of the *in vivo* drug-drug interaction potential for these compounds (49). Together, these data demonstrated that LSA, RMA, and SAA serve as potent competitive inhibitors of hOAT1 and hOAT3 and that there is strong potential for herb-drug interactions, such as altered pharmacokinetics and pharmacodynamics of co-administered clinical therapeutics that are OAT substrates.

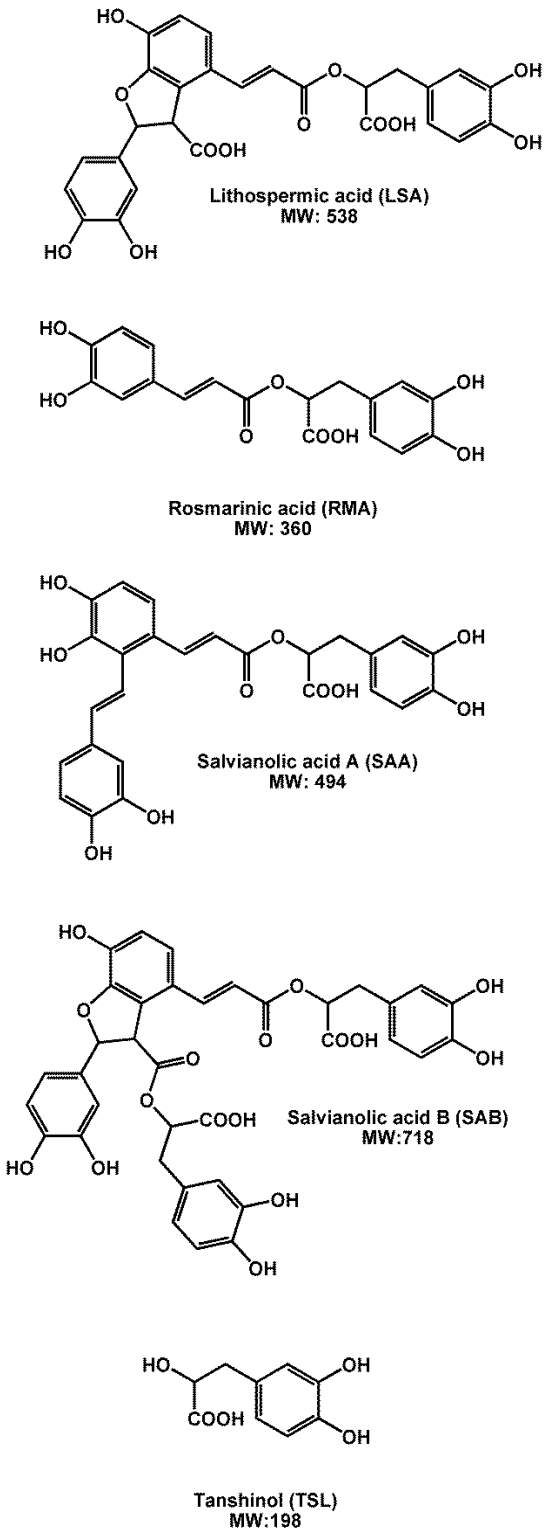

Figure 4.1. Chemical structures for the Danshen components LSA, RMA, and SAA.

MW, molecular mass.

4.B MATERIALS AND METHODS

4.B.1 Chemicals

Purified (≥ 96.0%) lithospermic acid (LSA), rosmarinic acid (RMA), salvianolic acid A (SAA), were purchased from Tauto Biotech (Shanghai, China). The chemical structures are shown in Figure 4.1. Tritiated *para*-aminohippuric acid ([^{3}H]PAH) and estrone sulfate ([^{3}H]ES) were purchased from PerkinElmer Life and Analytical Sciences (Waltham, MA). Unlabeled PAH, ES, and probenecid were obtained from Sigma-Aldrich (St. Louis, MO).

4.B.2 Tissue culture

The derivation of stably transfected Chinese hamster ovary (CHO) cells expressing hOAT1, human embryonic kidney 293 (HEK) cells expressing hOAT3, and their corresponding empty vector transfected control cell lines, has been described previously (20, 29). The CHO and HEK cell lines were maintained at 37°C with 5% CO_2 in DMEM F-12 or DMEM high glucose media (Mediatech, Inc., Herndon, VA) containing 10% serum, 1% Pen/Strep and either 1 mg/mL G418 (CHO cell lines) or 125 µg/ml hygromycin B (HEK cell lines), respectively.

4.B.3 Cell accumulation assays

Accumulation assay protocols were adapted from those previously published (82, 109). In brief, cells were seeded in 24-well tissue culture plates (2×10^5 cells/well) and grown in the absence of antibiotics for two days prior to uptake assays. Before initiation of transport experiments, the cells were equilibrated with 500 µL of transport buffer [Hanks' balanced salt solution containing 10 mM HEPES (Sigma-Aldrich, St. Louis, MO), pH 7.4] for 10 min. The equilibration buffer was replaced with 500 µL of fresh transport buffer containing 1 µM [^{3}H]PAH or 1 µM [^{3}H]ES (0.25 µCi/mL) in the presence or absence of inhibitors as indicated in the figure legends. Substrate concentration and accumulation time used for kinetic analysis of

hOAT1 (1 µM PAH for 3 min, K_m = 15.4 µM) were based upon previous determinations in this cell line (130) and those for hOAT3 were determined in this study. After incubation for the indicated time, cells were immediately rinsed three times with ice-cold transport buffer, lysed with 1 M NaOH, and neutralized with 1 M HCl and 0.1 M HEPEs. Aliquots were removed for liquid scintillation counting and total protein determination using a Bio-Rad Protein Assay Kit (Bio-Rad Laboratories, Hercules, CA). Substrate accumulation was calculated as picomoles of substrate per milligram of protein. Michaelis constant (K_m) and inhibition constants (K_i) were determined using nonlinear regression with the appropriate models in GraphPad Prism Software version 5.0 (GraphPad Software Inc., San Diego, CA). Mode of inhibition was identified by using mixed-model inhibition analysis as described in our previous work (49)**.** The mode of inhibition was determined by the parameter α. Large value of α (α > 1) indicates competitive inhibition. Results were confirmed by performing experiments at least three times with triplicate samples.

4.B.4 Statistics

Statistical analysis was done with one-way ANOVA followed by post-hoc analysis with Dunnett's t-test or using Student's two-tailed unpaired t-test (α for significance set at 0.05). Data are reported as mean ± S.D. or mean ± S.E.M., as indicated.

4.C RESULTS

4.C.1 Inhibitory effects of hydrophilic Danshen components on hOAT1 and hOAT3 function

The stably transfected hOAT1-expressing (CHO-hOAT1) cell line exhibited marked (~5x) accumulation of PAH relative to empty vector-transfected CHO-ev (background) cells (Figure 4.2A). CHO (background) cells exhibited a probenecid-insensitive background for PAH that was equal to ~20% of the total accumulation obtained in transporter expressing cells (CHO-ev (background): 0.93 ± 0.19 pmol/mg protein/10 min vs. CHO-hOAT1 (control): 4.39 ± 0.20 pmol/mg protein/10 min). This non-specific PAH signal was not significantly influenced by addition of the Danshen compounds (1 mM), indicating that the reduction in substrate accumulation in CHO-hOAT1 cells is attributable to inhibition of hOAT1 activity and this value represents an appropriate background correction factor (data not shown). Rudimentary assessment of the ability of the three Danshen components (1 mM), LSA, RMA, and SAA, to inhibit hOAT1 revealed that, similar to the OAT inhibitor probenecid, each of the compounds significantly inhibited (> 83%) PAH uptake in CHO-hOAT1 cells ($p < 0.001$) under these conditions (Figure 4.2A).

ES accumulation in hOAT3-expressing (HEK-hOAT3) cells was significantly greater of (~4-fold) than that observed in empty vector-transfected HEK-ev (background) cells (HEK-ev: 2.46 ± 0.80 pmol/mg protein/10 min vs. HEK-hOAT3: 9.55 ± 1.41 pmol/mg protein/10 min, Figure 4.2B). As with hOAT1, hOAT3-mediated uptake was significantly ($p < 0.001$) inhibited by each Danshen component (> 98% inhibition at 1 mM; Figure 4.2B). LSA, RMA, and SAA (1 mM) failed to significantly influence non-specific uptake of ES in HEK-ev (background) cells (data not shown). Thus, illustrating that hOAT3 expression correlates with ES accumulation and that HEK-ev ES level can be used for background correction.

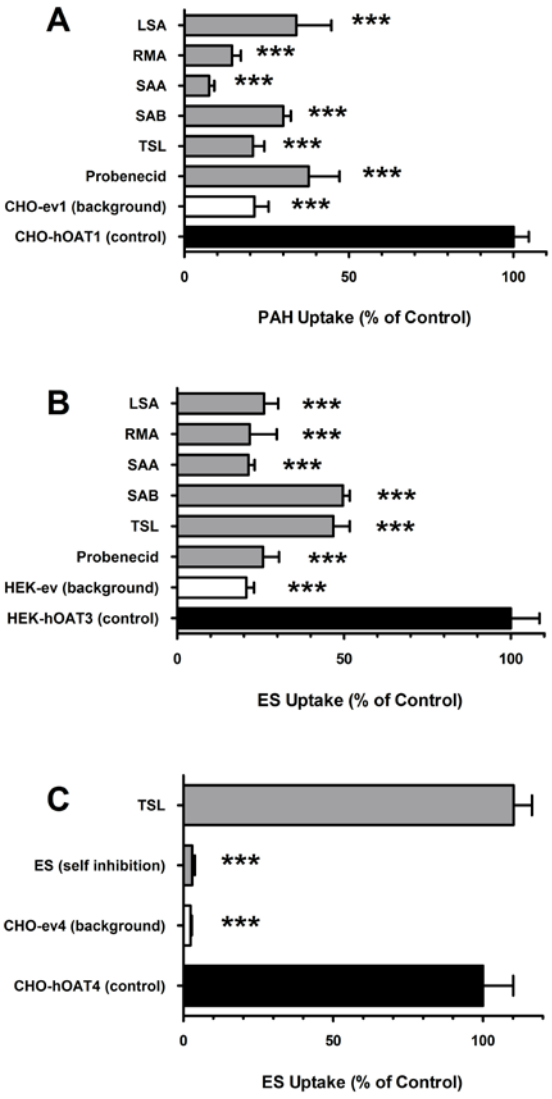

Figure 4.2. Inhibition of hOAT1- and hOAT3-mediated transport by Danshen components

A: Inhibition of hOAT1-mediated uptake of [^{3}H]PAH (1 µM) by LSA, RMA, SAA, and probenecid (1000 µM) was measured in the CHO-hOAT1 cell line (10 min). B: Inhibition of hOAT3-mediated uptake of [^{3}H]ES (1 µM) by LSA, RMA, SAA, and probenecid (1000 µM) was measured in the HEK-hOAT3 cells (10 min). Background PAH and ES accumulation was measured in the respective empty vector transfected control cell lines and is included to provide a clear gauge of the background in the experimental system. Graphs shown are from representative experiments with values plotted as mean ± S.D. of triplicate values. Black bars: substrate accumulation in the absence of inhibitor in transporter expressing cells, open bars: substrate accumulation in mock transfected cells, grey bars: substrate accumulation in the presence of inhibitors in transporter expressing cells; *** denotes $p < 0.001$ as determined by one-way ANOVA followed by Dunnett's t-test.

4.C.2 Mode of inhibition

In order to calculate the more universal kinetic parameter, K_i, studies were conducted to determine the mechanism of inhibition of hOAT1 and hOAT3 by LSA, RMA, and SAA. Substrate concentration and accumulation time used for kinetic analysis of hOAT1 (1 µM PAH for 3 min, K_m = 15.4 µM) were based upon previous determinations in this cell line (130). For HEK-hOAT3 cells, ES accumulation was linear through at least the first minute and K_m was estimated as 14.5 ± 4.5 µM (data not shown and Figure 4.3). These parameters were then used to design saturation analysis experiments for hOAT1 and hOAT3 in the absence vs. presence of two different concentrations of LSA, RMA, or SAA. Substrate uptake under these conditions was determined, background corrected, and fit to the mixed-model inhibition, which incorporates competitive, non-competitive, and uncompetitive inhibition modes. Estimated α values were much greater than 1, indicating that LSA, RMA, and SAA inhibition of hOAT1- and hOAT3-mediated transport was competitive in nature (Table 4.1).

4.C.3 Determination of inhibition potencies of LSA, RMA, and SAA for hOAT1 and hOAT3

Using increasing concentrations of unlabeled test compounds (10^{-9} to 2×10^{-4} M), inhibition of hOAT1- and hOAT3-mediated transport of ([^{3}H]PAH) or ([^{3}H]ES), respectively, was measured (Figures 4.4 and 4.5 and Table 4.2). As indicated above, LSA, RMA, and SAA were determined to be competitive inhibitors of hOAT1 and hOAT3, thus K_i, rather than IC_{50} values, could be calculated by selecting competitive inhibition during analysis. K_i values were estimated as 20.8 ± 2.1 µM for LSA, 0.35 ± 0.06 µM for RMA, and 5.58 ± 0.29 µM for SAA on hOAT1-mediated transport and as 0.59 ± 0.26 µM for LSA, 0.55 ± 0.25 µM for RMA, and 0.16 ± 0.03 µM for SAA on hOAT3-mediated transport. For all of these analyses the coefficient of determination (r^2) was > 0.9. The K_i values for LSA and SAA on hOAT3 were ~1-2 orders of

magnitude lower than those for hOAT1 ($p < 0.001$, K_i ratio = 35 for each), whereas the K_i for RMA was similar between the two transporters (Table 4.2).

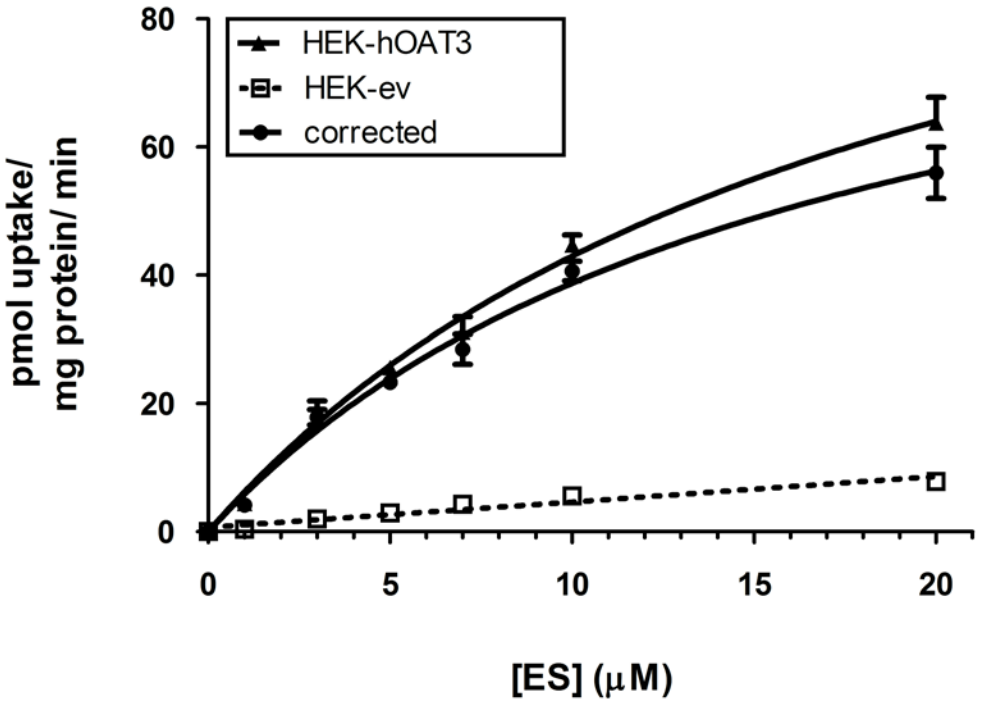

Figure 4.3. Michaelis-Menten kinetics of ES transport in HEK-hOAT3 cells

Uptake of [^{3}H]ES was measured for 1 min at room temperature in HEK-hOAT3 cells (closed triangles) and HEK-ev (background) cells (open squares) across increasing ES concentrations. The background corrected curve (closed circles) was obtained by subtracting the non-specific background uptake as measured in the HEK-ev cells from HEK-hOAT3 accumulation to allow analysis of hOAT3-mediated activity. Experiments were repeated three times in triplicate and Michaelis constant (K_m) values were calculated by nonlinear regression using the Michaelis-Menten model. The K_m for ES on hOAT3 was estimated as 14.5 ± 4.5 μM (mean ± S.E.M.). Graph shown is from a representative experiment with values plotted as mean ± S.D. (n=3).

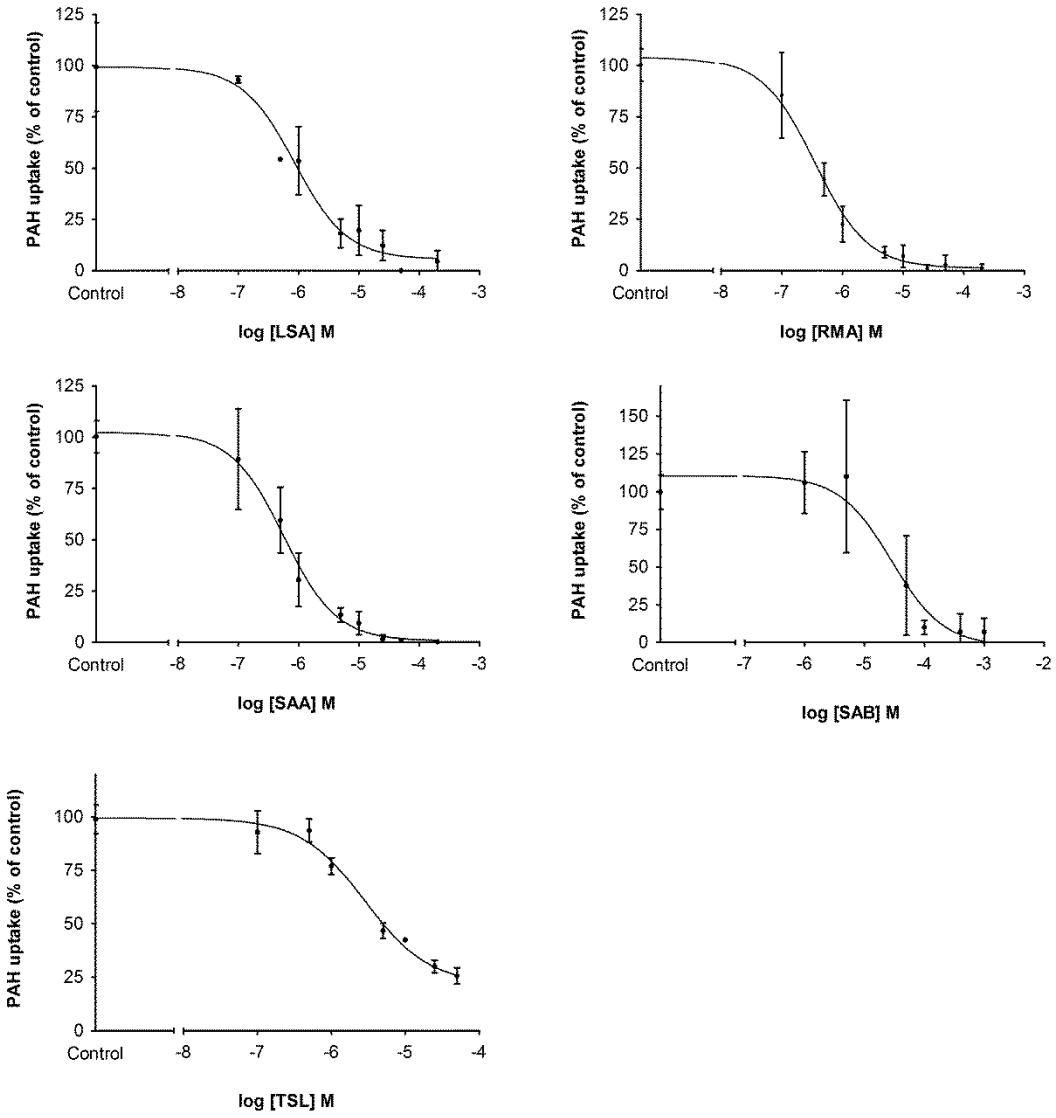

Figure 4.4. K_i determination for LSA, RMA, SAA, SAB, and TSL on hOAT1

One minute uptake of [^{3}H]PAH (1 µM) in CHO-hOAT1 cells was measured in the presence of increasing concentrations (10^{-7} to 2×10^{-3} M) of LSA, RMA, SAA, SAB, and TSL. Data were corrected for non-specific background measured in the CHO-ev1 (background) cells prior to kinetic analysis. K_i values were determined with non-linear regression and the "one-site competition" model using GraphPad Prism software. Experiments were repeated three times in triplicate with the mean K_i ± S.E.M. reported in Table 4.2. Graphs shown are from representative experiments with values plotted as mean ± S.D. (n=3).

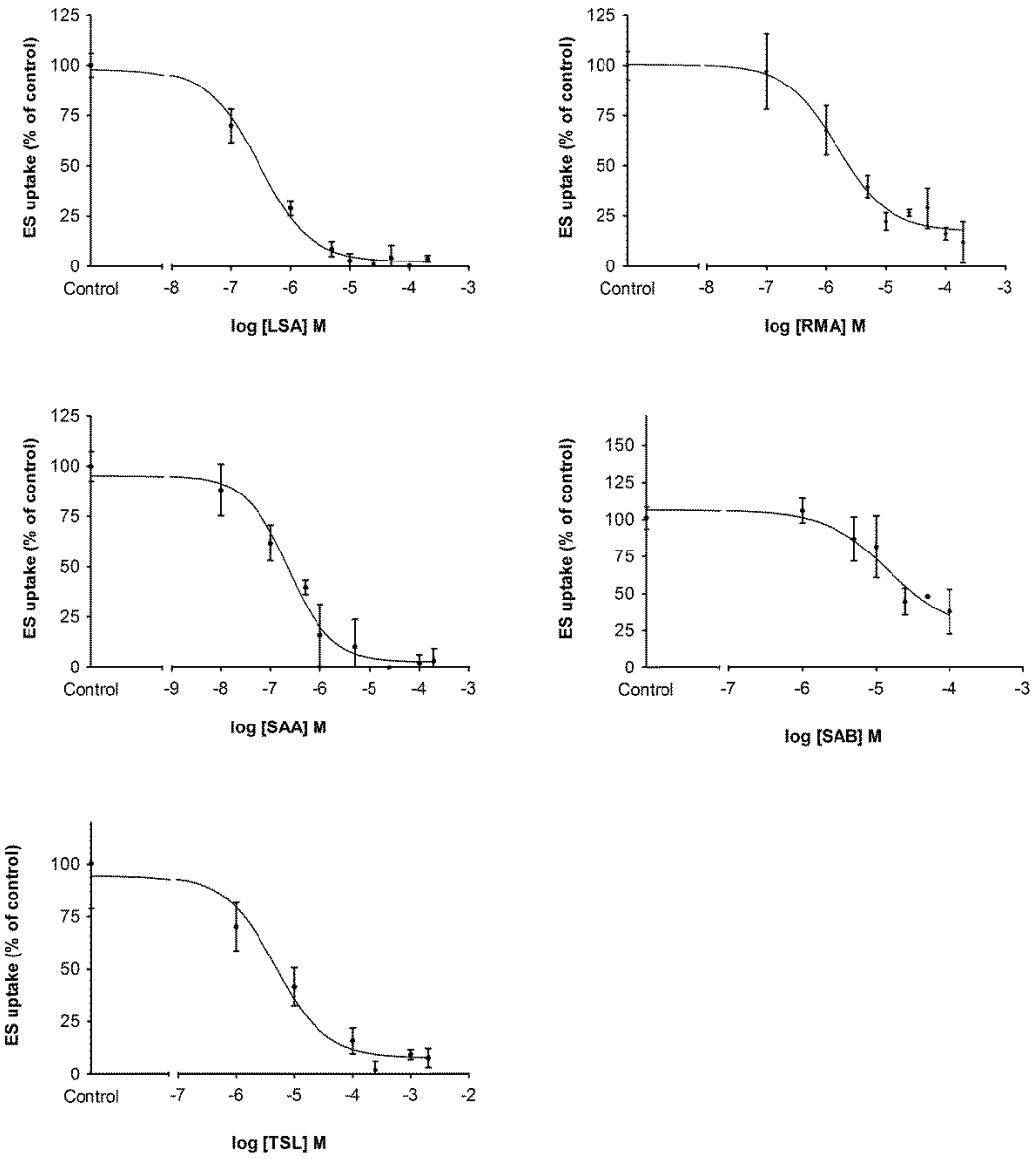

Figure 4.5. K_i determination for LSA, RMA, and SAA, SAB, and TSL on hOAT3

One minute uptake of [^{3}H]ES (1 µM) in HEK-hOAT3 cells was measured in the presence of increasing concentrations (10^{-8} to 2×10^{-3} M) of LSA, RMA, SAA, SAB, and TSL. Data were corrected for non-specific background measured in the HEK-ev (background) cells prior to kinetic analysis. K_i values were determined with non-linear regression and the "one-site competition" model using GraphPad Prism software. Experiments were repeated three times in triplicate with the mean K_i ± S.E.M. reported in Table 4.2. Graphs shown are from representative experiments with values plotted as mean ± S.D. (n=3).

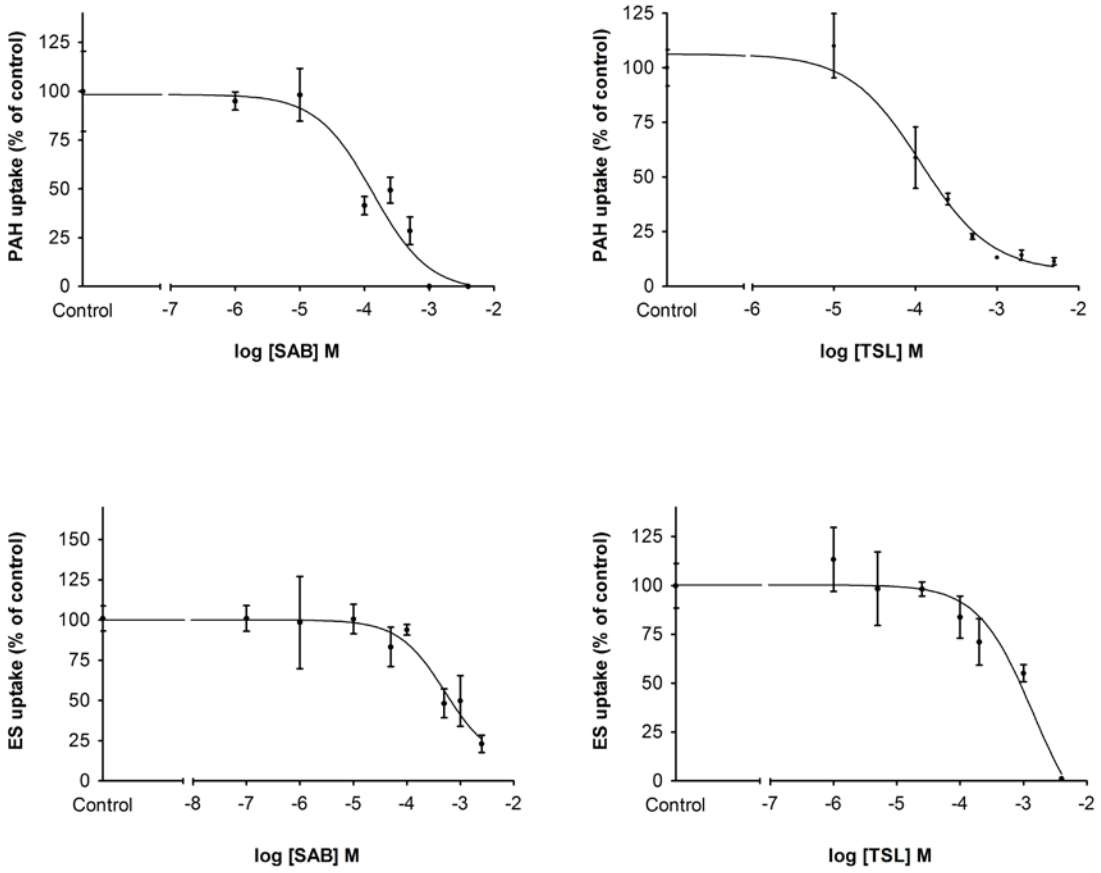

Figure 4.6. Dose-response curves for SAB and TSL with respect to mOat1 and mOat3

One minute uptake of [^{3}H]PAH or [^{3}H]ES (1 µM) in CHO-mOat1 (upper panels) or CHO-mOat3 (lower panels) cells was measured in the presence of increasing concentrations (10^{-7} to 5×10^{-3} M) of SAB and TSL. Data were corrected for non-specific background measured in the CHO-FRT (background) cells prior to kinetic analysis. IC_{50} values were determined with non-linear regression and the "log(inhibitor) *vs.* response" model using GraphPad Prism software. Experiments were repeated three times in triplicate with the mean IC_{50} ± S.E.M. reported in Table 4.3. Graphs shown are from representative experiments with values plotted as mean ± S.D. (n=3).

Table 4.1. Estimated α values from mixed-model inhibition analysis

Compound	hOAT1	hOAT3
LSA	1.5×10^{15}	9.6×10^{13}
RMA	2.1×10^{14}	3.2×10^{17}
SAA	3.1×10^{15}	4.2×10^{16}
SAB	6.8×10^{19}	8.2×10^{17}
TSL	8.8×10^{16}	3.5×10^{15}

Values are reported as mean. The S.E.M. is not applicable in this analysis.

Table 4.2. Estimated K_i values (µM) and DDI indices for hOAT1 and hOAT3

Compound	hOAT1	hOAT3	K_i Ratio (hOAT1/hOAT3)	f_u[a] (%)	DDI index[b] hOAT1	DDI index[b] hOAT3
LSA	20.8 ± 2.1	0.59 ± 0.26***	35	-[c]	0.01[d]	0.4[d]
RMA	0.35 ± 0.06	0.55 ± 0.25	0.6	9.5[e]	1.6	1.0
SAA	5.6 ± 0.3	0.16 ± 0.03***	35	-	-	-
SAB	22.2 ± 1.9	19.8 ± 8.4	1.1	6.8[e]	0.02	0.02
TSL	40.4 ± 12.9	8.6 ± 3.3	4.7	100[e]	0.5	2.1

Values are reported as mean ± S.E.M. (n=3). ***, significance of K_i values between hOAT1 and hOAT3 is $p < 0.001$ as determined by two-tailed Student's unpaired t-test. [a]f_u: Fraction unbound in plasma; [b]Clinical data taken from reference (104); [c]-: Unknown; [d]Assuming LSA is highly protein bound (f_u = 10%); [e] Fraction unbound in plasma from reference (137).

Table 4.3. Comparison of K_i values (μM) between mOat1 and mOat3 and their human orthologs

Compound	mOat1[a]	mOat3[a]	K_i Ratio (mOat1/hOAT1)	K_i Ratio (mOat3/hOAT3)
LSA	14.9 ± 4.9	31.1 ± 7.0	0.7	53*
RMA	5.5 ± 2.2	4.3 ± 0.2	16	7.8***
SAA	4.9 ± 2.2	21.3 ± 7.7	0.9	133
SAB	236 ± 90[b]	845 ± 287[b]	11	43*
TSL	136 ± 17[b]	1940 ± 486[b]	3.4*	226*

Values are reported as mean ± S.E.M. (n=3). * denotes significant difference between murine and human K_i values $p < 0.05$ and *** denotes significant difference between murine and human K_i values $p < 0.001$ as determined by two-tailed Student's unpaired t-test. [a]Data for LSA, RMA and SAA were taken from reference (49). [b]Corresponding K_i values assuming competitive inhibition (see text for explanation).

4.D DISCUSSION

The popularity of natural products as dietary supplements and/or alternative medicines has been increasing. Indeed, a recent survey found that ~20% of the adult population in the United States reported using one or more natural products (112). Because herbal medicines are produced from plants they are considered "natural" and, therefore, are often perceived as having no toxic effects by patients. However, many different side effects/adverse events are known to be associated with natural products, including herb-drug interactions (131, 132). A number of herb-drug interactions involving metabolic enzymes (*e.g.*, CYP450's) are well established, however, herb-drug interactions at the level of transporter proteins are not as well characterized.

Despite this, there is a growing literature base concerning the interaction of natural products with OATs. For example, the dietary polyphenol, ellagic acid, was found to potently inhibit hOAT1 (IC_{50} = 207 nM) and hOAT4 (48). The aglycone of the natural sweetener, stevioside, was identified as an inhibitor of both hOAT1 (K_i = 2.0 μM) and hOAT3 (K_i = 5.4 μM) (133). Similarly, dietary flavonoid and hydroxycinnamic acid aglycones, as well as their Phase II glucuronide and sulfate conjugates, produced pronounced inhibition of hOAT1- and hOAT3-mediated transport (50, 119). Finally, the nephrotoxin, aristolochic acid, the causative agent for "Chinese herbs nephropathy" which is found in herbal products containing *Aristolochia sp.*, exhibited significant interaction with hOAT1 (K_i = 600 nM), hOAT3 (K_i = 500 nM), and hOAT4 (K_i = 20.6 μM) (39). Thus, herb-drug interactions involving OATs and components of natural products, that impact the pharmacokinetics and pharmacodynamics of administered drugs, may occur.

In the present study, we sought to determine the inhibitory effects of three major Danshen components, LSA, RMA, and SAA on hOAT1- and hOAT3-mediated transport (Figures 4.2, 4.4,

and 4.5). In order to calculate K_i values on hOAT3, the K_m value for ES (test substrate) needed to be determined in the HEK-hOAT3 cell system (Figure 4.3). Saturation analysis revealed an estimated K_m of 14.5 ± 4.5 μM, which is similar to other reported values of 6.3-9.5 μM (98, 134, 135). LSA, RMA, and SAA were found to be potent competitive inhibitors of hOAT1- and hOAT3-mediated transport (Figures 4.4 and 4.5 and Tables 4.1 and 4.2). Their calculated K_i values are similar to reported K_m and K_i values for endogenous steroid and prostaglandin hormones on hOAT1 and hOAT3 (3). Therefore, LSA, RMA, and SAA may affect the disposition and elimination of not only co-administered drugs, but also of endogenous substances that are OAT substrates. The rank order of their potencies was different between the two transporters with RMA > SAA > LSA for hOAT1 and SAA > LSA ≈ RMA for hOAT3. Regardless, LSA and SAA exhibited significantly higher affinity (lower K_i values) for hOAT3 than for hOAT1, with each compound showing a ~35-fold preference, whereas, RMA exhibited similar affinity for both transporters (Table 4.2).

In the draft guidance for industry, "Drug Interaction Studies — Study Design, Data Analysis, Implications for Dosing, and Labeling Recommendations", re-issued by the Food and Drug Administration in February 2012, it was proposed that a DDI index, indicative of a compound's potential to cause marked *in vivo* drug-drug interactions when its value exceeds 0.1, can be calculated as the [unbound] C_{max}/K_i (or IC_{50}) ratio (136). In 2005, an *in vivo* pilot study conducted in healthy humans reported C_{max} values for LSA and RMA of 2.23 μM and 5.55 μM after *i.v.* administration of a Danshen product, in which the dose of LSA and RMA were 3 and 160 mg, respectively (104). Further, Yang *et al.* (2007) determined that, for RMA, the fraction unbound in plasma was 9.5% (137). Thus, using the published C_{max} and plasma protein binding values for RMA, as well as the K_i values determined in this study (Table 4.2), DDI indices of 1.6

and 1.0 were calculated for hOAT1 and hOAT3, respectively, indicating a strong potential for clinical herb-drug interactions. In the absence of plasma protein binding data for LSA, DDI indices for hOAT1 (0.01) and hOAT3 (0.4) were calculated assuming LSA to be highly (90%) protein bound (Table 4.2). Under such circumstances, the DDI index for hOAT3 would be greater than 0.1. The pharmacokinetic profile of SAA is virtually unknown. Clearly, greater understanding of the pharmacokinetic properties of LSA, RMA, and SAA, and the transporters that help determine them, is necessary to avoid potential herb-drug interactions. For Danshen pharmaceutical products this would be particularly relevant in coronary patients, where they may be taken in combination with drugs, such as angiotensin converting enzyme inhibitors, which are known to be hOAT1/hOAT3 substrates.

Additionally, there is marked variation in the amount of each active component in plant cultivated in different regions and in Danshen products prepared by different manufacturing processes (103, 104, 138). For example, the content of RMA in raw plant material varied as much as 16 fold between different cultivation regions and the dose of RMA ranged from 4.1-160 mg (~40 fold) in Danshen injectables produced by different manufacturers (103, 104). Moreover, the dose of RMA ranged from 1.16-3.47 mg from different batches of a Danshen injectable from the same pharmaceutical manufacturer (138). These data illustrate that clinically significant herb-drug interactions would or would not occur depending upon which manufacturer's product was administered and/or the diligence of the quality control protocol utilized by a single manufacturer. Therefore, although tanshinone II A, SAB, and protocatechuic aldehyde have been chosen as quality control markers for Danshen pharmaceutical dosage forms in accordance with the Chinese Pharmacopeia, our data suggest that the content of other Danshen components, *e.g.*, LSA and RMA, should be considered for monitoring and control as well.

Recently, we investigated the interaction between mOat1 and mOat3 and Danshen's hydrophilic components (49). As for the human orthologs, the rank order of potencies was slightly different between the two transporters with RMA≈ SAA > LSA for mOat1 and RMA > SAA ≈ LSA for mOat3. On comparing the mouse and human data, notable species differences appear to exist in terms of inhibitory potency (Table 4.3). Human OAT1 exhibited ~16-fold higher affinity for RMA as compared to mOat1, while LSA and SAA showed similar inhibition potencies across species. In contrast, all three compounds exhibited much higher affinity for hOAT3 over mOat3, by 1 order of magnitude for RMA and by ~2 orders of magnitude for LSA and SAA. Interestingly, for LSA and SAA the two species are reversed, with hOAT3 having higher affinity for both over hOAT1 vs. mOat1 having higher affinity for both over mOat3 (Tables 4.2 and 4.3). While the human orthologs had ~10 fold lower K_i values for RMA than the murine transporters, within species the values were similar for each transporter. These species differences indicate that any interactions observed *in vivo* in mice at clinically relevant doses of LSA, RMA, and SAA would potentially be of even greater magnitude in humans. This highlights the importance of delineating species differences in affinity *in vitro* prior to interpreting results from *in vivo* pharmacokinetic studies in pre-clinical models and attempting to extrapolate them to humans.

As discussed earlier, additional Danshen components also might show significant inhibitory effects on OATs. For example, caffeic acid was demonstrated to be an OAT inhibitor, with reported IC_{50} values of 16.6 µM for hOAT1 and 5.4 µM for hOAT3 (51). However, because of low plasma concentration (0.56 µM) and modest plasma protein binding (66%), the calculated DDI index is less than 0.1, indicating caffeic acid was not likely to cause significant OAT inhibition at clinically relevant concentrations (104, 139). Protocatechuic acid and some

hydroxycinnamates (major metabolites of chlorogenic acids) were also identified as inhibitors of hOAT1 and hOAT3 (52). However, again, the extremely low content in Danshen products renders them unlikely to contribute to OAT-mediated Danshen-drug interactions *in vivo*.

In summary, the active Danshen components, LSA, RMA, and SAA were demonstrated to elicit significant competitive inhibition on hOAT1- and hOAT3-mediated substrate uptake at clinically relevant concentrations. DDI indices for RMA on hOAT1 and hOAT3, and for LSA on hOAT3, suggest a strong potential for drug-drug interactions in patients when coadministered with drugs that are known hOAT1 and/or hOAT3 substrates. In addition, notable species differences were observed between human and murine OAT orthologs with human OATs showing higher affinity. All of these Danshen components preferentially interacted with hOAT3 compared to mOat3, while only RMA showed higher affinity with hOAT1 (vs. mOat1). This information should improve interpretation and extrapolation of pharmacokinetic data generated in pre-clinical studies. Finally, these components might serve as effective quality control markers to be monitored during the manufacturing process to improve product consistency, efficacy, and safety.

CHAPTER 5

POTENTIAL FOR FOOD/DRUG-DRUG INTERACTIONS BY PHENOLIC ACIDS ON HUMAN ORGANIC ANION TRANSPORTERS 1 (SLC22A6), 3 (SLC22A8), AND 4 (SLC22A11)

Drawn from manuscript published in *Biochem Pharmacol.* Oct 2012; 84(8): 1088-1095

5.A INTRODUCTION

The term, phenolic acid, describes a large group of compounds that contain an aromatic ring bearing hydroxyl and carboxyl substituents (140). In plants, phenolic acids are synthesized from phenylalanine or tyrosine via the shikimate pathway and they are widely distributed in fruits, vegetables, and beverages (43). As phenolic acids have been reported to possess anti-oxidant, anti-carcinogenic, and anti-inflammatory activities, they are believed to reduce the risk of developing chronic diseases, *e.g.*, diabetes, cardiovascular disorders, and certain cancers (43, 140, 141). A number of phenolic acids showed marked systemic exposure *in vivo* after daily consumption of phenolic acid-rich food (141, 142).

Additionally, *in vivo* metabolism generates phenolic acids. For example, gentisic acid was identified as one of the major metabolites of salicylate, and urinary elimination of gentisic acid accounted for 0.4-1.7% of the total administered dose of salicylate drugs (143, 144). Another study indicated that ferulic and isoferulic acids may be metabolites of caffeic acid (145). Finally,

anthocyanins (ACNs) were recently identified as an important dietary source of phenolic acids. ACNs are flavonoids which are widely distributed in flowers, berries, grapes, red wine, and blood orange juice, producing blue and red color (146). Daily consumption of ACNs was estimated as 3-215 mg (146). Yet, it was reported in clinical studies that the bioavailability of ACNs was poor (146). However, *in vitro* studies demonstrated that phenolic acids represent major stable degradation products of ACNs, and this was confirmed in clinical studies (44, 147, 148). Thus, phenolic acids are commonly found in the systemic circulation even in individuals not actively taking phenolic acid containing dietary supplements or alternative medicines.

Several transporter families are responsible for the systemic disposition of organic acids. Among these, the Solute Carrier 22 (SLC22; organic cation/anion/zwitterion transporters) family is a key mediator in the distribution and renal tubular secretion of a multitude of endogenous and exogenous organic anions (2, 3). Many toxins, toxicants, and drugs (including antibiotics, antiviral and anticancer agents) are known organic anion transporter (OAT) substrates (2, 3). Further, some phenolic acids, *e.g.*, tanshinol, rosmarinic acid, and salvianolic acid B, exhibit their highest tissue concentration in the kidney compared to other tissues, *e.g.*, liver, intestine, and brain, after dosing (116, 149). In accordance, the kidney is known to express more OAT family members than any other tissue (3). In particular, human organic anion transporter 1 (hOAT1; SLC22A6), hOAT2 (SLC22A7), and hOAT3 (SLC22A8), expressed in the basolateral membrane of renal proximal tubule cells, and hOAT4 (SLC22A11), hURAT1 (SLC22A12), and hOAT10 (SLC22A13) located in the apical membrane, are major constituents of the renal organic anion transport pathway.

OAT-mediated drug-drug interactions (DDIs), manifesting as altered renal clearance and longer terminal plasma half-life, have been observed in a number of clinical and pre-clinical

studies. For example, renal clearance of benzylpenicillin and ciprofloxacin was reduced when co-administered with probenecid, a known OAT inhibitor, in clinical practice (77, 129). In accord with these clinical findings, pharmacokinetic studies using organic anion transporter 3 knockout mice demonstrated significantly reduced renal elimination of benzylpenicillin, ciprofloxacin, and methotrexate (80, 81). In response to our increased knowledge of such clinically relevant drug-transporter interactions, and the impact they have on drug safety, the United States Food and Drug Administration (FDA) and the European Medicines Agency have issued guidance documents outlining conditions under which, prior to approval, any new drug entity should be investigated for potential DDIs on seven identified transporters; OAT1, OAT3, organic cation transporter 2 (OCT2), organic anion transporting polypeptide 1B1 (OATP1B1), OATP1B3, multidrug resistance transporter 1 (MDR1), and breast cancer resistance protein (BCRP) (http://www.fda.gov/downloads/Drugs/GuidanceComplianceRegulatoryInformation/Guidances/UCM292362.pdf

and http://www.ema.europa.eu/ema/index.jsp?curl=pages/includes/document/document_detail.jsp?webContentId=WC500090112&murl=menus/document_library/document_library.jsp&mid=WC0b01ac058009a3dc&jsenabled=true). Thus, the potential clinical significance of OAT1- and OAT3-mediated DDIs is already clearly recognized.

As most phenolic acids are small and mainly exist as anions at physiological pH, it is possible that they are OAT substrates or inhibitors. For example, some hydroxycinnamic acids, including caffeic acid, dihydrocaffeic acid, dihydroferulic acid, and ferulic acid were identified as hOAT1 and/or hOAT3 substrates (50). This study further demonstrated that these compounds, as well as their glucuronide- and sulfate-conjugated metabolites, inhibited hOAT1 or hOAT3 transport activity (50). Caffeic acid was identified as a competitive inhibitor for hOAT1 and

hOAT3, with IC_{50} estimates of 16.6 µM and 5.4 µM, respectively (51). As a consequence, hOAT1/hOAT3-mediated transport of antifolates and antivirals was inhibited by caffeic acid (51). Finally, ellagic acid, which is a dietary polyphenol found in many fruits and vegetables, was demonstrated to be a potent inhibitor for hOAT1 (IC_{50} = 207 nM) and hOAT4 (48). Therefore, it is necessary to explore the potential interaction of phenolic acids with OATs, in order to determine what transport processes influence the distribution and elimination (and hence efficacy and toxicity) of these compounds. This information is also vital to avoid potential drug/food-drug interactions.

In the present study, the inhibitory effects of nine dietary phenolic acids, *p*-coumaric acid, ferulic acid, gallic acid, gentisic acid, 4-hydroxybenzoic acid, protocatechuic acid, sinapinic acid, syringic acid, and vanillic acid, on the transport of *para*-aminohippuric acid (PAH) mediated by hOAT1 and the transport of estrone sulfate (ES) mediated by hOAT3 and hOAT4 were characterized. For potent inhibitors, dose-response studies were conducted in order to derive inhibitory constants (IC_{50} and K_i values) to aid evaluation of potential for clinical DDIs. Among these phenolic acids, gallic acid exhibited highest affinity for hOAT1 and hOAT3, with corresponding maximum DDI indices (unbound maximum plasma concentration/IC_{50}) of 5.52 and 0.76, respectively. Gentisic acid exhibited a marked DDI index of 7.25 for hOAT3 (assuming 90% binding to plasma protein). These findings suggested there is a strong potential for gallic acid- and gentisic acid-associated food/drug-drug interactions with co-administered clinical therapeutics that are OAT substrates, including altered drug pharmacokinetics, pharmacodynamics, and toxicity.

5.B MATERIALS AND METHODS

5.B.1 Chemicals

p-Coumaric acid, ferulic acid, gallic acid, gentisic acid, 4-hydroxybenzoic acid, sinapinic acid, and vanillic acid (≥97% purity) were purchased from Sigma-Aldrich (St. Louis, MO). Protocatechuic acid and syringic acid (≥95% purity) were obtained from Santa Cruz Biotechnology, Inc. (Santa Cruz, CA). The chemical structures for these compounds are shown in Figure 5.1. Tritiated *para*-aminohippuric acid ([^{3}H]PAH) and estrone sulfate ([^{3}H]ES) were purchased from PerkinElmer Life and Analytical Sciences (Waltham, MA) and unlabeled PAH, ES, and probenecid were purchased from Sigma-Aldrich.

5.B.2 Tissue culture

Derivation of stably transfected Chinese hamster ovary (CHO) cells expressing hOAT1 (CHO-hOAT1) and hOAT4 (CHO-hOAT4), as well as stably transfected human embryonic kidney 293 (HEK) cells expressing hOAT3 (HEK-hOAT3), and their corresponding empty vector transfected background control cell lines, has been described previously (82, 130, 150). CHO-hOAT1 cells were maintained at 37°C with 5% CO_2 in phenol red-free RPMI 1640 media (Gibco-Invitrogen, Grand Island, NY) containing 10% serum, 1% Pen/Strep and 1 mg/mL G418. CHO-hOAT4 cells were maintained at 37°C with 5% CO_2 in EMEM Alpha Modification media (Sigma-Aldrich) containing 10% serum, 1% Pen/Strep and 0.5 mg/mL G418. HEK cell lines were maintained at 37°C with 5% CO_2 in DMEM high glucose media (Mediatech, Inc., Herndon, VA) containing 10% serum, 1% Pen/Strep and 125 µg/ml hygromycin B.

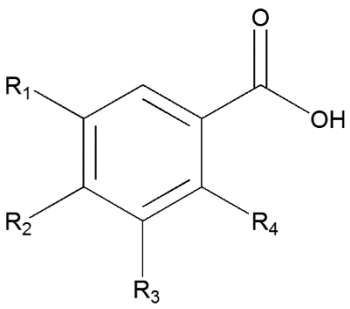

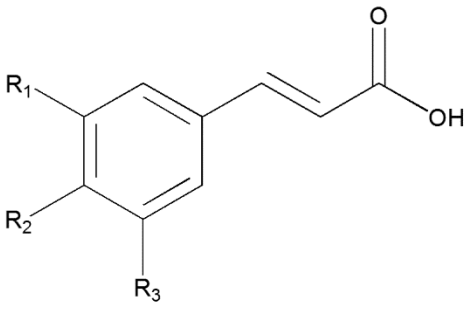

Compounds	R1	R2	R3	R4
Gallic acid	OH	OH	OH	H
Gentisic acid	OH	H	H	OH
4-Hydroxybenzoic acid	H	OH	H	H
Protocatechuic acid	OH	OH	H	H
Syringic acid	OCH_3	OH	OCH_3	H
Vanillic acid	OCH_3	OH	H	H

Compounds	R1	R2	R3
p-Coumaric acid	H	OH	H
Ferulic acid	OCH_3	OH	H
Sinapinic acid	OCH_3	OH	OCH_3

Figure 5.1. Chemical structures of the nine dietary phenolic acids investigated in this study

5.B.3 Cell accumulation assay

The procedure for the cell accumulation assay was described in previous publications (82). In brief, 2×10^5 cells/well were seeded in 24-well tissue culture plates and grown in the absence of antibiotics for 48 hr. Before initiating the cell transport experiment, cells were preincubated in transport buffer for 10 min [500 µL of Hanks' balanced salt solution containing 10 mM HEPES, pH 7.4]. After equilibration, this solution was replaced with 500 µL of fresh transport buffer containing 1 µM non-radiolabeled substrates spiked with trace amounts of [^{3}H]PAH (0.5 µCi/mL) or [^{3}H]ES (0.25 µCi/mL) with or without test compounds. At the end of incubation, cells were quickly rinsed three times with ice-cold transport buffer and lysed. The intracellular accumulation of tritiated substrates was counted by liquid scintillation and reported as picomoles of substrate per milligram total protein. All uptake data were corrected for background accumulation in corresponding control cells. Exposure to as high as 1 mM of each phenolic acid did not significantly influence the non-specific substrate signal observed in CHO empty vector control cells or HEK empty vector control cells, as compared to unexposed cells (data not shown). Therefore, substrate accumulation in corresponding empty vector control cell lines under control conditions represents appropriate values for background correction. Substrate concentrations and accumulation times used for kinetic analysis of hOAT1 (1 µM PAH for 3 min, K_m = 15.4 µM) were determined previously (130) and for kinetic analysis of hOAT3 (ES for 1 min, K_m = 14.5 ± 4.5 µM) were measured in our laboratory (data not shown). Kinetic calculations were performed using GraphPad Prism Software version 5.0 (GraphPad Software Inc., San Diego, CA). The half maximal inhibitory concentrations (IC_{50}) were calculated using nonlinear regression with the appropriate model. Assuming competitive inhibition, K_i values were derived using the Cheng-Prusoff equation: $K_i = IC_{50}/(1 + [\text{Substrate}]/K_m)$. Results were

confirmed by repeating all experiments at least three times with triplicate wells for each data point in every experiment.

5.B.4 Statistics

Data are reported as mean ± S.D. or mean ± S.E.M. as indicated. Statistical differences were assessed using one-way ANOVA followed by post-hoc analysis with Dunnett's t-test ($\alpha = 0.05$).

5.C RESULTS

5.C.1 Inhibitory effects of phenolic acids on hOAT1-mediated PAH uptake.

CHO-hOAT1 cells showed significant accumulation of PAH (6.23 ± 0.89 pmol mg protein^{-1} 10 min^{-1}) compared to that in the empty vector transfected background control cells (2.34 ± 0.50 pmol mg protein^{-1} 10 min^{-1}), and this OAT1-mediated accumulation was inhibited by probenecid (Figure 5.2). The dietary phenolic acids, *p*-coumaric acid, ferulic acid, gallic acid, gentisic acid, 4-hydroxybenzoic acid, protocatechuic acid, sinapinic acid, syringic acid, and vanillic acid, were assessed for inhibitory effects on PAH uptake in CHO-hOAT1 cells at 100 µM (Figure 5.2). Protocatechuic acid and vanillic acid produced approximately 53% and 80% inhibition, whereas ferulic acid, gallic acid, and sinapinic acid completely blocked PAH accumulation (> 99% inhibition). *p*-Coumaric acid produced no effect, while gentisic acid, 4-hydroxybenzoic acid, and syringic acid actually stimulated uptake. Exposure to 100 µM of each phenolic acid had no effect on CHO-hOAT1 cell viability or integrity (data not shown).

Dose-response studies, applying increasing concentrations of test compounds (10^{-7} to 5×10^{-4} M), were performed to determine the IC_{50} values for gallic acid, protocatechuic acid, sinapinic acid, and vanillic acid in order to allow direct comparison of inhibition potencies of these compounds (Figure 5.3 and Table 5.1). The IC_{50} value for ferulic acid on hOAT1 has been reported as 9.01 µM (50). Gallic acid showed stronger affinity with hOAT1 (IC_{50}=1.24 ± 0.36 µM), compared to protocatechuic acid (IC_{50}=18.08 ± 2.59 µM), sinapinic acid (IC_{50}=11.02 ± 1.55 µM), and vanillic acid (7.65 ± 2.92 µM). Previous studies investigating the type of inhibition (competitive vs. uncompetitive vs. noncompetitive) produced on hOAT1 and hOAT3 for a variety of compounds have all determined the interaction to be competitive (51, 151). Therefore, assuming competitive inhibition, inhibition constants (K_i) were estimated as 1.08 ±

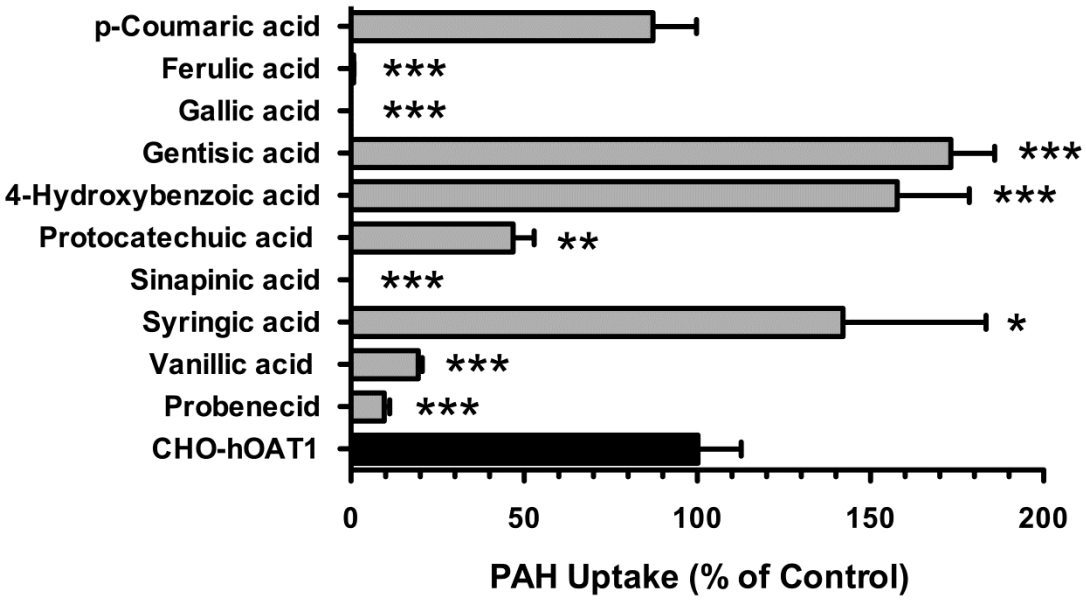

Figure 5.2. Inhibition of hOAT1-mediated uptake by dietary phenolic acids

Ten minute cellular uptake of [^{3}H]PAH (1 µM) was measured in CHO-hOAT1 cells in the absence (6.23 ± 0.89 pmol mg protein^{-1} 10 min^{-1}) and presence of dietary phenolic acids (100 µM) or probenecid (1,000 µM). All data were corrected by background PAH accumulation measured in corresponding empty vector transfected background control cell (2.34 ± 0.50 pmol mg protein^{-1} 10 min^{-1}). Values are mean ± S.D. of triplicate values. Significant inhibition denoted by ** $p <$ 0.01 and *** $p < 0.001$ as determined by one-way ANOVA followed by Dunnett's t-test.

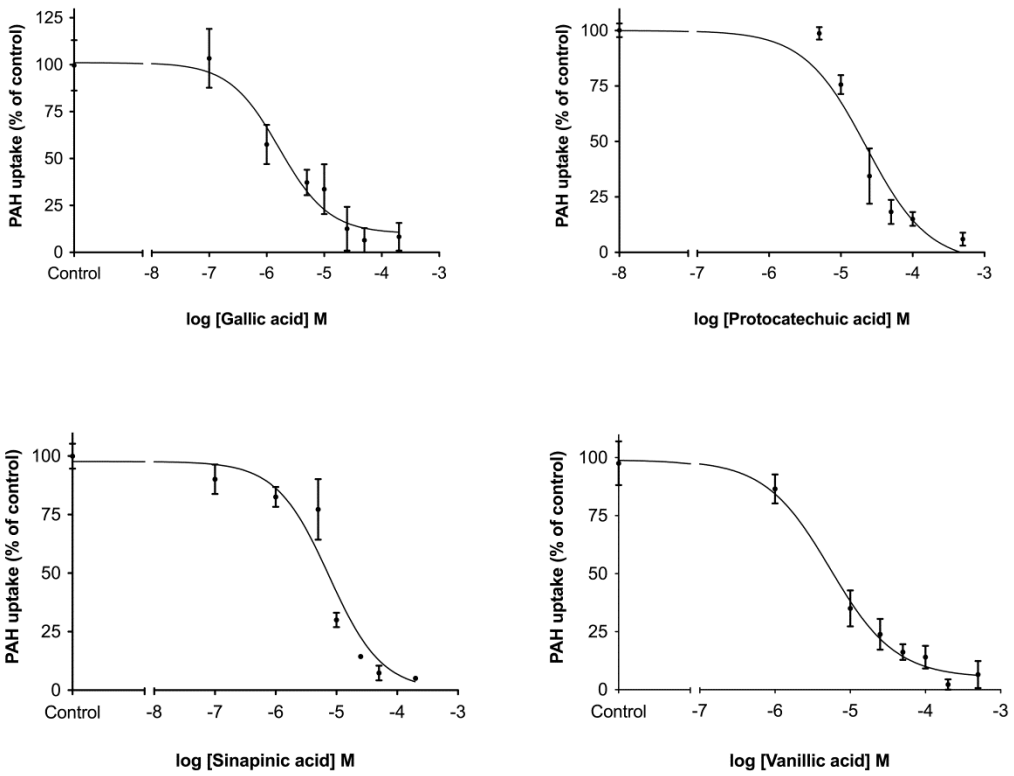

Figure 5.3. Dose-response curves for gallic acid, protocatechuic acid, sinapinic acid, and vanillic acid with respect to hOAT1

One minute uptake of [^{3}H]PAH (1 µM) in CHO-hOAT1 cells was measured in the presence of increasing concentrations (10^{-7} to 5×10^{-4} M) of test compounds. Data were corrected for non-specific background measured in the corresponding empty vector transfected background control cell. IC_{50} values were determined with nonlinear regression and the "log(inhibitor) vs. response" model using GraphPad Prism software. Experiments were repeated three times in triplicate with the mean IC_{50} ± S.E.M. reported in Table 5.1. Graphs shown are from representative experiments with values plotted as mean ± S.D. (n=3).

0.26 µM for gallic acid, 13.36 ± 1.60 µM for protocatechuic acid, 10.05 ± 1.74 µM for sinapinic acid, and 7.19 ± 2.74 µM for vanillic acid on hOAT1-mediated transport (Table 5.1).

5.C.2 Inhibitory effects of phenolic acids on hOAT3-mediated ES uptake.

We next examined the effects of these compounds on hOAT3-mediated transport. ES, a model substrate for hOAT3, was used to evaluate the transport activity of hOAT3 expressing cells. Significantly greater accumulation of ES (~5 fold) was observed in stably transfected hOAT3-expressing cells (HEK-hOAT3) relative to empty vector transfected background control cells (20.7 ± 3.5 vs. 4.10 ± 0.92 pmol mg protein^{-1} 10 min^{-1}, respectively). Similar to hOAT1, probenecid completely inhibited (> 99% inhibition) hOAT3-mediated ES uptake (Figure 5.4). However, unlike hOAT1, all of the tested compounds (100 µM) significantly inhibited hOAT3-mediated ES uptake. Gallic acid and sinapinic acid showed the strongest inhibitory effects on hOAT3-mediated ES uptake (> 84% inhibition), followed by ferulic acid (79% inhibition), gentisic acid (75% inhibition), and protocatechuic acid (61% inhibition). The inhibitory effects for the remaining compounds on hOAT3 transport activity were less than 60% (*p*-coumaric acid: 59% inhibition; 4-hydroxybenzoic acid: 38% inhibition; syringic acid: 46% inhibition; vanillic acid: 42% inhibition). Exposure to 100 µM of each phenolic acid had no effect on HEK-hOAT3 cell viability or integrity (data not shown).

Based on known plasma concentration levels, plasma protein binding, and the level of inhibition observed, kinetic studies were conducted to derive IC_{50} values for ferulic acid, gallic acid, gentisic acid, protocatechuic acid, and sinapinic acid on hOAT3 transport activity. Using increasing concentrations of unlabeled test compounds (10^{-6} to 10^{-3} M), IC_{50} values were measured as 7.35 ± 3.73 µM for ferulic acid, 9.02 ± 3.24 µM for gallic acid, 81.34 ± 20.50 µM for gentisic acid, 81.82 ± 26.82 µM for protocatechuic acid, and 24.08 ± 1.46 µM for sinapinic

acid (Figure 5.5 and Table 5.1). Estimated K_i values were calculated assuming that these compounds were competitive inhibitors (Table 5.1).

5.C.3. Inhibitory effects of hydrophilic Danshen components on hOAT4-mediated ES uptake.

As shown in Figure 5.6, stably transfected hOAT4-expressing (CHO-hOAT4) cells showed marked accumulation of ES (~13 fold) compared to empty vector transfected background control cells (64.1 ± 6.6 vs. 5.34 ± 0.36 pmol mg protein^{-1} 10 min^{-1}, respectively). ES (1 mM) exhibited self-inhibition on hOAT4-mediated ES uptake (> 99% inhibition). Among the test compounds, only sinapinic acid (100 µM) showed a significant inhibitory effect (33% inhibition). Accordingly, the IC_{50} value for sinapinic acid on hOAT4 transport activity is likely to be greater than 100 µM, therefore, no further kinetic studies were performed. As observed for hOAT1, but in contrast to hOAT3, syringic acid showed significant stimulation (35%) of hOAT4-mediated ES uptake.

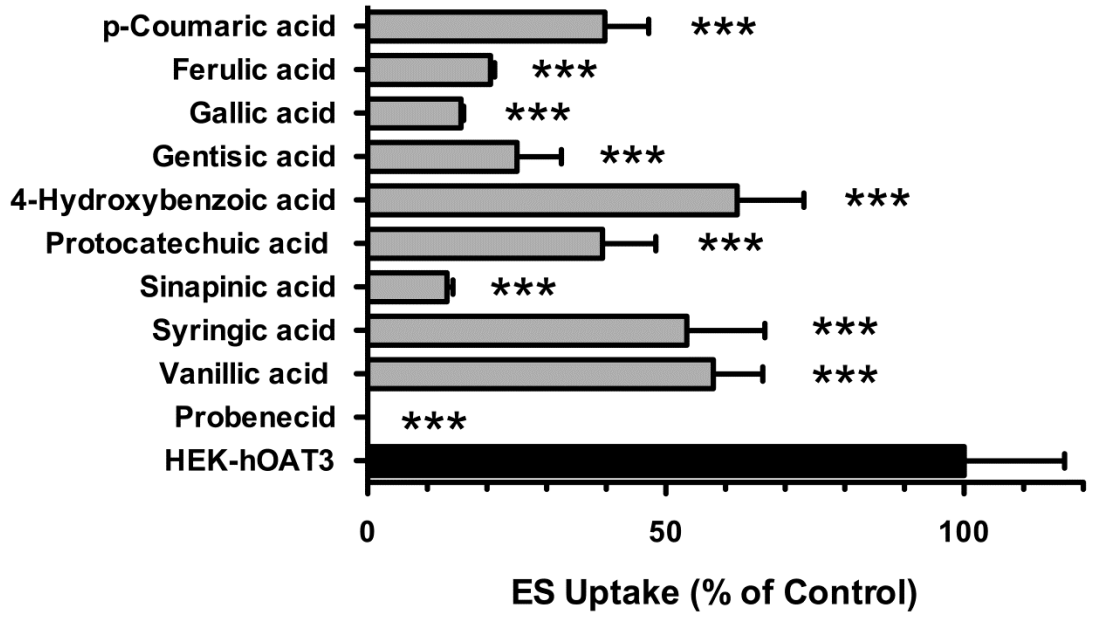

Figure 5.4. Inhibition of hOAT3-mediated uptake by dietary phenolic acids

Ten minute cellular uptake of [^{3}H]ES (1 µM) was measured in HEK-hOAT3 cells in the absence (20.7 ± 3.5 pmol mg protein^{-1} 10 min^{-1}) and presence of dietary phenolic acids (100 µM) or probenecid (1,000 µM). All data were corrected by background ES accumulation measured in HEK-FRT cells (4.10 ± 0.92 pmol mg protein^{-1} 10 min^{-1}). Values are mean ± S.D. of triplicate values. Significant inhibition denoted by *** $p < 0.001$ as determined by one-way ANOVA followed by Dunnett's t-test.

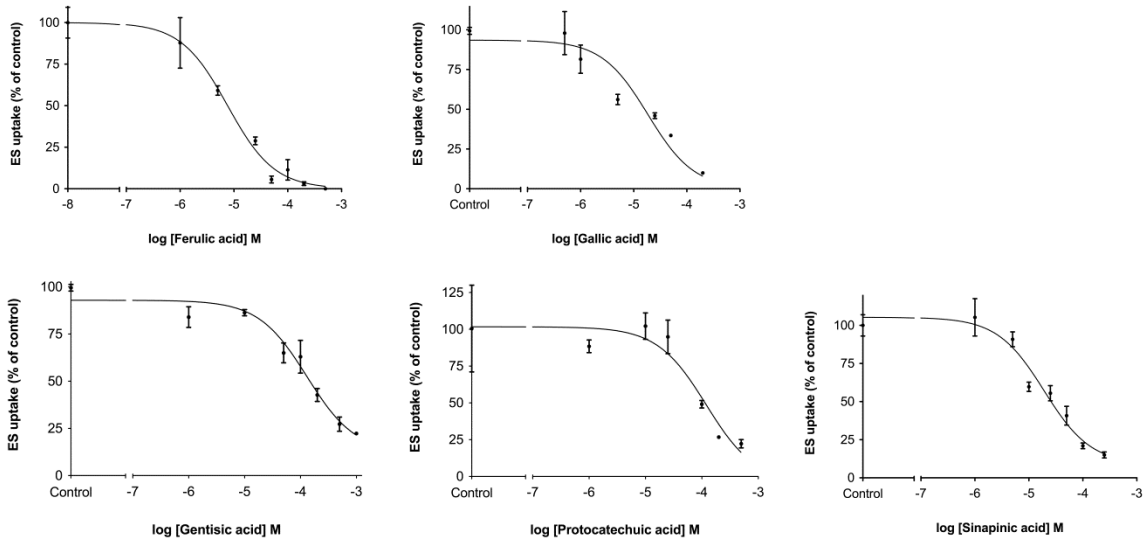

Figure 5.5. Dose-response curves for ferulic acid, gallic acid, gentisic acid, protocatechuic acid, and sinapinic acid, with respect to hOAT3

One minute uptake of [^{3}H]ES (1 µM) in HEK-hOAT3 cells was measured in the presence of increasing concentrations (10^{-6} to 10^{-3} M) of tested compounds. Data were corrected for non-specific background measured in the HEK-FRT cells. IC_{50} values were determined with non-linear regression and the "log(inhibitor) vs. response" model using GraphPad Prism software. Experiments were repeated three times in triplicate with the mean IC_{50} ± S.E.M. reported in Table 5.1. Graphs shown are from representative experiments with values plotted as mean ± S.D. (n=3).

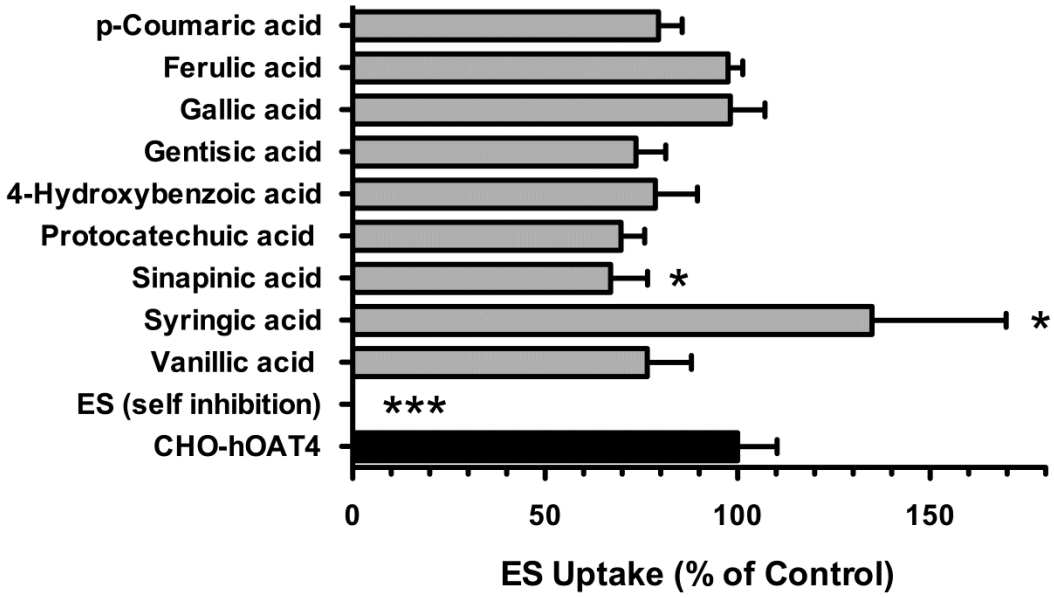

Figure 5.6. Inhibition of hOAT4-mediated uptake by dietary phenolic acids

Ten minute cellular uptake of [^{3}H]ES (1 µM) was measured in CHO-hOAT4 cells in the absence (64.1 ± 6.6 pmol mg protein^{-1} 10 min^{-1}) and presence of dietary phenolic acids (100 µM) or unlabeled ES (1,000 µM). All data were corrected by background ES accumulation measured in corresponding empty vector transfected background control cell (5.34 ± 0.36 pmol mg protein^{-1} 10 min^{-1}). Values are mean ± S.D. of triplicate values. Significant inhibition denoted by * $p <$ 0.05 as determined by one-way ANOVA followed by Dunnett's t-test.

Table 5.1. Estimated IC_{50} (μM), K_i (μM) and DDI index values for hOAT1- and hOAT3-mediated transport of dietary phenolic acids

Compounds	hOAT1		hOAT3		f_u [b] (%)	Reported C_{max} (μM)	DDI index		References (for f_u and C_{max})
	IC_{50} (μM)	K_i (μM)[a]	IC_{50} (μM)	K_i (μM)			hOAT1	hOAT3	
Ferulic acid	9.01[c]	ND[d]	7.35±3.73	6.87±3.49	26.5	0.012-1.04	0.0004-0.03	0.0004-0.04	(142, 152-154)
Gallic acid	1.24±0.36	1.08±0.26	9.02±3.24	8.44±3.03	68.4	0.22-10	0.12-5.52	0.02-0.76	(142, 154, 155)
Gentisic acid	ND	ND	86.81±21.78	81.34±20.50	?[e]	0.7-6,290	ND	0.0008-7.25	(156-159)
Protocatechuic acid	18.08±2.59	13.36±1.60	87.36±28.57	81.82±26.82	79.3	0.12-0.49	0.005-0.02	0.001-0.004	(148, 154, 156, 160, 161)
Sinapinic acid	11.02±1.55	10.05±1.74	25.74±1.56	24.08±1.46	?	?	?	?	
Vanillic acid	7.65±2.92	7.19±2.74	ND	ND	43.7	0.03-0.10	0.002-0.006	ND	(154, 156, 161)

Values are reported as mean ± S.E.M. [a] K_i values were estimated assuming competitive inhibition; [b] f_u: Fraction unbound in plasma; [c] Reported from (50); [d] ND: Not determined; [e] ?: unknown; [f] Assuming gentisic acid is highly protein bound (f_u = 10%)

5.D DISCUSSION

Phenolic acids have consistently displayed beneficial therapeutic effects for cardiovascular diseases, cancers, and chronic inflammation both *in vitro* and *in vivo* (160). In addition to 'natural' exposure to phenolic acids through dietary sources such as many fruits and vegetables, phenolic acids are increasingly used in clinical practice as complementary/alternative medicines (162). This has resulted in a greater understanding of the clinical pharmacokinetic properties of phenolic acids. However, to understand their pharmacological actions and pharmacokinetic behaviors at the biochemical level and, thus, better predict potential DDIs and/or toxicities, it is essential to identify and characterize the active transport mechanisms that impact these processes. Such information may explain how and why these compounds are targeted to specific organ(s) for therapeutic effects and elimination from the body.

In the present study, we characterized the interactions of nine phenolic acids with three human OATs; hOAT1, hOAT3, and hOAT4. All of the phenolic acids examined are bioavailable as indicated by plasma or urinary data. As illustrated, each transporter exhibited a unique pattern of interaction with the examined phenolic acids (Figures 5.2, 5.4, and 5.6). In general, all of the compounds produced an effect on hOAT1 and hOAT3, whereas, only two compounds showed interaction with hOAT4. All of the tested compounds exhibited significant inhibition for hOAT3 transport activity at 100 µM, while there were only five compounds (ferulic acid, gallic acid, protocatechuic acid, sinapinic acid, and vanillic acid) that significantly blocked hOAT1-mediated PAH uptake under the same condition. Sinapinic acid (100 µM) was the only phenolic acid showing significant inhibition of hOAT4-mediated ES uptake. However, given the modest nature of the interaction on hOAT4 at 100 µM, it was concluded that this was highly unlikely to be clinically relevant. Overall, these data implicated hOAT1 and hOAT3, but not hOAT4, as having

an important role in potential food/drug-drug interactions involving these phenolic acids. Whether or not these transporters handle these compounds as actual substrates requires further investigation.

Compounds reported to have relatively high C_{max} values in humans (except for sinapinic acid) and producing inhibition > ~60% at 100 µM on hOAT1 and/or hOAT3 were selected for IC_{50} (K_i) determination (Figures 5.3 and 5.5 and Table 5.1). Subsequently, C_{max}, % protein binding, and IC_{50} values were used to calculate the drug-drug interaction index [DDI = unbound C_{max} / IC_{50}] for each relevant transporter:compound combination (Table 5.1), where a value greater than 0.1 indicates the potential for drug-drug interactions and the need for an *in vivo* DDI study for any investigational drug (recommended by FDA Guidance for Drug Interaction Studies). Clearly, gallic acid (maximum DDI index of 5.52 and 0.76 for hOAT1 and hOAT3, respectively) and gentisic acid (maximum DDI index of 7.25 for hOAT3) have a very strong potential for producing DDIs *in vivo*.

Gallic acid has been demonstrated to have anti-oxidant, anti-inflammatory, anti-allergenic, and anti-cancer properties (162). Currently, gallic acid is consumed as a major component in fruits, vegetables, beverages, herbal supplements, homeopathic remedies, and pharmaceutical products (162, 163). Pharmacokinetic studies have reported maximum plasma concentrations for gallic acid ranging from 0.22-10 µM in humans after drinking red wine (300 mL) or after oral administration of acidum gallicum tablets (50 mg GA), Assam black tea brews (50 mg GA), or a dietary herbal supplement (800 mg GA) (142, 155). Since the renal clearance of gallic acid was ~8.4 L/h, the unbound renal clearance of gallic acid was estimated as 206 mL/min, which is 1.7 fold higher than the glomerular filtration rate (~120 mL/min) (163). Thus, gallic acid might undergo active tubular secretion in the kidney. In this study, gallic acid emerged as a potent

inhibitor for hOAT1 and hOAT3 (IC_{50}: 1.24 and 9.02 µM, respectively), indicating that these transporters might be involved in its active secretion. Furthermore, the DDI index for hOAT1 at the lowest reported C_{max} (0.22 µM) is 0.12 and, thus, still meets the criteria for warranting *in vivo* DDI studies. Human OAT3 requires a C_{max} of only 1.5 µM (reported range 0.22-10 µM) to reach a DDI index > 0.1. Future studies also should focus on gallic acid's major metabolites, particularly 4-O-methylgallic acid, which showed an even higher C_{max} than unchanged gallic acid (142). Since these compounds possess a carboxyl group in the aromatic ring, they might be OAT substrates or inhibitors, and potentially exacerbate gallic acid-associated DDIs.

For gentisic acid on hOAT3 (IC_{50} = 86.81 µM), the DDI index becomes 0.1 at a C_{max} of just 10 µM (reported range 0.7-6,290 µM), if we assume high protein binding of 90% (actual lower protein binding would serve to decrease the C_{max} at which the 0.1 cut-off is reached). Clinically, gentisic acid becomes very important, as it is a major metabolite of salicylate, one of the most commonly used non-steroidal anti-inflammatory drugs (NSAIDs) (164). For example, in clinical practice methotrexate is often taken concomitantly with NSAIDs in the treatment of rheumatoid arthritis. However, it was reported that this combined therapy might increase methotrexate-related adverse effects, and aspirin was found to reduce the renal clearance of methotrexate by 30% (164, 165). Although NSAIDs can reduce glomerular filtration of methotrexate and influence its fraction of plasma protein binding, inhibition of active renal tubular secretion via OATs might be an important elimination mechanism, as methotrexate is an organic acid mainly excreted unchanged in the urine (166, 167). Accordingly, transport of methotrexate by hOAT1 (K_m = 554 µM) and hOAT3 (K_m = 21.1 µM) was investigated and results indicated a possible role for hOAT3 in its renal elimination, yet, salicylate showed extremely poor affinity for hOAT3 (K_i = 2.2 mM) (168). However, as the results of the present study suggest, gentisic acid, formed as a

salicylate metabolite, could inhibit hOAT3 transport activity at clinical concentrations (2-6.29 mM) and be responsible for the observed DDIs (157-159). This may prove to be particularly relevant for the pediatric population, as the highest reported C_{max} value was observed in a clinical study with subjects aged 2 to 16 y (159).

As indicated, gentisic acid and 4-hydroxybenzoic acid stimulated hOAT1-mediated uptake and syringic acid stimulated both hOAT1- and hOAT4-mediated uptake, yet all three compounds inhibited hOAT3 (Figures 5.2, 5.4 and 5.6). Thus, the stimulatory effects were varied and no consistent pattern or association with compound structural features was identified. Such sporadic *in vitro* stimulation/inhibition of transporter activity has been reported previously in the literature for several drug classes including steroids, anticancer chemotherapeutics, non-steroidal anti-inflammatory drugs, and fluoroquinolone antimicrobials (82, 169, 170). For example, ciprofloxacin stimulated hOAT1 transport activity, but inhibited hOAT3 (82). Stimulation of MRP2 was observed for sparfloxacin (170). It has been theorized that these effects might be the result of allosteric interactions with the transporters, with binding promoting conformational changes that modulate the transport kinetics of substrates (169, 170). The interactions reported here are certainly consistent with this theory, however the nature and position of any potential allosteric binding sites within the hOATs remains unclear and requires further investigation, particularly given the close sequence homology of the OATs and varied effects of the studied phenolic acids. Regardless, such stimulatory interactions could have important *in vivo* consequences. For example, while a gentisic acid-drug interaction on hOAT3 might produce altered drug pharmacokinetics exhibiting decreased drug elimination and increased terminal half-life, such an interaction on hOAT1 might produce the opposite effect, resulting in increased elimination and shortened terminal half-life causing a marked loss of drug efficacy.

Recent studies have identified that some ACNs are degraded to phenolic acids (44, 147, 148). It was identified *in vitro* that 4-hydroxybenzoic acid, protocatechuic acid, syringic acid, and vanillic acid, are the major degradation products of cyanidin, malvidin, peonidin, and pelargonidin (44). In addition, 4-hydroxybenzoic acid and protocatechuic acid were confirmed as the major human metabolites of cyanidin-glucosides and pelargonidin-3-glucoside, respectively, *in vivo* (148, 160). Thus, while the bioavailability of ACNs is poor, a large portion of ACNs are degraded to phenolic acids and the concentration of these phenolic acid metabolites might reach much higher levels than indicated by their bioavailability and actual quantity in dietary sources. Due to the large amount of ACNs in the human diet, it is vital to investigate the potential transporter-mediated DDIs induced by these ACN metabolites.

Over 170 species of plants have been used as herbal medicines in the treatment of kidney injury and disease, and phenolic acids (*e.g.*, *p*-coumaric acid, ferulic acid, gallic acid, sinapinic acid) were identified as major components in them (171). Oxidative damage induced by the formation of free radicals is one mechanism that results in nephropathy (171). Phenolic acids, bearing oxidizable functional groups, exhibit strong reactive oxygen species/free radical scavenging ability (140, 172, 173). A ranked order of antioxidant activity for some phenolic acids, according to their EC_{50} values, has been reported as gallic acid (0.0237 µM) > gentisic acid (0.0292 µM) > syringic acid (0.0427 µM) > caffeic acid (0.0478 µM) > protocatechuic acid (0.0574 µM) > sinapinic acid (0.0724 µM) > ferulic acid (0.0927 µM) > isoferulic acid (5.68 µM) > vanillic acid (14.37 µM) > *p*-coumaric acid (66.29 µM) > *o*-coumaric acid (130.05 µM) > *m*-coumaric acid (>300 µM) > 4-hydroxybenzoic acid (>800 µM)≈ salicylic acid (>800 µM) (172, 173). All of the compounds tested in the present study showed significant interactions with

hOAT3, while five of them showed significant inhibition on hOAT1, thus OAT-mediated accumulation in renal proximal tubule cells might explain their nephroprotective effects.

In addition, these phenolic acids might have the potential to treat renal injury induced by nephrotoxic drugs including β-lactam antibiotics (cephalosporins and penems) and antivirals (adefovir and cidofovir). OATs have been demonstrated to be involved in the uptake of these nephrotoxic drugs in proximal tubule cells (174, 175). Some OAT inhibitors, including probenecid and NSAIDs, efficiently attenuated this drug-induced renal damage at clinically relevant concentrations (130, 176). Therefore, phenolic acids might prove useful as an alternative treatment in the management of OAT-mediated nephrotoxicity of drugs, without producing side effects.

In summary, we have demonstrated the interaction of dietary phenolic acids with hOAT1, hOAT3, and hOAT4. These results indicated that OAT-mediated food/drug-drug interactions involving these phenolic acids might occur *in vivo*. Among the tested compounds, gallic acid and gentisic acid showed strong potential for food/drug-drug interactions. In the absence of protein binding and C_{max} information, the DDI potential of sinapinic acid could not be fully addressed, however the IC_{50}/K_i values are consistent with this possibility. Future *in vivo* interaction studies between gallic acid and gentisic acid and clinical therapeutics that are known hOAT1 and hOAT3 substrates appear necessary in order to establish safety guidelines for relevant pharmaceutical products.

CHAPTER 6

INTERACTION OF NATURAL DIETARY AND HERBAL ANIONIC COMPOUNDS AND FLAVONOIDS WITH HUMAN ORGANIC ANION TRANSPORTERS 1 (SLC22A6), 3 (SLC22A8), AND 4 (SLC22A11)

Drawn from manuscript published in *Evid Based Complement Alternat Med*. Vol.2013, Article ID 612527, 7 pages, 2013.

6.A INTRODUCTION

In concert with our growing knowledge of drug transporter expression and function, transporter-mediated drug-drug interactions (DDIs) are being increasingly identified by numerous *in vitro* and *in vivo* studies (3, 177). Recently, government agencies in the United States (Food and Drug Administration) and Europe (European Medicines Agency), as well as the pharmaceutical industry, have acknowledged that transporters play a key role in the absorption, distribution, and excretion of many clinical therapeutics. Organic anion transporter 1 (OAT1; SLC22A6), OAT3 (SLC22A8), and OAT4 (SLC22A11) are among the transporters identified, thus far, to impact the pharmacokinetics, and hence dosing, efficacy and toxicity, of some drugs. OAT1 and OAT3, expressed in the basolateral membrane of renal proximal tubule cells in both humans and preclinical species, function as key mediators for organic solute flux from blood to the glomerular filtrate (3, 177). Additionally, OAT4, which is exclusively expressed in the apical

membrane of human proximal tubules, reabsorbs anionic compounds from the urine (177). Further, many endogenous substances, including hormones, neurotransmitters and toxins, have been identified as substrates and/or inhibitors of OATs (3, 177). Thus, the potential clinical significance of OAT-mediated DDIs is firmly recognized.

Although many studies have exhibited OAT-mediated DDIs for synthesized drugs, relatively little is known about the potential interaction between OATs and natural products, including various organic anions, phenolic acids and flavonoids found in herbal supplements and food. Several dietary flavonoids and their metabolic conjugates (*e.g.*, sulfates and glucuronides) were identified as potent inhibitors and/or substrates of human (h) OAT1, hOAT3 and hOAT4 (48, 119). Phenolic acids, *e.g.*, contained in the widely used Chinese herbal medicine Danshen (*Salvia miltiorrhiza*) or common berries such as strawberries or blueberries, were similarly demonstrated to interact with these three transporters (52). These studies highlight the strong potential for hOAT-mediated natural product-drug interaction and the need to investigate further anionic compounds and flavonoids that are found in popular complementary/alternative medicines and natural supplements.

Catechin and epicatechin are major components of tea products, possessing anti-oxidative and purported anti-cancer properties (178, 179). 1,3- and 1,5-dicaffeoylquinic acids are two enantiomers of dicaffeoylquinic acid with various pharmacological effects, which are widely distributed in plants (*e.g.*, coffee beans, sweet potato leaves, and fennels) (180). Indeed, 1,3-dicaffeoylquinic acid (also known as cynarin) is being actively investigated for its anti-HIV and immunosuppressive properties (181). Extracts of *Ginkgo biloba* have gained popularity as an herbal supplement because they are believed to improve mental sharpness and memory, while slowing brain aging, and were hoped to be effective in relieving symptoms associated with

Alzheimer's disease. Regardless, it is well recognized that several ginkgolic acids, particularly (13:0), (15:1) and (17:1) (designating the number of carbon atoms in the alkyl side chain) can produce severe allergic, cytotoxic, mutagenic, carcinogenic, and genotoxic effects (182). Licorice root (*Radix Glycyrrhizae*) is employed to relieve a number of maladies including stomach ulcers, colic, chronic gastritis, sore throat, bronchitis, osteoarthritis, liver disorders, malaria and tuberculosis. One major component of *Radix Glycyrrhizae* preparations, glycyrrhizin, gives rise to two bioactive metabolites, 18α- and 18β-glycyrrhetinic acid, thought to play a role in these beneficial effects (183). Ursolic acid is a pentacylic triterpene acid occurring naturally in herbs and fruits. It exhibits anti-inflammatory and anti-carcinogenic activities (184) and is marketed as an herbal supplement to promote weight loss. Since these compounds have been identified as major components of first-line/complementary/alternative medicines, foods, and beverages, humans can be exposed to these compounds through clinical therapies and the daily diet. Many of these compounds have shown systemic exposure in humans (Table 6.1). Based on their chemical structures and previous studies, these compounds have the potential to interact with OATs. Thus, OAT-mediated DDIs may occur *in vivo* when combined with known OAT substrates and such information should prove helpful in guiding the safe use and development of products that contain these compounds.

Therefore, the purpose of the present study was to investigate the inhibitory potential of these nine compounds, catechin, epicatechin, 1,3- and 1,5-dicaffeoylquinic acids, ginkgolic acids (13:0), (15:1) and (17:1), 18β-glycyrrhetinic acid, and ursolic acid, on hOAT1-, hOAT3- and hOAT4-mediated transport. In addition to generating transporter specific inhibition profiles, dose-response studies were conducted for potent inhibitors in order to derive inhibitory constants (IC_{50} and K_i values) to aid evaluation of their potential for clinical OAT-mediated DDIs.

Table 6.1. Maximum plasma concentration (C_{max}) reported in human subjects

Compound	C_{max} (μM)	Route of administration	Dose (mg)	Reference
Epicatechin	0.20	Oral	37	(178)
1,5-Dicaffeoylquinic acid	0.14	Oral	600	(185)
18β-Glycyrrhetinic acid	0.11-2.9[a]	Oral	130-144 (Glycyrrhizin)	(183, 186, 187)
Ursolic acid	7.4	i.v.	186	(184)

[a]Assuming plasma concentration of 18α- and 18β-glycyrrhetinic acid is about 1:3 as reported in (183).

6.B MATERIALS AND METHODS

6.B.1 Purified chemicals

Catechin, 1,3- and 1,5-dicaffeoylquinic acids, epicatechin, ginkgolic acids (13:0), (15:1), and (17:1), and ursolic acid (all≥ 97% purity) were purchased from Tauto Biotech (Shanghai, China). 18β-Glycyrrhetinic acid (≥ 97% purity) was obtained from Sigma -Aldrich (St. Louis, MO). The chemical structures of these compounds are shown in Figure 6.1. Tritiated *p*-aminohippuric acid ([^{3}H]PAH) and estrone sulfate ([^{3}H]ES) were purchased from PerkinElmer Life and Analytical Sciences (Waltham, MA) and unlabeled PAH, ES, and probenecid were purchased from Sigma-Aldrich (St. Louis, MO).

6.B.2 Cell culture

Derivation and culture of stably transfected Chinese hamster ovary (CHO) cells expressing hOAT1 (CHO-hOAT1) and hOAT4 (CHO-hOAT4), and stably transfected human embryonic kidney 293 (HEK) cells expressing hOAT3 (HEK-hOAT3), as well as their corresponding empty vector transfected background control cell lines, has been described previously (82, 130, 150).

6.B.3 Cell accumulation assays

The cell accumulation assay protocol was performed as described in our recent publications with minor modifications (82, 109). In brief, 2×10^5 cells/well were seeded in 24-well tissue culture plates and grown in the absence of antibiotics for two days. For transport experiments cells were pre-incubated in transport buffer without substrates or inhibitors for 10 min after which time the buffer was replaced with 400 µL of fresh transport buffer containing 1 µM [^{3}H]PAH (0.5 µCi/mL) or [^{3}H]ES (0.25 µCi/mL) with or without test compounds. After incubation for times specified in the figure legends, cellular uptake was quenched by quickly rinsing each well three times with fresh ice-cold transport buffer. Cells were lysed with 1 M

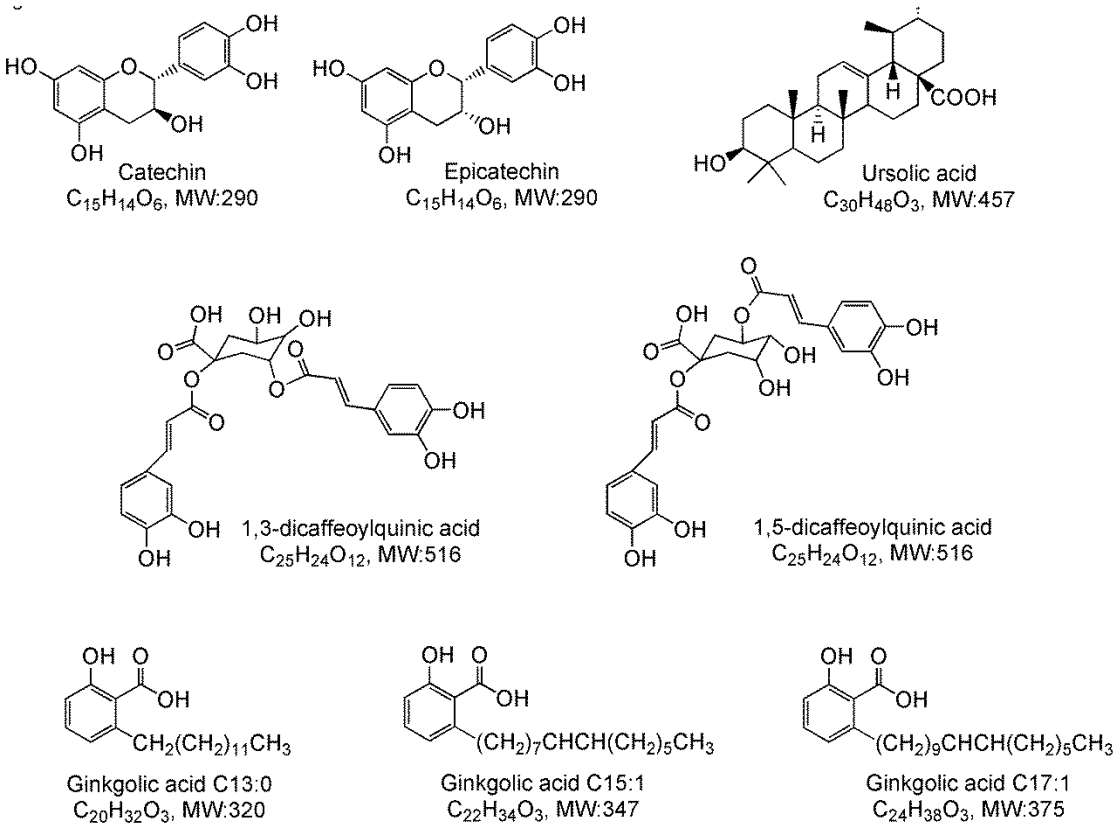

Figure 6.1. Chemical structures of compounds investigated in this study.

MW, molecular weight.

NaOH and radioactivity was measured with a liquid scintillation counter and reported as picomoles of substrate per milligram total protein. All intracellular uptake data were corrected for background accumulation in corresponding empty vector transfected control cells. Kinetic calculations were performed using GraphPad Prism Software version 5.0 (GraphPad Software Inc., San Diego, CA). The half maximal inhibitory concentrations (IC_{50}) and inhibitory constants (K_i) were calculated using nonlinear regression with the appropriate models. Results were confirmed by repeating all experiments at least three times with triplicate wells for each data point. For kinetic analysis, hOAT1 expressing cells showed linear PAH uptake for the initial 3 min with K_m = 15.4 µM (130), while hOAT3 expressing cells exhibited linear ES uptake for the initial 1 min with K_m = 14.5 µM (52).

6.B.4 Statistics

Values are expressed as mean ± S.D. or mean ± S.E.M. as indicated. Statistical differences were assessed using one-way analysis of variance (ANOVA) followed by post-hoc analysis with Dunnett's t-test ($\alpha = 0.05$).

6.C RESULTS

6.C.1 Inhibition of hOAT1 by natural anionic compounds and flavonoids

Approximately three fold greater accumulation of PAH was observed in CHO-hOAT1 cells (6.30 ± 0.97 pmol mg protein^{-1} 10 min^{-1}) than in empty vector transfected background control cells (2.12 ± 0.19 pmol mg protein^{-1} 10 min^{-1}). The hOAT1-mediated PAH accumulation was almost completely inhibited by probenecid (Figure 6.2). The nine test compounds, catechin, 1,3- and 1,5-dicaffeoylquinic acid, epicatechin, ginkgolic acids (13:0), (15:1) and (17:1), 18β-glycyrrhetinic acid, and ursolic acid, were assessed for inhibitory effects on hOAT1-mediated uptake (Figure 6.2). 1,3- and 1,5-Dicaffeoylquinic acid (64% and 22% inhibition, respectively), ginkgolic acid (17:1) (42% inhibition) and 18β-glycyrrhetinic acid (56% inhibition) each significantly inhibited hOAT1-mediated PAH uptake at 50 fold excess. Ursolic acid produced a significant stimulation of uptake and the other compounds were without effect. Since 1,3-dicaffeoylquinic acid and 18β-glycyrrhetinic acid produced inhibition greater than 50%, they were further characterized by dose-response studies (0.01–500 μM, shown in Figure 6.3). Estimated IC_{50} values were 1.2 ± 0.4 μM for 1,3-dicaffeoylquinic acid and 2.7 ± 0.2 μM for 18β-glycyrrhetinic acid. Numerous studies investigating the mode of inhibition produced on hOAT1 and hOAT3 for a broad array of compounds have demonstrated the interaction to be competitive (51, 151, 188-190). Therefore, assuming competitive inhibition of hOAT1, inhibition constants (K_i) were estimated as 1.1 ± 0.2 μM for 1,3-dicaffeoylquinic acid and 2.5 ± 0.2 μM for 18β-glycyrrhetinic acid.

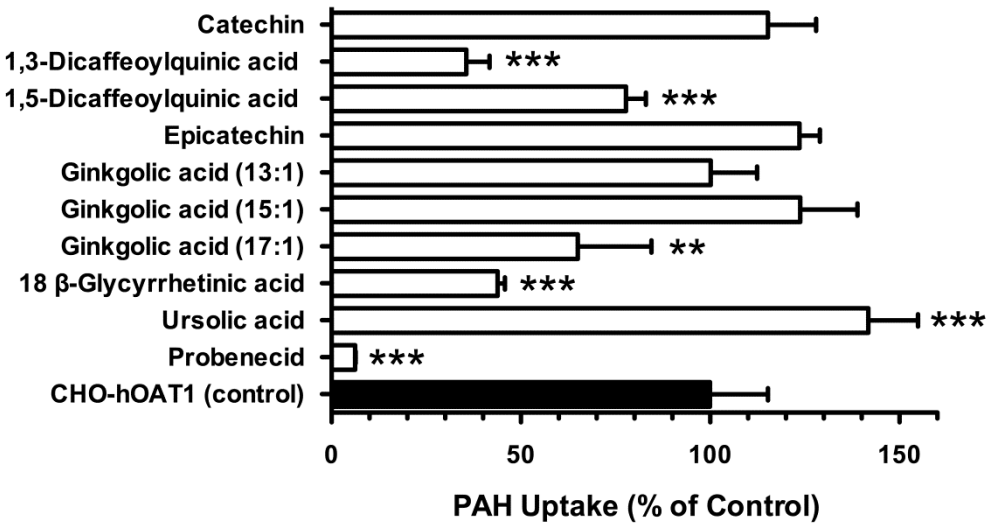

Figure 6.2. Inhibitory effects of the nine test compounds on hOAT1-mediated PAH uptake

Ten minute uptake of [^{3}H]PAH (1 µM) was measured in CHO-hOAT1 cells in the absence and presence of test compounds (50 µM) or probenecid (1000 µM). Data represent hOAT1-mediated transport specifically, *i.e.*, data have been corrected for background PAH accumulation measured in empty vector transfected cells. Values are mean ± S.D. of triplicate values from a representative experiment. ** denotes $p < 0.01$, and *** denotes $p < 0.001$ as determined by one-way ANOVA followed by Dunnett's t-test.

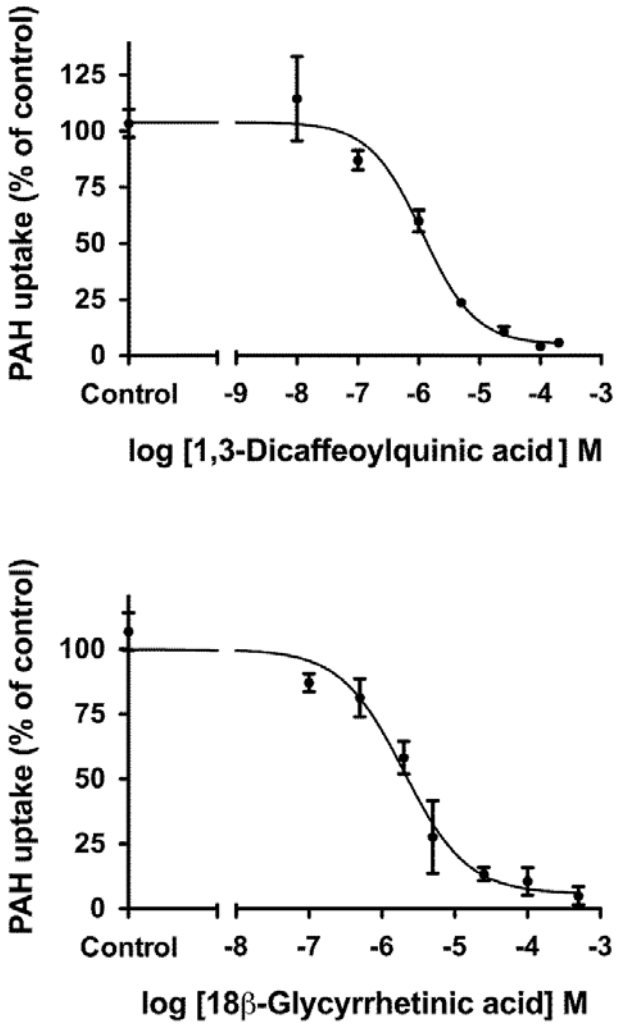

Figure 6.3. Dose-response effects for 1,3-dicaffeoylquinic acid and 18β-glycyrrhetinic acid on hOAT1-mediated PAH transport

One minute uptake of [^{3}H]PAH (1 µM) in CHO-hOAT1 cells was measured in the presence of increasing concentrations (10^{-7} to 5×10^{-4} M) of test compounds. Data were corrected by subtracting background PAH accumulation measured in empty vector transfected cells. IC_{50} values were determined with nonlinear regression and the "log(inhibitor) vs. response" model using GraphPad Prism software. Experiments were repeated three times with triplicate samples and graphs shown are from representative experiments with values plotted as mean ± S.D. (n=3). The data were used to generate mean IC_{50} ± S.E.M. estimates.

6.C.2 Inhibition of hOAT3 by natural anionic compounds and flavonoids

Human OAT3 expressing cells showed about 4 fold greater accumulation of ES as compared to background control cells (10.6 ± 0.5 vs. 2.6 ± 0.3 pmol mg protein^{-1} 10 min^{-1}, respectively). Similar to hOAT1, hOAT3-mediated ES uptake was completely (> 96% inhibition) blocked by probenecid (Figure 6.4). Five of the compounds, 1,3- and 1,5-dicaffeoylquinic acid, epicatechin, and ginkgolic acids (15:1) and (17:1) significantly inhibited hOAT3-mediated transport at 50 fold excess (Figure 6.4). 1,3-Dicaffeoylquinic acid and ginkgolic acid (17:1) exhibited 41% inhibition, while 30-35% reduction of hOAT3-mediated ES uptake was observed for 1,5-dicaffeoylquinic acid, epicatechin, and ginkgolic acid (15:1). Catechin, 18β-glycyrrhetinic acid and ursolic acid failed to produce significant inhibition. Based on the level of inhibition observed, IC_{50} values for all of these compounds would be greater than 50 µM, much higher than clinically relevant concentrations (Table 6.1). Therefore, further dose-response studies were not performed.

6.C.3 Inhibition of hOAT4 by natural anionic compounds and flavonoids

Stably transfected hOAT4-expressing cells showed ~18 fold higher accumulation of ES than background control cells (42.5 ± 5.1 vs. 2.4 ± 0.2 pmol mg protein^{-1} 10 min^{-1}, respectively). Human OAT4-mediated ES uptake was virtually completely blocked (> 96% inhibition) by self-inhibition (Figure 6.5). Catechin (50 µM) was the only compound that showed a significant inhibitory effect (32%) on hOAT4 (Figure 6.5). 1,5-Dicaffeoylquinic acid and 18β-glycyrrhetinic acid produced significant stimulation of ES uptake. Accordingly, the IC_{50} value for catechin on hOAT4 transport activity should be greater than 50 µM and no further kinetic studies were performed.

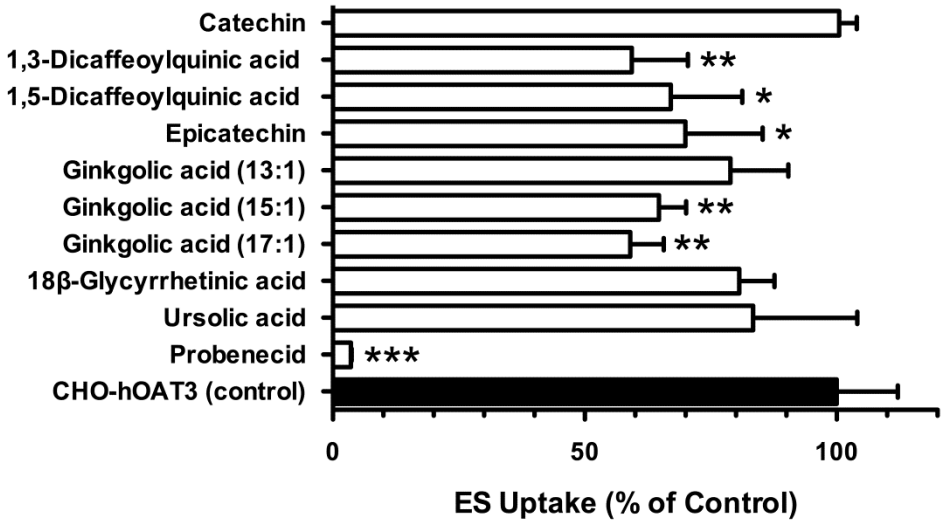

Figure 6.4. Inhibitory effects of the nine test compounds on hOAT3-mediated ES uptake

Ten minute uptake of [^{3}H]ES (1 µM) was measured in HEK-hOAT3 cells in the absence and presence of test compounds (50 µM) or probenecid (1000 µM). Data represent hOAT3-mediated transport specifically, *i.e.*, data have been corrected for background ES accumulation measured in empty vector transfected cells. Values are mean ± S.D. of triplicate values from a representative experiment. * denotes $p < 0.05$, ** denotes $p < 0.01$, and *** denotes $p < 0.001$ as determined by one-way ANOVA followed by Dunnett's t-test.

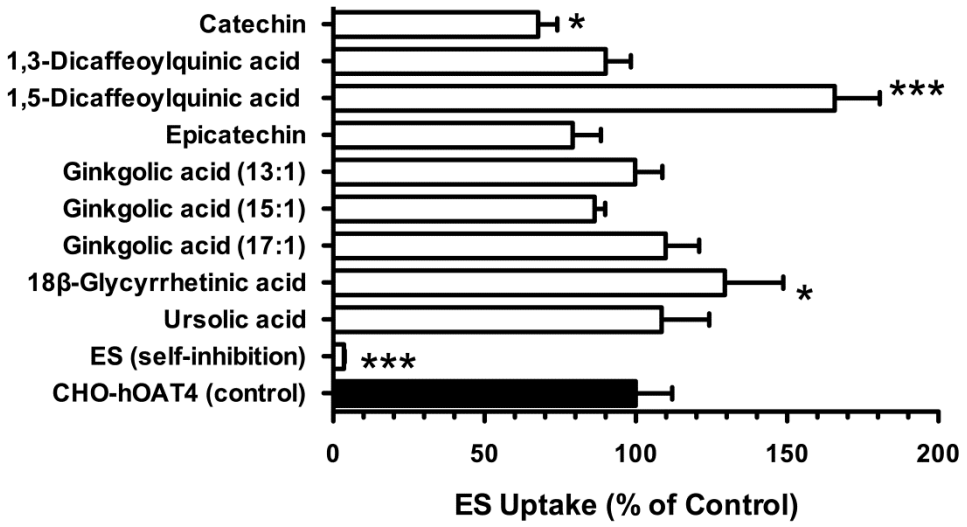

Figure 6.5. Inhibitory effects of the nine test compounds on hOAT4-mediated ES uptake

Ten minute uptake of [^{3}H]ES (1 µM) was measured in CHO-hOAT4 cells in the absence and presence of test compounds (50 µM) or ES (1000 µM for self-inhibition). Data represent hOAT4-mediated transport specifically, *i.e.*, data have been corrected for background ES accumulation measured in empty vector transfected cells. Values are mean ± S.D. of triplicate values from a representative experiment. * denotes $p < 0.05$, and *** denotes $p < 0.001$ as determined by one-way ANOVA followed by Dunnett's t-test.

6.D DISCUSSION

Literally hundreds of therapeutic and endogenous compounds have been demonstrated to interact with OATs (3, 177). Precisely because of their broad, polyspecific nature, OATs are likely sites for DDIs *in vivo*. As a consequence, they have been identified worldwide as a family of "clinically relevant" transporters in recent government guidances to the pharmaceutical industry (3, 177). Unlike Western drugs, the pharmacokinetic and pharmacological properties of botanical drug products and natural supplements have not been well investigated. Being naturally derived, people often view these compounds as "safe" and without potential for causing adverse events. However, there is increasing evidence demonstrating potent interactions between components of natural products and OATs, resulting in possible toxicity and DDIs (3, 177). For example, aristolochic acid, a potent nephrotoxic contaminant sometimes found in certain Chinese herbal therapies, was identified as a high affinity substrate of murine Oat1, Oat2 and Oat3, as well as a potent inhibitor of hOAT1, hOAT3 and hOAT4 (36, 39). Additional studies have demonstrated the OAT-mediated DDI potential for common flavonoid and phenolic acid components of foods and herbal medicines (48, 119). These investigations showed that many dietary/phytomedicine-derived organic acids and flavonoids have a high inhibitory potency for hOAT1, hOAT3 and/or hOAT4 and, according to proposed guidelines established by the FDA and EMA, high likelihood to result in significant DDIs *in vivo* (3, 48, 119, 177). Therefore, further studies on OAT-mediated natural product/drug interactions are needed in order to establish informed safety and efficacy profiles for botanical products.

In the present study, we characterized the interactions of nine chemically diverse compounds including flavonoids, chlorogenic acids, phenolic acids, and other organic acids, found as major dietary or phytomedicine components, with three human OATs: hOAT1, hOAT3, and hOAT4.

As illustrated, most of the compounds produced significant inhibition of hOAT1 and hOAT3 at a 50 fold excess concentration (Figures 6.2 and 6.4). In marked contrast, only catechin significantly inhibited hOAT4 under this condition (Figure 6.5). Interestingly, ursolic acid caused a significant stimulation of hOAT1-mediated PAH uptake while it was without effect on either hOAT3 or hOAT4 transport activity. Similarly, 1,5-dicaffeoylquinic acid and 18β-glycyrrhetinic acid appeared to significantly stimulate hOAT4 transport while decreasing hOAT1- and hOAT3-mediated uptake. Such sporadic transporter stimulation/inhibition has been previously reported in the literature for other compounds. For example, for fluoroquinolone antimicrobials, ciprofloxacin inhibited hOAT3, but stimulated hOAT1 (82) and sparfloxacin was reported to stimulate multidrug resistance-associated protein 2 activity (170). Such stimulation of transport activity *in vitro* also has been reported for steroids, chemotherapeutic agents, and non-steroidal anti-inflammatory drugs (82, 169, 170, 191). One potential explanation is allosteric binding of the compounds to the transporters with subsequent alteration of substrate affinity (169, 170). However, these transporters share a high degree of sequence identity and no readily discernible structural differences corresponding to such a binding site are apparent, and these effects do not exhibit a consistent pattern among the hOATs. Whether these effects will be observed *in vivo* is yet to be determined, however, in such an instance increased (vs. decreased) elimination and shortened (vs. lengthened) terminal half-life of victim drugs could occur causing loss of efficacy.

The FDA guidance on drug interaction studies proposed using the DDI index, calculated as the ratio of unbound C_{max} over IC_{50} or K_i, as an indicator for the assessment of a compound's DDI potential, with a value greater than 0.1 indicating the potential need to perform an *in vivo* DDI study for an investigational drug. In the current study, 18β-glycyrrhetinic acid exhibited

strong inhibition of hOAT1 with an estimated IC_{50} of 2.7 ± 0.2 µM or K_i of 2.5 ± 0.2 µM (Figures 6.3). Human exposure studies reported C_{max} values ranging from 0.11 to 2.9 µM (Table 6.1), perhaps due to interindividual variability, different doses, and/or dosing regimen (single dose vs. repeated dose). As such, the maximum DDI for 18β-glycyrrhetinic acid is ~1.1; although this value does not account for plasma protein binding as this is unknown. However, if we assume it to be highly plasma protein bound, *e.g.,* 90%, the DDI index would be 0.12, meeting the FDA guidance threshold of 0.1. Therefore, 18β-glycyrrhetinic acid may affect hOAT1-mediated renal elimination of coadministered therapeutics that are hOAT1 substrates.

1,3-Dicaffeoylquinic acid is a major component found in artichoke and *Echinacea purpurea* (192, 193). Pharmacological studies demonstrated that it exhibits antimicrobial and antioxidant activity (192, 194). Moreover, it has garnered increased interest because of its anti-HIV and immunosuppressive properties. 1,3-Dicaffeoylquinic acid blocked HIV-1 integrase activity, leading to interference of insertion of viral DNA into the genome of the victim cell (181). Another study demonstrated that it inhibited the interaction between CD28 of T-cell receptor and CD80 of antigen presenting cells, blocking "signal 2" of T-cell activation (193). Due to its potential development as a therapeutic agent, systemic exposure in clinical applications may reach high levels. In the present study, 1,3-dicaffeoylquinic acid showed high affinity with hOAT1 (IC_{50} = 1.2 ± 0.4 µM; K_i = 1.1 ± 0.2 µM). Therefore, the dose-systemic exposure relationship and plasma protein binding should be elucidated as part of the future drug development process for this compound.

It has been reported that flavonoids can interact with OATs (48). Therefore, catechin and epicatechin, two flavonoid components from green tea were investigated for potential interaction with hOAT1, hOAT3 and hOAT4. Both compounds exhibited significant inhibition of hOAT4

and hOAT3 when present at a 50 fold excess, however no inhibition was observed for hOAT1. Because of low reported clinical plasma concentrations (Table 6.1), these flavonoids were determined to be unlikely to cause DDIs after normal consumption of tea products. However, OATs might promote entry of these antioxidants into renal proximal tubules, providing a nephroprotective effect.

In summary, we investigated the potential interaction of nine flavonoids, phenolic acids, chlorogenic acids, and other organic acids with hOAT1, hOAT3, and hOAT4. Among the examined compounds, 1,3-dicaffeoylquinic acid and 18β-glycyrrhetinic acid showed marked affinity with hOAT1. In humans, systemic exposure of 18β-glycyrrhetinic acid may induce significant hOAT1-associated DDIs. Future *in vivo* interaction studies between 18β-glycyrrhetinic acid or 1,3-dicaffeoylquinic acid and clinical therapeutics known to be hOAT1 substrates may be necessary to establish safety guidelines for use of pharmaceutical products containing these compounds to avoid potential DDIs.

CHAPTER 7

SIMULTANEOUS DETERMINTION OF GALLIC ACID AND GENTISIC ACID IN ORGANIC ANION TRANSPORTER EXPRESSING CELLS BY LIQUID CHROMATOGRAPHY-TANDEM MASS SPECTROMETRY

Drawn from manuscript submitted in *J Chromatogr B.* 2013

7.A INTRODUCTION

Over the last two decades, impressive progress has been made to elucidate the impact of drug transporters in drug absorption, disposition, and elimination, therapeutic efficacy and adverse drug reactions (3, 177). In order to understand the role of drug transporters in pharmacokinetics and avoid potential drug-drug interactions (DDIs), the United States Food and Drug Administration (FDA) has recently issued guidance documents, requiring investigations on potential new drug entity-drug transporter interaction on seven identified transporters; organic anion transporter 1 (OAT1), OAT3, organic cation transporter 2, organic anion transporting polypeptide 1B1, organic anion transporting polypeptide 1B3, multidrug resistance transporter 1, and breast cancer resistance protein, prior to approval (52).

Numerous studies demonstrated that OATs handle substances carrying negative charge(s) at physiological pH (3, 177). Phenolic acids (plant secondary metabolites that are widely distributed in fruits, vegetables, and beverages) might be OAT substrates, since the PK_a values

for these compounds are much less than 7.4 (43). They are characterized by hydroxylated aromatic ring(s) bearing carboxyl substituents (140). In general, phenolic acids, including gallic acid and gentisic acid, possess anti-oxidant, anti-carcinogenic, and anti-inflammatory activities (162, 163). Gallic acid, in addition to fruits and vegetables, is a major component in herbal supplements, homeopathic remedies, and pharmaceutical products (139, 162, 163). Gentisic acid was identified as a major metabolite of salicylate (143). Pharmacokinetic studies have shown that these compounds undergo renal elimination as the unchanged parent form (144, 163). Our previous work demonstrated that gallic acid and gentisic acid have high affinity for human OAT1 and OAT3, with IC_{50} values in the low micromolar range (52). However, whether these compounds are actually OAT substrates, or only non-transported inhibitors, remains unclear. This information is key to determining whether OAT-mediated active secretion is involved in the renal elimination of these compounds. In addition, since such interaction would result in preferential tissue distribution, the findings would be helpful to show the target organ(s) in which these compounds exert beneficial therapeutic effects.

To address this issue, a sensitive, robust, and precise bioanalytical method is required for quantification of gallic acid and gentisic acid in cell lysate. Compared with other routine analytical techniques, liquid chromatography (LC) interfaced to mass spectrometry (MS) or tandem mass spectrometry (MS/MS) has facilitated sensitive and selective quantification in pharmaceutical studies. For published assays describing LC-MS/MS based measurement of gallic acid and gentisic acid in a biological matrix, insufficient sensitivity (LLOQ of 0.5 and 9.4 ng/mL, respectively) and limited linear dynamic range (0.5-500 and 9.4-191.5 ng/mL, respectively) make these methods less desirable for quantifying drug transporter mediated-cellular uptake of gallic acid and gentisic acid (195, 196). In addition, the run-time of the

reported quantification method for gentisic acid is long (17 min) (196). Furthermore, electrospray ionization (ESI), which allows analysis of non-volatile, polar molecules compared with other ion source designs (*e.g.*, atmospheric pressure chemical ionization (APCI)), is more susceptible to matrix effects, exhibiting as impaired assay accuracy and precision. Unfortunately, previously published assays did not evaluate matrix effect (195, 196), or only investigated plasma-derived matrix effect (195, 196). For the purpose of cell-based bioassay, the potential matrix effect caused by cell lysate matrix should be studied. To the best of our knowledge, however, no liquid chromatography-tandem mass spectrometry (LC/MS-MS) based assay has been established to directly measure the uptake of gallic acid or gentisic acid in cell lysate.

In the present study, a rapid, sensitive, and reproducible LC/MS-MS method was developed and validated to simultaneously determine the concentrations of gallic acid and gentisic acid in cell lysate. The method requires 100 μL of cell lysate to obtain a lower limit of quantification of 0.33 ng/mL and a chromatographic run time of 3 min for both analytes. Results from post-column infusion and the post extraction addition method indicate that the quantification of both analytes was not affected by matrix effects. Compared with previously described methods, this new method exhibits higher analytical performance with respect to sensitivity, linear dynamic range, and speed. Following validation, the assay utility was demonstrated in a measurement of a cellular uptake study of gallic acid and gentisic acid in OAT-expressing cells.

7.B MATERIAL AND METHODS

7.B.1 Chemicals and reagent

Gallic acid, gentisic acid, probenecid, and sodium L-ascorbate (≥ 97% purity) were purchased from Sigma-Aldrich (St. Louis, MO). Danshensu (≥ 96% purity) was used as the internal standard (IS) and purchased from Tauto Biotech (Shanghai, China). The chemical structures of gallic acid, gentisic acid, and the IS are shown in Figure 7.1. HPLC-grade acetic acid (CH_3COOH, 99.93%), acetonitrile (CH_3CN 99.9%), ethyl acetate (EtOAc, 99.84%), and formic acid (HCOOH, 99.93%) were purchased from Merck (Darmstadt, Germany). Deionized water was generated from a Direct-Q1 3 UV water purifying system (Millipore, Bedford, MA).

7.B.2 Instrumentation

An API 4000Qtrap hybrid triple quadrupole/linear ion trap mass spectrometer (AB Sciex., Foster City, CA) was interfaced with an electrospray ionization source with liquid chromatography including a Waters Acquity UPLC® system (Waters Corporation, Milford, PA). Analyst 1.5 data acquisition software (Waters Corp., Milford, MA, USA) was used to control the LC-MS/MS system, as well as for data acquisition and processing. Nitrogen gas was generated from a Parker Hannifin (Haverhill, MA, USA) Tri-Gas Generator LC/MS 5000.

7.B.3 LC-MS/MS condition

The analytes and the IS were separated on a Gemini C18 column (100 mm × 2.0 mm I.D., 5 μm) with a Security Guard column (Gemini C18, 4 mm × 2.0 mm, 5 μm) from Phenomenex (Torrance, CA, USA). Mobile phases consisted of 0.1% acetic acid in water (A) and 0.05% formic acid in acetonitrile (B). An isocratic elution (40% A) was conducted with a flow rate of 0.35 mL/min. The total run time was 3 min.

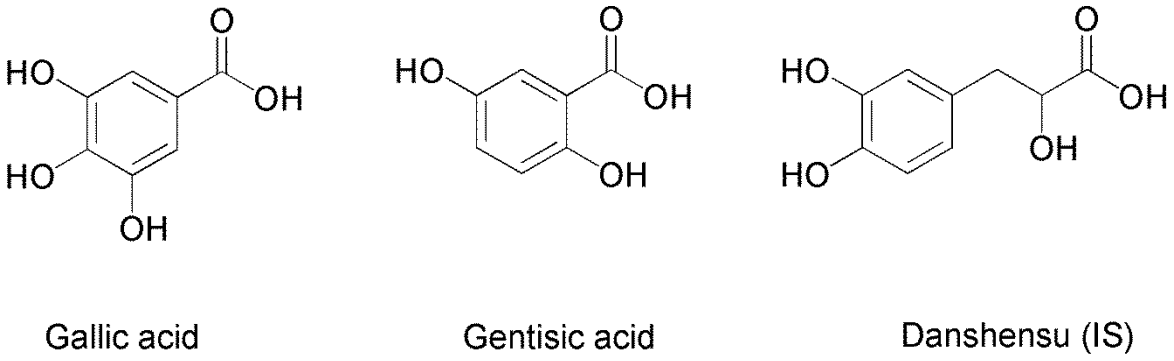

Figure 7.1. Chemical structures of gallic acid, gentisic acid, and Danshensu (IS) were drawn using ChemDraw Ultra (PerkinElmer Inc., Waltham, MA)

The mass spectrometer was operated in the negative ESI mode with selected reaction monitoring (SRM). The optimized mass spectrometric parameters were as follows: ion source temperature (TEM = 325 °C), ion transfer voltage (ITV = –4500 V), collision gas (CAD = high), curtain gas (CUR = 14), ion source gas 1 (GS1 = 55) and ion source gas 2 (GS2 = 20). The units for gases are arbitrary. The dwell time was 200 ms for all test compounds. SRM transitions, collision energies (CE), declustering potential (DP), and Q3 fragment ion descriptions are shown in Table 7.1.

7.B.4 Cell culture

Derivation of stably transfected Chinese hamster ovary (CHO) cells expressing murine Oat1 (CHO-mOat1) and murine Oat3 (CHO-mOat3), and corresponding empty vector transfected background control cell line (CHO-FRT), has been described previously (82). CHO cell lines were maintained at 37°C with 5% CO_2 in DMEM F-12 media (Mediatech, Inc., Herndon, VA) containing 10% serum, 1% Pen/Strep and 125 µg/ml hygromycin B.

7.B.5 Sample preparation

Cell lysate samples (100 µL) were mixed with 10 µL of the 1000 ng/mL IS working solution and 10 µL of the 50 µM ascorbic acid working solution to prevent oxidation. Then the sample was acidified with 5 µL of 2N hydrochloric acid and extracted with 900 µL of EtOAc by vortex-shaking for 10 min. After centrifugation at 13000 rpm for 5 min, the upper EtOAc phase (800 µL) was removed and reduced to dryness under a stream of nitrogen at 40°C at 15-20 PSI. The dry residue was reconstituted in 150 µL of reconstitution solvent (acetonitrile/H_2O; 25:75 v/v) containing 0.1% acetic acid and 5 µM ascorbic acid, centrifuged at 13000 rpm for 5 min, and 20 µL of the supernatant was introduced into the LC-MS/MS system.

7.B.6 Calibration and validation.

Blank cell lysate samples (995 µL) were spiked with 5 µL of the gallic acid and gentisic acid working solution (1000 µg/mL) and then serially diluted with blank cell lysate to generate nominal concentrations of 2400, 1000, 500, 200, 80, 32, 12.8, 5.12, 2.05, 0.82 and 0.33 ng/mL for both analytes, respectively. These matrix-based calibration standards were extracted with EtOAc for analysis. Calibration curves were constructed using linear regression of the peak area ratio of the analytes to the IS (Y) against the corresponding nominal concentrations of the analytes in cell lysate (X, ng/mL) with a weighting factor of $1/x^2$.

The extraction efficiency was assessed by comparing the peak areas of the analytes added to blank cell lysate at three levels (1, 50, and 2000 ng/mL) before sample clean-up with the same amount of the analytes added to post-extraction cell lysate blanks (n=6). The stability test included freeze/thaw stability in cell lysate during and after three -80°C↔25°C (room temperature) cycles at two levels (1 and 2000 ng/mL), short-term stability in cell lysate at 25°C for 6 h and long term stability in cell lysate at -80°C for 1 month at two levels (1 and 2000 ng/mL), and post-preparation stability in reconstitution solution at 4°C for 24 h at three levels (1, 50, and 2000 ng/mL). The long term stock solution stability (6 months) was also investigated. For each concentration level, quality control (QC) standards were prepared and extracted n=6.

QC samples at 1, 50, and 2000 ng/mL (n=6) were determined on the same day or three different days to evaluate intra-day or inter-day precision and accuracy, respectively. Intra-day/inter-day accuracy and precision were calculated as the percentage of mean measured concentration to the corresponding nominal concentration and coefficient of variation of the measured concentrations. The lower limit of quantification (LLOQ) was determined based on the criterion of being within ±20% of precision and accuracy.

7.B.7 Matrix effects evaluation

Matrix effects were assessed by both post-column infusion and post extraction method. The procedure for post-column infusion was described previously (197). Briefly, the prepared blank cell lysate sample was injected while infusing the analytes and the IS (1000 ng/mL) in reconstitution solution at 15 µL/min into the ESI interface through a mixing tee. Compared to resulting profiles of mobile phase injection, response change observed from the blank cell lysate sample indicates ionization suppression or enhancement. Post extraction method was conducted by comparing the peak areas of the analytes (1, 50, and 2000 ng/mL) and the IS (100 ng/mL) dissolved in reconstitution solution versus post-spiked extracted cell lysate (n=6). The ratio of mean peak areas for the test compounds in pure reconstitution solution to those with sample matrix was used to quantify matrix effects.

7.B.8 Application to cellular uptake study

The protocol for the cellular accumulation studies was adapted from a previously published study with minor modifications (52). In brief, cells were seeded in 24-well tissue culture plates at a density of 2×10^5 cells/well and grown in the absence of antibiotics for 48 h. Then, the cells were equilibrated with 500 µL of transport buffer [Hanks' balanced salt solution containing 10 mM HEPES (Sigma-Aldrich, St. Louis, MO), pH 7.4] for 10 min. The equilibration buffer was then replaced with 500 µL of fresh transport buffer containing 10 µM gallic acid or gentisic acid. After incubation for 10 min, cells were immediately rinsed three times with ice-cold transport buffer, and lysed with 200 µL 1 N NaOH. Cell lysate was neutralized with 2 M HCl (100 µL). Aliquots (100 µL) were extracted as described in Section 2.4 for LC-MS/MS analysis and total protein determination using a Bio-Rad Protein Assay Kit (Bio-Rad Laboratories, Hercules, CA).

7.C RESULTS AND DISCUSSION

7.C.1 LC-MS/MS

The chemical structures of gallic acid and gentisic acid indicate that they are more likely to be deprotonated to produce $[M–H]^-$ in the ESI source, and this was confirmed by comparing the response of the analytes between positive and negative ESI mode. Parameters for mass spectrometry were optimized for quantification of gallic acid and gentistic acid in negative mode. Product ions for gallic acid and gentisic acid were chosen based upon intensity and reproducibility. A fast isocratic program was used to achieve optimal chromatographic behavior, with total run time of 3 min. Retention times were 0.98, 2.09, and 1.03 min for selected transitions of gallic acid (m/z 169.0→125.0), gentisic acid (m/z 153.1→108.0), and the IS (m/z 196.8→135.2), respectively. The chosen mobile phase additive conditions (0.1% acetic acid in mobile phase A and 0.05% formic acid in mobile phase B) improved chromatographic peak shape and intensity of the analytes. However, other mobile phase additives (0.1% acetic acid in mobile phase A and B, 0.05% formic acid in mobile phase A and B, and 0.1% formic acid in mobile phase A and B) were not suitable for gallic acid, as they resulted in asymmetrical peak shape or poor retention. Gallic acid and gentisic acid fragmentation patterns were identical with those previously described (196). Representative chromatograms of blank cell lysate, blank cell lysate spiked with gallic acid (200 ng/mL), gentisic acid (200 ng/mL), and the IS (100 ng/mL) are shown in Figure 7.2.

7.C.2 Validation of the analytical method

7.C.2.1 Linearity and specificity

The intensity, shown as peak area ratio of gallic acid or gentisic acid to the IS in cell lysate, was linear over the range 0.33-2400 ng/mL. The calibration curves for quantification of the

tested compounds in cell lysate showed a correlation coefficient (r^2) greater than 0.995. A weighting factor of $1/x^2$ was used for both analytes. The magnitude of linear dynamic range was much wider than previously reported methods (195, 196). The percent relative standard deviation for the mean back-calculated values fell within 15%, showing good accuracy for calibration standards. As shown in Figure 7.2, no co-elution of matrix components from cell lysate was observed at retention times corresponding to the analytes, demonstrating that the method had good specificity. Moreover, no cross-interference among the analytes and the IS was found. No significant peaks were found at retention times corresponding to the analytes and the IS in blank sample immediately following the calibration standards at upper limit of quantification (2400 ng/mL), suggesting insignificant carryover for this method. An extract peak with constant signal (1500-3000 cps) was observed in the gallic acid channel, which was not seen in the blank cell lysate. While the exact reason for this extra peak is unknown, the proposed isocratic elution was capable of separating this peak from the peak for gallic acid, with retention times of 1.30 min and 0.98 min, respectively. This extra peak did not affect the calculation of peak area for gallic acid.

7.C.2.2 Accuracy and precision

Intra-day and inter-day precision and accuracy for the analytes are shown in Table 7.2. The maximum deviation of accuracy and precision for intra-day and inter-day validation were well below 13.5%. The LLOQ was determined at 0.33 ng/mL for both analytes, with the precision and accuracy within +14.1%.

7.C.2.3 Extraction recovery

The mean extraction efficiency for gallic acid in cell lysate determined by analyzing the cell lysate QC standards at 1, 50, and 2000 ng/mL were 77.3 ± 9.8%, 76.5 ± 4.8% and 88.2 ± 4.6% respectively. The results for gentisic acid show a mean extraction recovery of 77.6-86.9% with the RSD below 3.5% (86.0 ± 3.5%, 86.9 ± 2.2% and 77.6 ± 0.9% for 1, 50, and 2000 ng/mL, respectively). The extraction recovery of the IS was 51.7 ± 2.3% at 100 ng/mL. As gallic acid, gentisic acid and the IS each carry a carboxylic group, a low pH environment favors maintaining unionized compounds in the sample, facilitating extraction. In this study, the chosen condition (5 µL 2N hydrochloric acid) markedly improved extraction efficiency compared with the untreated condition.

Table 7.1. Selected reaction monitoring transitions and the optimum LC-MS/MS conditions

Compound	Q1 (Da)	Q3 (Da)	DP[a]	CE[b]
Gallic acid	169.0	125.0	–26	–25
Gentisic acid	153.1	108.0	–26	–39
Danshensu (IS)	196.8	135.2	–27	–24

[a] Declustering potential; [b] Collision energy.

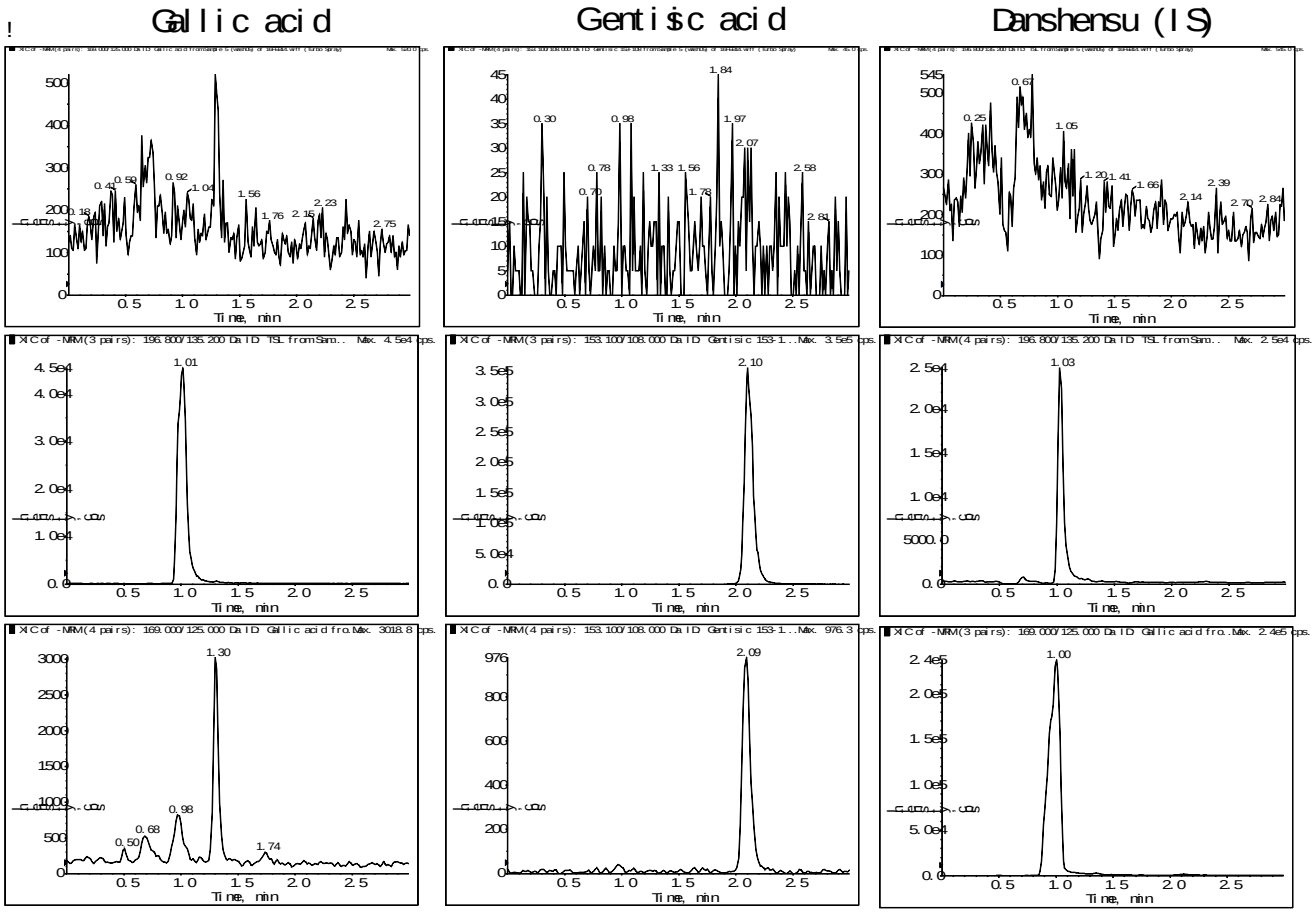

Figure 7.2. Example chromatograms for the analytes and IS in a typical blank cell lysate (upper panels), analytes and the IS dissolved in pure reconstitution solution (middle panels), and extracted cell lysate sample spiked with the analytes at LLOQ and the IS at 100 ng/mL (lower panels)

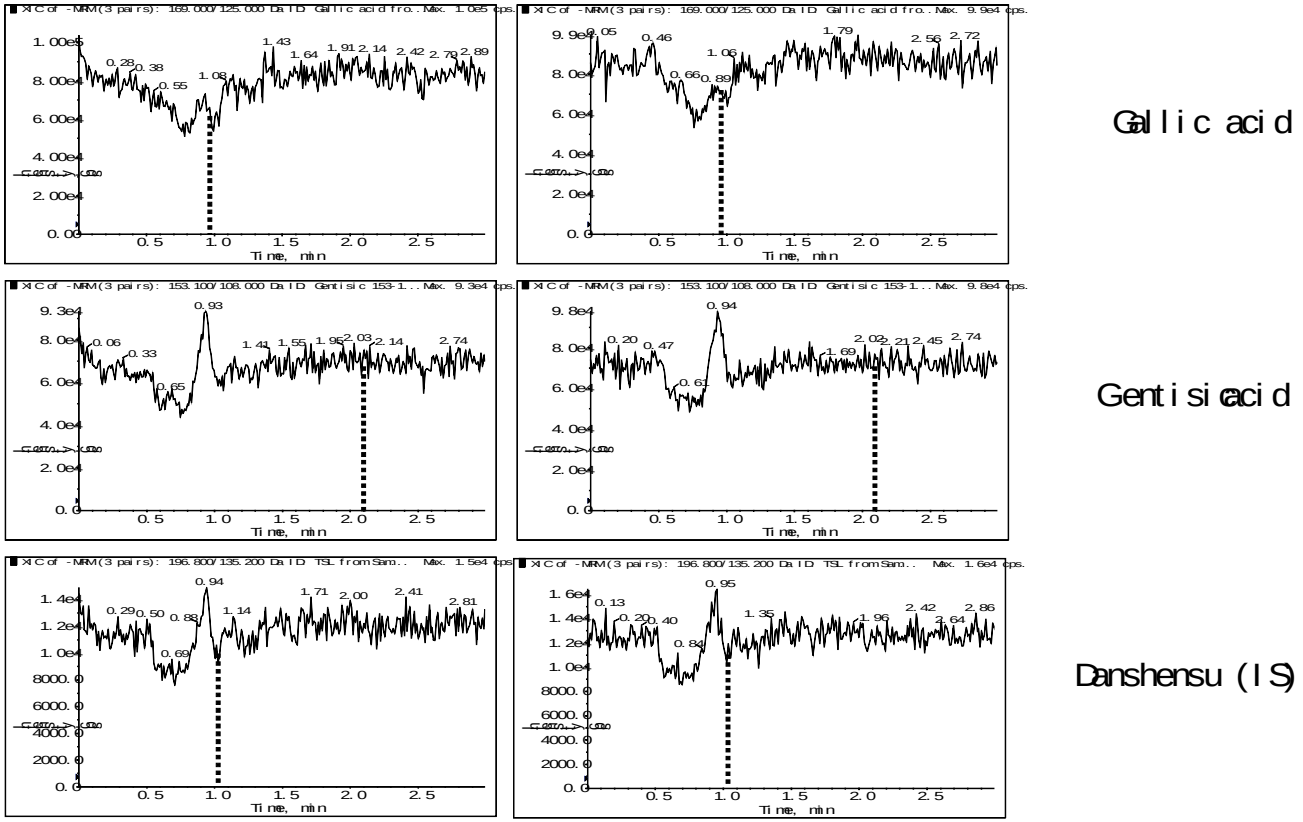

Figure 7.3. Post-column infusion profiles of the analytes and the IS (1000 ng/mL) in the absence (left panels) or presence (right panels) of cell lysate-derived matrix. Dashed lines indicate the retention time of the test compound

Table 7.2. Intra- and inter-day precision and accuracy in determination of gallic acid and gentisic acid

	Gallic acid			Gentisic acid		
Nominal Conc. (ng/mL)	1	50	2000	1	50	2000
Intra-day						
Measured Conc. (ng/mL) mean ± SD, n =6	1.06±0.11	50.6±2.08	1745±68.8	1.09±0.08	55.5±1.94	1832±56.9
Precision (RSD, %)	10.4	4.11	3.94	7.34	3.50	3.11
Accuracy (% bias)	6	1	-12.7	9	11	-8.4
*Inter-day**						
Measured Conc. (ng/mL) mean ± SD, n =6	0.99±0.10	45.2±5.00	1845±143	1.00±0.10	49.1±6.59	1868±100
Precision (RSD, %)	10.1	11.1	7.75	10.0	13.4	5.35
Accuracy (% bias)	-0.7	-9.5	-7.7	0	-1.8	-6.6

*QCs analyzed n =3 in three separate days

7.C.2.4 Matrix effects

Matrix effects were firstly evaluated by post-column infusion of test compounds dissolved in reconstitution solution at 1000 ng/mL. Post-column infusion profiles were obtained in the ESI negative mode (shown in Figure 7.3) exhibiting matrix effects of EtOAc-extracted cell lysate on the response of the tested compounds. When compared to post-column infusion profiles for mobile phase, no significant matrix effects (indicated by ionization suppression or enhancement) were observed throughout the entire sample-run window in the presence of matrix components in the ESI source. The post-extraction addition study revealed that co-eluting matrix failed to exhibit significant suppression or enhancement (<15%) on the ESI response of both gallic acid and gentisic acid, confirming that matrix effects did not impact the established assay method.

7.2.C.5 Stability

Stability assessment was conducted by determination of QC standards treated under different conditions representing post-preparation stability, short and long term storage stability, stock solution stability, and freeze-thaw stability. Since phenolic compounds can be easily oxidized, an anti-oxidant was necessary to keep the analytes and the IS stable in the sample during preparation. In the present study, ~5 µM of ascorbic acid was determined to be sufficient for preventing oxidation while 20 µM impaired the chromatographic peak shape of gallic acid (data not shown). The accuracy of treated QC standards was calculated by freshly prepared calibration standards. QC standards for post-preparation stability exhibited acceptable accuracy and precision (±7%) at 1, 50, and 2000 ng/mL. Short and long term storage stability results ranged from −4.2% to 12.5% biases for test levels (1 and 2000 ng/mL). Gallic acid and gentisic acid in stock solution stored at –80°C for 6 months was stable, with peak area response difference never exceeding 1.7%. Freeze-thaw stability was assessed for three cycles at two levels (1 and 2000

ng/mL), resulting in biases ranged from 3.6 to 8.2%. The IS, Danshensu, failed to show significant degradation in reconstitution solution at 4°C for 24h, with a peak area response difference of 10.9%.

7.C.3 Determination of the intracellular concentration of gallic acid and gentisic acid in OAT-expressing cells.

The suitability of the LC-MS/MS method presented here to determine gallic acid and gentisic acid levels in cell lysates from a cellular uptake study using murine (m)Oat1- or mOat3-expressing cells (CHO-mOat1 cells and CHO-mOat3 cells, respectively) was tested. Inhibitor (probenecid)-sensitive transport activity of these transfected cells was confirmed previously (49). When incubated with gallic acid (10 µM) for 10 min, the intracellular concentration of gallic acid in CHO-mOat1 cells was 1.12 ± 0.33 ng/mL, while the concentrations of gallic acid in CHO-mOat3 cells, CHO-FRT(control cells), or probenecid-treated cells were below the LLOQ (Figure 7.4). These data indicate markedly increased intracellular uptake in the CHO-mOat1 cells, as compared with CHO-FRT and CHO-mOat3 cells. The absorptive uptake was completely inhibited by probenecid (known OAT inhibitor) at 1 mM. Normalized with the protein content in cell lysate, the cellular uptake rate of gallic acid in mOat1-expressing cells was 10.4 ± 3.7 ng/mL/mg protein/10 min. The intracellular concentration of gentisic acid in CHO-mOat1, CHO-mOat3 and CHO-FRT background control cells after incubation were below the LLOQ (Figure 7.4).

These results indicate that gallic acid is a substrate for mOat1 and suggest that human OAT1 might be involved in the active renal secretion of gallic acid. This finding is consistent with a previous clinical pharmacokinetic study showing that the unbound renal clearance of gallic acid was 1.7 fold higher than the glomerular filtration rate (~120 mL/min) (163). Collectively, these

data show that the newly developed analytical method can be used to assess cellular uptake of gallic acid and gentisic acid.

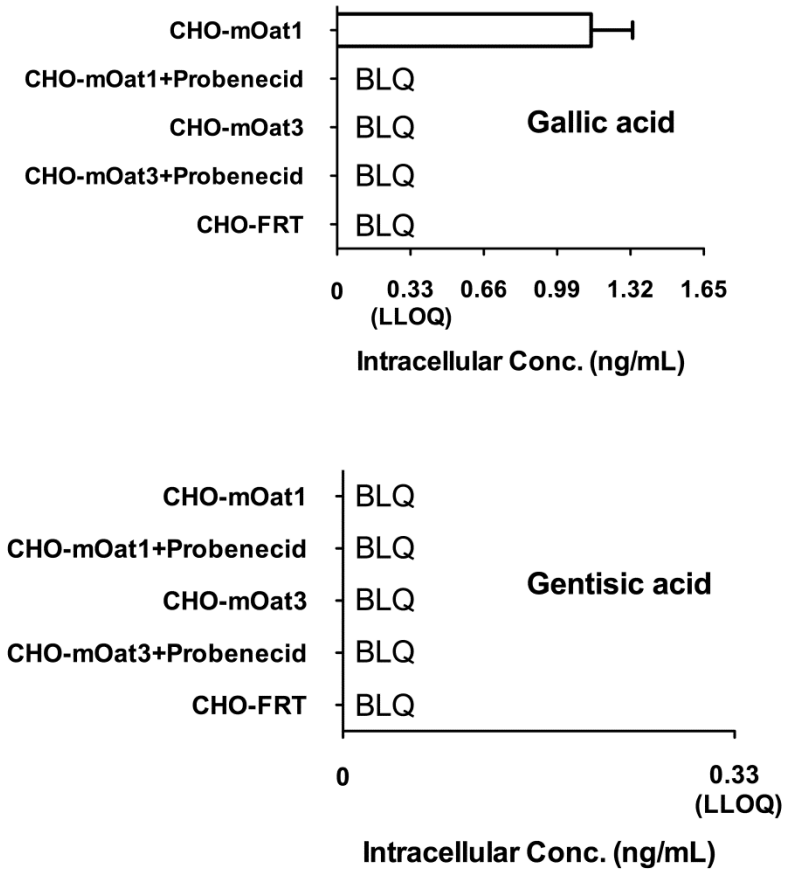

Figure 7.4. Cellular uptake of gallic acid and gentisic acid in mOat1- and mOat3-expressing cells, as well as empty vector transfected background control cell line (CHO-FRT). The concentration of gallic acid, gentisic acid, and probenecid (known OAT inhibitor) for incubation were 10 µM, 10 µM, and 1000 µM. LLOQ, lower limit of quantification; BLQ, below LLOQ.

7.D CONCLUSIONS

As the FDA has suggested that potential drug transporter-mediated DDI should be investigated to avoid unexpected adverse effects, validated bioanalytical methods to directly measure drug transporter-mediated cellular uptake are needed. In the present study, we reported a specific, sensitive, and reliable LC-MS/MS method for analysis of gallic acid and gentisic acid from complex cell lysate samples, with LLOQ of 0.33 ng/mL. Good linearity was obtained with concentrations ranging from 0.33 to 2400 ng/mL. Method validation results showed acceptable intra-/inter-day accuracy and precision as well as stability, and insignificant matrix effects. Compared with previous reported methods, this assay was highly sensitive and rapid, with wider linear dynamic range, which fits for the purpose of cell-based *in vitro* novel substrate identification and screening of potential DDI. Finally, the suitability of this method was demonstrated in a cellular uptake study in which the intracellular concentrations of gallic acid and gentisic acid in OAT-expressing cells was measured. The method described here can be applied to study potential interaction of gallic acid or gentisic acid with any transporter family, *e.g.*, OATs (SLC22 transporter family), multidrug resistance-associated proteins (MRPs; ABCC transporter family), and organic anion transporting polypeptides (OATPs; SLCO family), as well as to investigate their absorption and metabolism profiles with *in vitro* models, *e.g.*, Caco-2 cells and primary hepatocytes.

CHAPTER 8

SYSTEMIC LEVEL EVALUATION OF ORGANIC ANION TRANSPORTER-MEDIATED DRUG-DRUG INTERACTION POTENCY IN SALVIA MITIORRHIZA (DANSHEN) PREPARATIONS: FOCUSING ON CUMULATIVE EFFECTS FROM MULTIPLE COMPONENTS

8.A INTRODUCTION

Danshen, the dried root of *Salvia miltiorrhiza*, is used by patients as a part of traditional Chinese medicine in the treatment of cardiovascular disease (100, 101). The major pharmacological effects in cardiovascular therapy may include improvement of microcirculation, preventing platelet adhesion and aggregation, and inhibiting the formation of thromboxane (100, 101). Presently, there are more than 900 commercial Danshen preparations manufactured in China, and injectables account for ~30% of total Danshen products (http://www.sda.gov.cn/WS01/CL0001/). Typical of herbal medicines, Danshen pharmaceutical products are actually a mixture of ingredients, including phenolic acids such as lithospermic acid (LSA), rosmarinic acid (RMA), salvianolic acid A (SAA), salvianolic acid B (SAB, also named lithospermic acid B), and tanshinol (TSL, also named danshensu), each of which has been identified as a major component in these preparations (103, 104, 116, 198). However, because of variations in cultivars, cultivation regions, manufacturing, and lack of standard quality control

criteria, the content of such components in Danshen preparations can exhibit wide variation among products from different sources. Such lack of standardization of the major Danshen components makes it difficult to predict systemic and peak exposure of these components between products, or to evaluate any exposure-related toxicity and drug-drug interaction (DDI) potential in clinical applications for products from various manufacturers (103, 199).

The number of reports on drug transporter-mediated DDIs from numerous preclinical and clinical studies has increased (136). Among these transporter families, the organic anion transporter (OAT; SLC22) family mediates the renal transcellular solute flux of a multitude of endogenous substances and xenobiotics that carry negative charge(s) at physiological pH (3). Because of their broad substrate specificity, many clinically important therapeutics have been identified as OAT substrates and/or inhibitors, such as antibiotics, antiviral and anticancer agents, statins, and angiotensin-converting enzyme inhibitors (3). As a result, United States Food and Drug Administration (FDA) regulatory, industrial and scientific experts have developed recommendations under what circumstances DDIs with seven selected transporters, including OAT1 and OAT3, need to be investigated (118, 136).

The DDI index is introduced as the unbound maximum plasma concentration (C_{max} or C_{ss}) of a drug component of interest at the highest clinically relevant dose over the *in vitro* transporter inhibition potency of the compound (K_i or IC_{50}) as an indicator of DDI potential. Conservatively, follow-up clinical DDI investigations are recommended when the DDI index ≥ 0.1 (136). For the majority of drug products, the DDI index is affected by only one or a few ingredients with constant content even between different manufacturers. However, for herbal medicines and natural products, the DDI index estimation becomes more complicated as they contain numerous components that can interfere with drug transporter activity, whether identified as an active

component or not. These components, in most cases, show marked similarity in chemical structure. This fact is quite important for assessment of DDI potential, since drug transporters, including OATs, interact with an array of compounds with marked diversity in their chemical structure (136). As a result, it is highly probable that more than one component in an herbal product could demonstrate a strong potential to interact with any specific transporter. Therefore, a new parameter to express this multifaceted inhibition potential on transporters, the cumulative DDI index, is proposed. This parameter, shown as the sum of each component's DDI index, reflects the overall DDI potential for multiple-component herbal preparations at clinically relevant concentrations.

Using Danshen as an example of herbal medicine, our previous work demonstrated that LSA, RMA, SAA, SAB and TSL each showed significant competitive inhibitory effects on human (h)OAT1- and hOAT3-mediated substrate uptake, and their corresponding K_i values on hOAT1 and hOAT3 are shown in Table 8.1 (190). Since all of these Danshen components showed competitive inhibition on human OAT transport activity, it is likely that these compounds share the same binding site such that cumulative inhibitory effects would emerge after administration of Danshen products with varying composition of these ingredients. The first aim of the present study was to compare the inhibitory effects of individual Danshen components (LSA, RMA, and TSL) vs. a mixture of components on hOAT1 and hOAT3. Pharmacokinetic modeling was used to predict plasma concentrations for Danshen products after *i.v.* bolus and *i.v.* infusion administration of clinically relevant doses. Finally, the new index, the cumulative DDI index, was evaluated for Danshen injectables from different manufacturers and different lots/batches from the same manufacturer. Results from this study demonstrate that the cumulative DDI index, which shows the overall inhibition potential of Danshen preparations, was significantly higher

than the DDI index from any single component, indicating that the DDI index for any single component in a complex mixture is likely to underestimate the true DDI potential of that product. Additionally, the cumulative DDI indices are highly variable between Danshen injectables from different manufactures as well as between different lots/batches produced by the same manufacturer. Such information might be useful in guiding quality control in the manufacture and clinical application of such pharmaceutical products.

8.B MATERIALS AND METHODS

8.B.1 Materials

The Danshen components LSA, RMA, and TSL (≥ 96% purity) were obtained from Tauto Biotech (Shanghai, China). Tritiated PAH ([^{3}H]PAH) and ES ([^{3}H]ES) were purchased from PerkinElmer Life and Analytical Sciences (Waltham, MA) and unlabeled PAH, ES, and probenecid were purchased from Sigma-Aldrich (St. Louis, MO).

8.B.2 Tissue culture

Derivation of stably transfected Chinese hamster ovary (CHO) cells expressing hOAT1 and stably transfected human embryonic kidney 293 (HEK) cells expressing hOAT3, and their corresponding empty vector transfected control cell lines, has been described previously (52). CHO cell lines were cultured in phenol red-free RPMI 1640 medium (Gibco Invitrogen., Grand Island, NY) containing 1 mg/mL G418. HEK cell lines were cultured in DMEM High glucose medium (Mediatech, Inc., Herndon, VA) containing 125 µg/ml hygromycin B. All cultures contained 10% FBS and 1% Pen/Strep, and were maintained at 37°C with 5% CO_2.

8.B.3 Cell accumulation assays

Cell transport assay procedures were adapted from those previously published (52). In brief, 2×10^5 cells/well were seeded in 24-well tissue culture plates and grown in the absence of antibiotics for 48 hr. On the day of the experiment cells were equilibrated with transport buffer for 10 min [500 µL of Hanks' balanced salt solution containing 10 mM HEPES, pH 7.4]. Equilibration buffer was replaced with 500 µL of fresh transport buffer containing 1 µM [^{3}H]PAH (0.5 µCi/mL) or 1 µM [^{3}H]ES (0.25 µCi/mL) with or without inhibitors. After incubation, cells were immediately rinsed three times with ice-cold transport buffer, lysed, and analyzed via liquid scintillation counting. Substrate accumulation was reported as picomoles of

substrate per milligram protein. The concentrations of LSA, RMA, and TSL were chosen to exhibit mild inhibition (≤ 61%). Results were confirmed by repeating all experiments at least three times with triplicate wells for each data point in every experiment.

8.B.4 Derivation of cumulative DDI index

Commonly, the influence of a single competitive inhibitor on transporter activity is described as follows;

$$\frac{V_0}{V_i} = 1 + \frac{I}{K_i}$$

where V_0, V_i, and I represent V_{max} in the absence of inhibitor, V_{max} in the presence of inhibitor and the relevant concentration of the inhibitor, respectively. According to the "Guidance for Industry: Drug Interaction Studies" issued by the FDA, I/K_i was proposed as an indicator for estimating the DDI potential (118). However, assuming independent competitive inhibition by all inhibitors in the presence of multiple (n) inhibitors, the influence on transport activity becomes;

$$\frac{V_0}{V_i} = 1 + \frac{I_1}{K_{i,1}} + \frac{I_2}{K_{i,2}} + \cdots + \frac{I_n}{K_{i,n}}$$

where I_n and $K_{i,n}$ represent the relevant concentration and inhibition constant of the individual inhibitors (n), respectively. As illustrated, the sum of $I_n/K_{i,n}$ for n inhibitors plays an equivalent role on transporter function as I/K_i for a single competitive inhibitor. As a result, for Danshen preparations, which include multiple components known to be competitive OAT inhibitors (190), the sum of $I_n/K_{i,n}$, designated as the cumulative DDI index, was used to describe the DDI potential of these complex mixtures.

8.B.5 Pharmacokinetic modeling

In order to determine relevant plasma concentrations for various doses of the different Danshen components, pharmacokinetic models had to be developed. Pharmacokinetic modeling was performed with WinNonlin software (version 5.2.1, Pharsight, St. Louis, MO, USA) using plasma concentration data from a previously reported clinical pharmacokinetic study on human subjects after a single 60 min *i.v.* infusion of a Danshen injectable (104). The doses were 5 mg, 3 mg, 160 mg, 65 mg, and 90 mg for caffeic acid (CA), LSA, RMA, SAB, and TSL, respectively (104). All observed plasma concentrations were above the assay LLOQ (8 ng/mL for all components), except for those of RMA at the last two time points (104). As a result, these two points were excluded from pharmacokinetic calculations. Initially, several pharmacokinetic compartment models were investigated during the model selection process. An *i.v.* infusion two-compartment model with first-order elimination was chosen as the final pharmacokinetic model based on the law of parsimony (simplest model) and goodness of fit including Akaike Criteria (AIC), Schwarz Bayesian Criterion (SBC), Weighted Sum of Square of Residuals (WSSR), visual inspection of weighted residuals versus observed concentrations, and fitted and observed plasma concentrations versus time. The schematic representation of this model is as follows

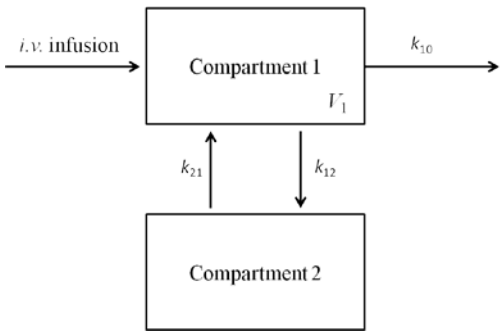

where k_{10} is the elimination rate constant from compartment 1, k_{12} is the distribution rate constant from compartment 1 to compartment 2, k_{21} is the distribution rate constant from compartment 2

to compartment 1, and V_1 represents volume of compartment 1. Compartments 1 and 2 represent central and peripheral compartments, respectively.

8.B.6 Simulation of plasma concentrations and estimation of cumulativeDDI index

The content of the Danshen components, LSA, RMA, SAB and TSL in Danshen injectables from different manufacturers, or from different lots/batches produced by a single manufacturer, were obtained from the literature (103, 104, 138, 198, 200). In order to estimate the DDI index, the plasma concentration-time profile of each Danshen component was simulated for patients administered these Danshen injectables under two clinically relevant scenarios: *i.v.* bolus administration and 60 min *i.v.* infusion administration. Simulated plasma concentration-time profiles were generated using a two compartment model with first-order elimination, assuming that all four Danshen components follow dose-proportional pharmacokinetics. The final pharmacokinetic model parameters were fixed. In addition, Yang *et al.* (2007) determined that, for RMA, SAB, and TSL, the fraction unbound in human plasma was 9.5%, 6.8%, and 100% (137). In the absence of LSA plasma binding data, it was assumed that LSA is highly protein bound (90%), leaving the fraction unbound in human plasma as 10%. Unbound plasma concentrations were estimated as the product of plasma concentration times, the fraction unbound in plasma. The DDI index was estimated as the predicted unbound C_{max} or C_{ss} in plasma over K_i for each component. The cumulative DDI index for a specific Danshen preparation was calculated as the sum of individual DDI indices for each component.

8.B.7 Statistics

Data are reported as mean ± S.D. Statistical differences were assessed using one-way ANOVA followed by post-hoc analysis with Dunnett's t-test ($\alpha = 0.05$).

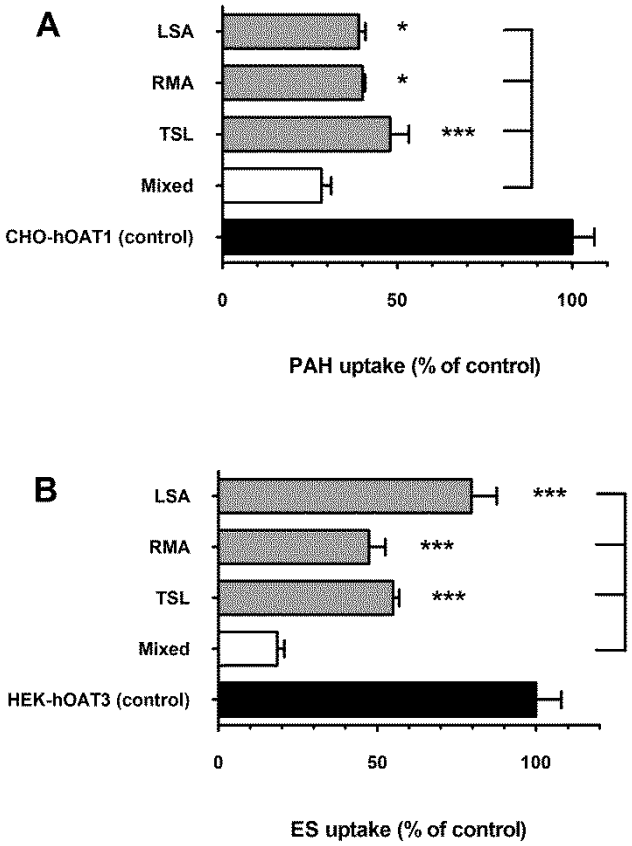

Figure 8.1. Cumulative inhibitory effects of LSA, RMA, and TSL on hOAT1 and hOAT3

A: Inhibition of hOAT1-mediated uptake of [^{3}H]PAH (1 µM) by LSA (10 µM), RMA (1 µM), and TSL (50 µM) individually or the mixture of these three components was measured in CHO-hOAT1 cells (10 min). B: Inhibition of hOAT3-mediated uptake of [^{3}H]ES (1 µM) by LSA (0.5 µM), RMA (0.5 µM), and TSL (10 µM) individually or as mixture of these three components was measured in the HEK-hOAT3 cells (10 min). All data were corrected by background substrate accumulation measured in corresponding empty vector control cells. OAT-expressing cell showed signicantly reduced cellular uptake of substrate ($p < 0.001$) when treated with single Danshen component or the mixture. Values are mean ± S.D. of triplicate values. All treated groups showed significant inhibiton on hOAT1 and hOAT3 ($p < 0.001$). *** denotes $p < 0.001$ and *denotes $p < 0.05$ as determined by one-way ANOVA followed by Dunnett's t-test to compare invidual compounds group *vs.* mixed group.

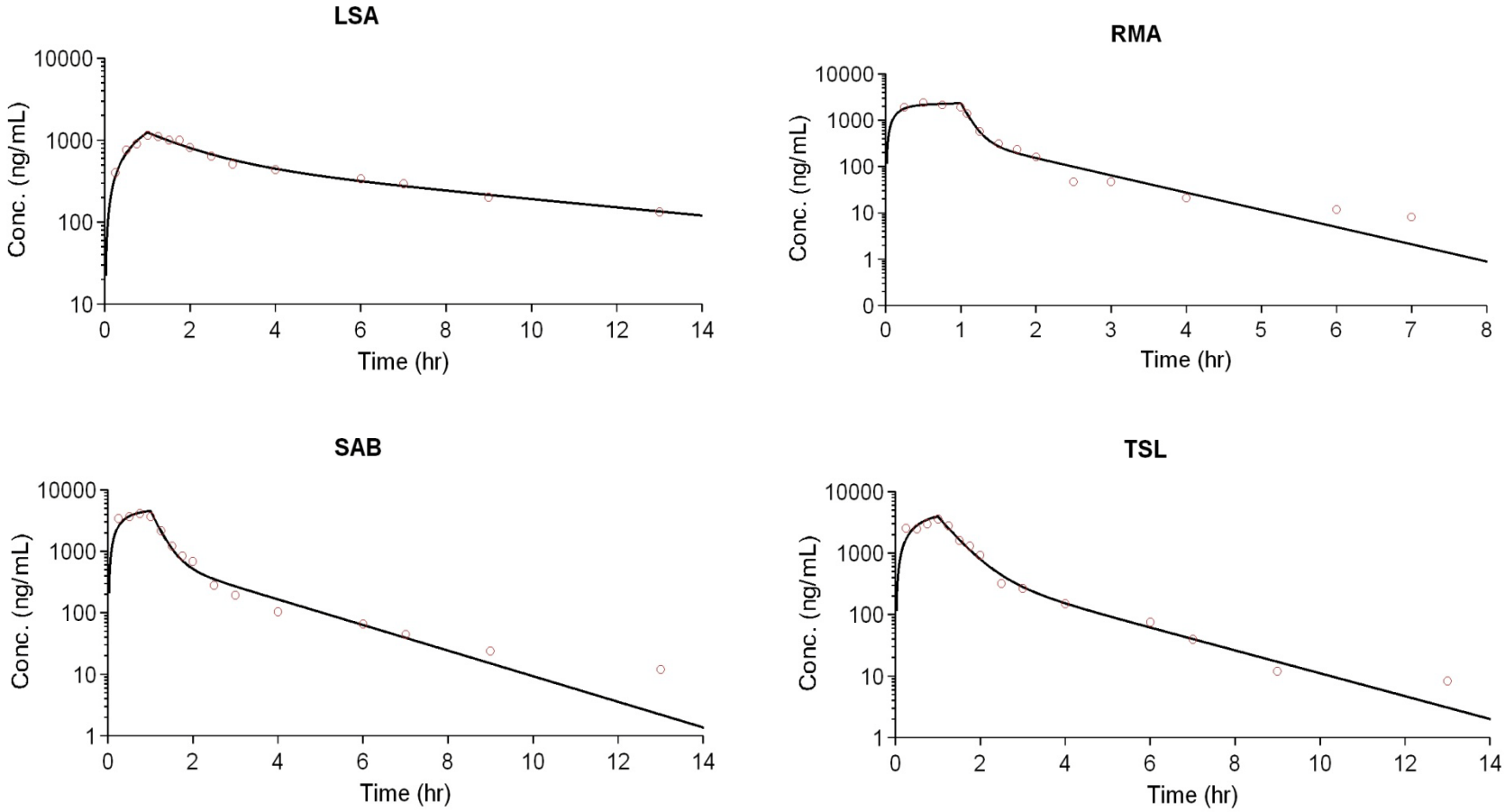

Figure 8.2. Modeling of published experimental data for human plasma concentrations of Danshen components, LSA, RMA, SAB, and TSL after i.v. infusion using a two-compartment model.

Original data (shown as open circle) were taken from reference (104). The doses were 3 mg, 160 mg, 65 mg, and 90 mg for LSA, RMA, SAB, and TSL, respectively.

Table 8.1. Estimated K_i values (μM) of Danshen components for hOAT1 and hOAT3

Compound	hOAT1	hOAT3
LSA	20.8 ± 2.1	0.59 ± 0.26
RMA	0.35 ± 0.06	0.55 ± 0.25
SAA	5.6 ± 0.3	0.16 ± 0.03
SAB	22.2 ± 1.9	19.8 ± 8.4
TSL	40.4 ± 12.9	8.6 ± 3.3

Values are reported as mean ± S.E.M. (n=3). These values were obtained from reference (190).

Table 8.2. Estimated parameters for two-compartment model with first-order elimination to describe pharmacokinetic properties of Danshen components after *i.v.* infusion

Compound	V_1 (L)	k_{10} (1/hr)	k_{12} (1/hr)	k_{21} (1/hr)	V_{dss} (L)	CL_{tot} (L/hr)	$t_{1/2}^{elimination}$ (hr)
LSA	1.9±0.1	0.25±0.03	0.29±0.07	0.35±0.15	3.43±0.53	0.48±0.04	6.04±1.78
RMA	18.9±3.3	3.30±0.34	0.28±0.07	0.44±0.09	23.4±4.0	61.6±2.8	0.81±0.23
SAB	4.1±0.6	2.74±0.38	0.86±0.34	0.60±0.25	9.44±1.94	11.2±0.7	1.45±0.48
TSL	10.4±1.3	1.58±0.19	0.32±0.21	0.55±0.35	16.4±3.4	16.4±1.1	1.62±0.87

Values are reported as mean ± S.E.M.

Table 8.3. Reported content of Danshen components in injectables from different manufacturers

Manufacturer	Maximum Dose (mg)[a]				Reference
	LSA	RMA	SAB	TSL	
1	NR[b]	10.2	17.2	21.2	(103)
2	NR	4.2	13.8	41.4	(103)
3	NR	4.6	7.0	31.2	(103)
4	NR	5.6	16.2	29.8	(103)
5	NR	12	12.6	80.6	(103)
6	3.88	10.3	39.5	37.8	(198)
7	1.7	3.4	6.8	45.2	(198)
8	NR	6.6	ND[c]	98.4	(200)
9	NR	14.1	343	ND	(200)
10	NR	5.1	2.0	25.4	(200)
11	NR	18.1	50.16	42.9	(200)
12	NR	4.4	2.9	59.7	(200)
13	NR	3.2	2.5	49.0	(200)
14	NR	7.7	16.8	52.5	(200)
15	NR	3.5	10.0	51.5	(200)
16	3	160	63	90	(104)

[a] Used for *i.v.* infusion administration, which is four-fold of the maximum dose for *i.v.* bolus administration; [b]Not reported; [c]Not detectable (value set to 0 for DDI index calculations in Tables 8.5 and 8.6)

Table 8.4. Reported content of Danshen components in injectables from a single manufacturer with different batches/lots. Data were reported from reference (138).

Batches	Maximum Dose (mg)[a]		
	RMA	SAB	TSL
1	1.9	1.3	24.7
2	3.5	1.7	29.0
3	2.5	1.5	25.9
4	2.7	2.0	24.9
5	2.4	1.6	23.1
6	2.0	1.0	19.1
7	3.3	1.4	27.1
8	2.5	1.7	24.8
9	2.2	1.1	21.3
10	2.5	1.9	27.3
11	1.2	0.3	9.0
12	2.6	1.7	27.1
13	2.7	1.6	28.5
14	3.4	1.9	28.9

[a] Used for *i.v.* infusion administration, which is four-fold of the maximum dose for *i.v.* bolus administration

Table 8.5. Estimation of individual and cumulative DDI indices for Danshen injectables from different manufacturers after *i.v.* bolus administration on hOAT1 and hOAT3

Manufacturers	Dose-related DDI index for hOAT1					Dose-related DDI index for hOAT3				
	LSA	RMA	SAB	TSL	Cumulative	LSA	RMA	SAB	TSL	Cumulative
1	—[a]	*0.10*	<0.005	0.06	*0.16*	—	0.06	0.01	*0.30*	*0.37*
2	—	0.04	<0.005	*0.12*	*0.16*	—	0.03	<0.005	*0.58*	*0.61*
3	—	0.05	<0.005	0.09	*0.14*	—	0.03	<0.005	*0.44*	*0.47*
4	—	0.06	<0.005	0.09	*0.15*	—	0.04	<0.005	*0.42*	*0.46*
5	—	*0.12*	<0.005	*0.24*	*0.36*	—	0.08	<0.005	***1.14***	***1.22***
6	0	*0.10*	0.01	*0.11*	*0.21*	0.16	0.07	0.01	*0.54*	*0.78*
7	0	0.03	<0.005	*0.14*	*0.17*	0.07	0.02	<0.005	*0.64*	*0.73*
8	—	0.07	0	*0.30*	*0.37*	—	0.04	0	***1.40***	***1.44***
9	—	*0.14*	0.09	0	*0.23*	—	0.09	*0.10*	0	*0.19*
10	—	0.05	<0.005	0.08	*0.13*	—	0.03	0	*0.36*	*0.39*
11	—	*0.18*	0.01	*0.13*	*0.32*	—	*0.11*	0.01	*0.61*	*0.73*
12	—	0.04	<0.005	*0.18*	*0.22*	—	0.03	<0.005	*0.85*	*0.88*
13	—	0.03	<0.005	*0.15*	*0.18*	—	0.02	<0.005	*0.70*	*0.72*
14	—	0.08	<0.005	*0.16*	*0.24*	—	0.05	<0.005	*0.74*	*0.79*
15	—	0.03	<0.005	*0.15*	*0.18*		0.02	<0.005	*0.73*	*0.75*
16	<0.005	***1.60***	0.02	*0.27*	***1.89***	*0.13*	***1.02***	0.02	***1.27***	***2.43***

[a]— DDI index could not be calculated as no value was reported (NR in Table 8.3). Values in *italic* indicate DDI index ≥ 0.1 threshold value. Values in bold ***italic*** indicate DDI index ≥ 1.

Table 8.6. Estimation of individual and cumulative DDI indices for Danshen injectables from different manufacturers after *i.v.* infusion administration on hOAT1 and hOAT3

Manufacturers	Dose-related DDI index for hOAT1					Dose-related DDI index for hOAT3				
	LSA	RMA	SAB	TSL	Cumulative	LSA	RMA	SAB	TSL	Cumulative
1	—[a]	*0.11*	0.01	*0.12*	*0.24*	—	0.07	0.01	*0.55*	*0.63*
2	—	0.05	<0.005	*0.23*	*0.28*	—	0.03	<0.005	***1.08***	***1.11***
3	—	0.05	<0.005	*0.17*	*0.22*	—	0.03	<0.005	*0.81*	*0.84*
4	—	0.06	<0.005	*0.16*	*0.22*	—	0.04	0.01	*0.77*	*0.82*
5	—	*0.13*	<0.005	*0.45*	*0.58*	—	0.08	<0.005	***2.09***	***2.17***
6	0.01	*0.11*	0.01	*0.21*	*0.33*	0.51	0.07	0.01	*0.98*	***1.57***
7	0.01	0.04	<0.005	*0.25*	*0.29*	0.22	0.02	<0.005	***1.17***	***1.41***
8	—	0.07	0	*0.54*	*0.61*	—	0.05	0	***2.56***	***2.61***
9	—	*0.15*	*0.10*	0	*0.26*	—	*0.10*	*0.12*	0	*0.22*
10	—	0.06	<0.005	*0.14*	*0.20*	—	0.04	<0.005	*0.66*	*0.70*
11	—	*0.20*	0.02	*0.24*	*0.46*	—	*0.13*	0.02	***1.11***	***1.26***
12	—	0.05	<0.005	*0.33*	*0.38*	—	0.03	<0.005	***1.55***	***1.58***
13	—	0.03	<0.005	*0.27*	*0.30*	—	0.02	<0.005	***1.27***	***1.29***
14	—	0.08	0.01	*0.29*	*0.38*	—	0.05	0.01	***1.36***	***1.42***
15	—	0.04	<0.005	*0.28*	*0.32*	—	0.02	<0.005	***1.34***	***1.36***
16	0.01	***1.76***	0.02	*0.50*	***2.28***	*0.39*	***1.12***	0.02	***2.34***	***3.87***

[a]— DDI index could not be calculated as no value was reported (NR in Table 8.3). Values in *italic* indicate DDI index ≥ 0.1 threshold value. Values in bold ***italic*** indicate DDI index ≥ 1**.**

Table 8.7. Estimation of DDI index for Danshen injectables from different batches in the same manufacturer after *i.v.* bolus administration on hOAT1 and hOAT3

Batches	Dose-related DDI index for hOAT1				Dose-related DDI index for hOAT3			
	RMA	SAB	TSL	Cumulative	RMA	SAB	TSL	Cumulative
1	0.02	<0.001	0.07	0.09	0.01	<0.001	*0.35*	*0.36*
2	0.03	<0.001	0.09	*0.12*	0.02	<0.001	*0.41*	*0.43*
3	0.02	<0.001	0.08	*0.10*	0.02	<0.001	*0.37*	*0.39*
4	0.03	<0.001	0.07	*0.10*	0.02	<0.001	*0.35*	*0.37*
5	0.02	<0.001	0.07	0.09	0.02	<0.001	*0.33*	*0.35*
6	0.02	<0.001	0.06	0.08	0.01	<0.001	*0.27*	*0.28*
7	0.03	<0.001	0.08	*0.11*	0.02	<0.001	*0.38*	*0.40*
8	0.02	<0.001	0.07	0.09	0.02	<0.001	*0.35*	*0.37*
9	0.02	<0.001	0.06	0.08	0.01	<0.001	*0.30*	*0.31*
10	0.02	<0.001	0.08	*0.10*	0.02	<0.001	*0.39*	*0.41*
11	0.01	<0.001	0.03	0.04	0.01	<0.001	*0.13*	*0.14*
12	0.03	<0.001	0.08	*0.11*	0.02	<0.001	*0.38*	*0.40*
13	0.03	<0.001	0.09	*0.12*	0.02	<0.001	*0.40*	*0.42*
14	0.03	<0.001	0.09	*0.12*	0.02	<0.001	*0.41*	*0.43*

Values in *italic* indicate DDI index ≥ 0.1 threshold value.

Table 8.8 Estimation of DDI index for Danshen injectables from different batches in the same manufacturer after 1 hr *i.v.* infusion administration on hOAT1 and hOAT3

Batches	Dose-related DDI index for hOAT1				Dose-related DDI index for hOAT3			
	RMA	SAB	TSL	Cumulative	RMA	SAB	TSL	Cumulative
1	0.02	<0.001	*0.14*	*0.16*	0.01	<0.001	*0.64*	*0.65*
2	0.04	<0.001	*0.16*	*0.20*	0.02	<0.001	*0.75*	*0.77*
3	0.03	<0.001	*0.14*	*0.17*	0.02	<0.001	*0.67*	*0.69*
4	0.03	<0.001	*0.14*	*0.17*	0.02	<0.001	*0.65*	*0.67*
5	0.03	<0.001	*0.13*	*0.16*	0.02	<0.001	*0.60*	*0.62*
6	0.02	<0.001	*0.11*	*0.13*	0.01	<0.001	*0.50*	*0.51*
7	0.04	<0.001	*0.15*	*0.19*	0.02	<0.001	*0.70*	*0.72*
8	0.03	<0.001	*0.14*	*0.17*	0.02	<0.001	*0.64*	*0.66*
9	0.02	<0.001	*0.12*	*0.14*	0.02	<0.001	*0.55*	*0.57*
10	0.03	<0.001	*0.15*	*0.18*	0.02	<0.001	*0.71*	*0.73*
11	0.01	<0.001	0.05	0.06	0.01	<0.001	*0.23*	*0.24*
12	0.03	<0.001	*0.15*	*0.18*	0.02	<0.001	*0.70*	*0.72*
13	0.03	<0.001	*0.16*	*0.19*	0.02	<0.001	*0.74*	*0.76*
14	0.04	<0.001	*0.16*	*0.20*	0.02	<0.001	*0.75*	*0.77*

Values in *italic* indicate DDI index ≥ 0.1 threshold value.

8.C RESULTS

8.C.1 Cumulative inhibitory effects of LSA, RMA, and TSL on hOAT1 and hOAT3

Accumulation of PAH in the CHO-hOAT1 cell line (4.6 ± 0.3 pmol/mg protein/10 min) was markedly greater than that in the empty vector background CHO-EV cells (0.9 ± 0.3 pmol/mg protein/10 min; Figure 8.1A). LSA (10 µM), RMA (1 µM) and TSL (50 µM) produced 61 ± 3%, 60 ± 1%, and 52 ± 6% inhibition on hOAT1-mediated PAH uptake, respectively. Further, application of these three compounds together (at the specified concentrations) yielded a significantly increased inhibition (72 ± 7%) on hOAT1 transport activity, compared to the individual inhibitory effects of each compound (Figure 8.1A). Stably transfected hOAT3-expressing (HEK-hOAT3) cells showed significantly enhanced accumulation of ES (~4 fold) relative to empty vector background HEK-EV cells (6.2 ± 0.5 vs. 1.5 ± 0.2 pmol/mg protein/10 min, respectively; Figure 8.1B). Similarly, LSA (0.5 µM), RMA (0.5 µM) and TSL (10 µM) produced approximately 20 ± 2%, 53 ± 6%, and 45 ± 2% inhibition, respectively. When these compounds were included as a mixture in the incubation solution at the above concentrations, the observed inhibition significantly increased to 81 ± 10%. Therefore, LSA, RMA and TSL, known competitive inhibitors for hOAT1 and hOAT3, showed a cumulative inhibitory effect on hOAT1- and hOAT3-mediated uptake.

8.C.2 Pharmacokinetic modeling of clinical data

Performing an iterative model discrimination process revealed that an open two-compartmental model with *i.v.* infusion and first-order elimination yielded the lowest values of AIC, SBC, and WSSR, and this model was used to fit the plasma concentration-time profile data for LSA, RMA, SAB and TSL (Figure 8.2). Moreover, weighted residuals were randomly distributed in the weighted residuals vs. observed concentrations plot (data not shown). The

observed and predicted concentration-time profiles for each Danshen component are shown in Figure 8.2. Final pharmacokinetic model parameter estimates for each Danshen component are summarized in Table 8.2. Data for CA, another component in Danshen preparations, failed to fit any of the tested models. Overall, the model produced excellent fits of the actual data.

8.C.3 Estimation of cumulative DDI index and evaluation of OAT-mediated DDI potency for Danshen injectables

In clinical practice, Danshen injectables are commonly administered by *i.v.* bolus injection or *i.v.* infusion. The model parameters for LSA, RMA, SAB and TSL were used to simulate plasma concentration using the two compartment model with *i.v.* bolus or *i.v.* infusion administration and first-order elimination for a given dose, assuming the examined Danshen components exhibit "dose-proportional pharmacokinetics" and that the pharmacokinetic behavior of each Danshen component is not affected by the presence of any of the other components. As the plasma concentration of LSA, RMA, SAB or TSL did not reach steady-state (C_{ss}) after 60 min *i.v.* infusion, C_{max} values (plasma concentration at 1 h) were used for estimation of individual DDI index and cumulative DDI index.

As shown in Table 8.3, the content of Danshen components in injectables from different manufacturers has been determined (103, 104, 198, 200). Marked variation was observed between Danshen products from different manufacturers, with the content of LSA, RMA, SAB and TSL, showing 2.3-, 73-, 175-, and 4.9-fold variation, respectively. In addition, for Danshen injectables produced by a single manufacturer, the content of RMA, SAB, and TSL showed 3-, 6.7-, and 3.2-fold variation between different lots/batches (Table 8.4). As a consequence, the predicted C_{max} values of of LSA, RMA, SAB and TSL in these injectables exhibited the same range of variation. With this information, the DDI index (for individual components) and the

cumulative DDI index (for mixtures) were calculated (Tables 8.5 and 8.6). Most of these investigated Danshen injectables showed hOAT1- and hOAT3-mediated DDI potential (cumulative DDI index > 0.1), and the majority of preparations exhibited stronger interaction potential with hOAT3 compared to hOAT1. Among Danshen components, TSL emerged as making the greatest contribution to DDI potential, while LSA and RMA also showed substantial individual contribution in some products. SAB failed to exhibit DDI potential in most injectables. The DDI indices for individual components and the cumulative DDI indices were also calculated for different batches/lots of a Danshen injectable produced by the same manufacturer (Tables 8.7 and 8.8) (138). These Danshen products showed significant hOAT3-mediated DDI potential for both *i.v.* bolus injection and *i.v.* infusion use. In addition, the RMA and TSL content in some batches were high enough to cause hOAT1-mediated DDIs when delivered as *i.v.* bolus or *i.v.* infusion administration.

8.D DISCUSSION

Botanical drug products are currently increasing in popularity because of renewed interest in complementary and alternative therapies. Herbal medicines, which are derived from plants, are always considered "natural" and, therefore, are often perceived as safe by patients and the general public. However, because of their wide use as complementary and alternative medicines, they are often used in combination therapy with other prescribed and OTC drugs. As a result, numerous clinical cases of phytomedicine-associated DDIs have been identified (201-203), making it necessary to explore the DDI potential between herbal medicines and co-administered drugs more systemically. Because herbal drugs contain mixtures of plant components or extracts, they are extraordinarily complex in their composition, particularly when compared with prescription medications, which commonly contain a few active ingredients. An important caveat to herbal medicines is that some of the major components may not have any therapeutic benefit, but still possess significant DDI potential due to high systemic/peak exposure *in vivo*. Further, these components often share structural and physicochemical properties and, as such, might exert cumulative DDI effects. Currently, most transporter-mediated DDI studies focus on the interaction of each single component with the drug in question and, therefore, may underestimate the overall DDI potential for complex botanical drug products (201-203).

Presently, the individual DDI index, calculated as [unbound]C_{max}/K_i (or IC_{50}), is thought to reasonably predict *in vivo* DDI potential for a compound on a specific transporter. However, for herbal medicines, it is necessary to consider the overall inhibitory effects induced by all of the components in order for the DDI index to reflect the interaction potential for the product as a whole. In addition, the content of major components in herbal products is often influenced by factors such as extraction methods, cultivars, cultivation region, manufacturing processes, and

quality control criteria, which differ among manufacturers. Therefore, it might be more relevant to explore pharmaceutical product-specific DDI indices rather than compound-related indices.

In this study, the cumulative inhibitory effect of major Danshen components on OAT-mediated substrate uptake was assessed. Human OAT1 and hOAT3 transport activity was significantly lower when the components were applied as a mixture (LSA, RMA and TSL) as compared with being applied individually. These results suggested that in some situations the traditional DDI index might not reflect the true inhibition level of a multi-component system. Therefore, the cumulative DDI index, calculated as the sum of DDI indices for each individual component, was proposed in the present study to evaluate the DDI potential for such mixture. The individual DDI indices for the single compounds, LSA (10 µM), RMA (1 µM), and TSL (50 µM), as well as the cumulative DDI index for a mixture at those concentrations, on hOAT1 were 0.45, 2.9, 1.2, and 4.6, respectively. Such DDI indices predicted inhibition levels of 33%, 74%, 55%, and 82% for LSA, RMA, TSL, and the mixture, respectively, which corresponded closely with the observed inhibition profiles, 61 ± 3%, 60 ± 1%, 52 ± 6%, and 72 ± 7% for RMA, TSL, and the mixture, respectively. Similarly, the individual DDI indices for LSA (0.5 µM), RMA (0.5 µM) and TSL (10 µM), as well as the cumulative DDI index for the mixture, were 0.9, 0.9, 1.2, and 3.0, respectively, indicating that the predicted inhibition levels (46%, 48%, 54%, and 74% for LSA, RMA, TSL and the mixture, respectively) were comparable with the observed values, (61 ± 3%, 60 ± 1%, 52 ± 6%, and 81 ± 10% for LSA, RMA, TSL and the mixture, respectively). These data support use of the cumulative DDI index as a suitable indicator for evaluation of the DDI potential for complex mixtures.

The same threshold value of DDI index≥ 0.1 (transport activity decreased by 9%), as currently recommended for further individual component assessment, was maintained for the

cumulative DDI index. The estimated cumulative DDI indices for investigated Danshen injectables on hOAT1 and hOAT3 were greater than 0.1 in most cases. In addition, the cumulative DDI indices for hOAT3 were much greater than those for hOAT1 for most investigated Danshen injectables. As shown in Tables. 8.5 and 8.6, the cumulative DDI indices for hOAT3 exceeded 1 for a number of Danshen injectables, administered by *i.v.* bolus injection and 60 min *i.v.* infusion administration, indicating that more than 50% of hOAT3 transport function could be inhibited. Only one product induced a cumulative DDI index > 1 on hOAT1 due to a high RMA content. In general, the results demonstrate a strong potential that OAT function likely would be impaired *in vivo* after administration of these products, manifesting as reduced renal elimination of co-administered drugs that undergo OAT-mediated active secretion (Tables 8.5-8.8).

Among these Danshen components, TSL can be identified as the main contributor to the cumulative DDI index because of its relatively high content in preparations and low degree of plasma protein binding. Collectively, TSL exhibited higher DDI indices for hOAT1 and hOAT3 compared to the other components. Further, the data suggested that the contribution of SAB can be ignored. However, the impact of LSA and RMA on DDI potential cannot be ignored. In some Danshen injectables, RMA showed equal or greater contribution to the cumulative DDI index for hOAT1 (Tables 8.5 and 8.6). The content of LSA was available only for two investigated products. Nevertheless, LSA's high affinity for hOAT3 yielded an individual DDI index for LSA that accounts for a significant portion of the cumulative DDI index (Tables 8.5 and 8.6). Similarly, as shown in Table 8.7, such effects can yield a cumulative DDI index above the threshold value (0.1), while neither of the single component (RMA and TSL) DDI indices were greater than 0.1. In other words, considering only single component DDI assessment would

suggest no concern for Danshen-mediated *in vivo* DDIs, whereas the cumulative DDI index would indicate such a concern.

Like other herbal medicines, there is great variation in the content of major constituents of Danshen injectables. The content of LSA, RMA, SAB, and TSL, showed 2.3-, 73-, 175-, and 4.9-fold variation between Danshen products from different manufacturers (Table 8.3). Additionally, RMA, SAB and TSL showed 3-, 6.7- and 3.2-fold variation in content between different lots/batches of a product produced by a single manufacturer (Table 8.4). As a result, such variation leads to marked differences in the cumulative DDI indices for these products. According to Tables 8.5 and 8.6, Danshen products from different manufacturers exhibited 2.3- and 3.1-fold difference in the hOAT1-associated cumulative DDI index for *i.v* bolus and *i.v.* infusion administration, respectively. Such discrepancy was even higher for the hOAT3-associated cumulative DDI index, which exhibited 7.6- and 11.9-fold differences for *i.v* bolus and *i.v.* infusion administration, respectively. Variability in composition between batches/lots led to ~3-fold range in cumulative DDI indices (Tables 8.7 and 8.8). Clearly, estimating a general DDI potential for the range of Danshen injectables is difficult. In order to help address this problem, standardization of content and quality control measures should be established.

Danshen also is used in clinical therapy as tablets and "dripping pills" (100). The phenolic acid components investigated in the present work are also major components in these oral dosage forms. Unlike injections, TSL was the only component detectable in plasma after oral administration of Danshen products (116, 204). Therefore, TSL might be the only component with the potential of causing OAT-mediated DDIs *in vivo* after oral administration of Danshen preparations. However, there is a marked discrepancy in plasma concentration of TSL in clinical pharmacokinetic studies. Pei *et al.* reported that C_{max} of TSL was ~7.5 µg/mL (38 µM) after oral

administration of 250 mg Danshen pills (204), while another independent investigation revealed that the C_{max} of TSL was much lower (~50 ng/mL or 0.25 µM) even with a higher dose (750 mg Danshen pills) (116). Knowing that Danshen pills used in these studies were produced by the same manufacturer, the large difference in TSL C_{max} might be due to variation in the content of TSL between different batches. Unfortunately, the actual content of TSL was not reported (204). Without further studies to demonstrate the peak exposure of TSL, it is impractical to estimate DDI potential for Danshen oral dosages forms. However, a TSL C_{max} = 7.5 µg/mL might be sufficient to cause significant DDI (DDI index = 0.9 and 6 for hOAT1 and hOAT3, respectively), while a C_{max} of 50 ng/mL is not (DDI index < 0.1 for both hOAT1 and hOAT3).

There are some limitations to the present study. Currently, there is a lack of clinical pharmacokinetic data for the Danshen components CA and SAA, which are also potent OAT inhibitors (51, 190). Potential phase 2 metabolites of Danshen components may also impact OAT function. As a result, the contribution of these compounds to OAT-mediated DDIs cannot be estimated, potentially indicating that even the cumulative DDI potentials reported herein may actually underestimate the true DDI potential of Danshen injectables. Additionally, DDIs between each compound likely may occur, especially for TSL, which could undergo OAT-mediated renal elimination *in vivo*. The presence of CA, LSA, SAA and SAB in Danshen preparations might affect this renal elimination of TSL, and plasma concentration of TSL may be elevated depending on the achieved systemic exposures of CA, LSA, SAA and SAB, which in turn, influences TSL-associated DDIs. Finally, such DDI potential estimation was based on the peak exposure level. As shown in Table 8.2, considering the relative $t_{1/2}^{elimination}$ of these Danshen components, especially for TSL ($t_{1/2}^{elimination}$ = 1.6 hr), the main determinant for DDI potential of Danshen injectables, the DDI duration window might be short (< 2 hr).

In conclusion, the major Danshen components, LSA, RMA, and TSL, were demonstrated to elicit cumulative inhibitory effects on hOAT1- and hOAT3-mediated substrate uptake. The cumulative DDI index was introduced as a more comprehensive index to evaluate DDI potential for multiple-component Danshen injectables. Even though TSL appears to exert a dominant contribution to the cumulative DDI index, the potential impact of LSA and RMA cannot be ignored. The large cumulative DDI indices (particularly those $\gg$ 1) suggested that Danshen injectables have a strong potential to cause OAT-mediated DDIs *in vivo* and underscore the need for improved manufacturing standards to eliminate such wanton product variability and protect the public.

CHAPTER 9

OVERALL CONCLUSIONS AND FUTURE DIRECTIONS

Natural products have been used as first-line therapeutics, complementary/alternative medicines, and dietary supplements for thousands of years (205). Currently, herbal therapy is receiving renewed interest throughout the world as products produced from plants are considered "natural" and therefore often perceived as having no potential for toxic effects by patients. However, information about the safety and efficacy profiles for these compounds is still limited compared to western drugs. Indeed, many side effects associated with natural products have been reported over the last two decades (131, 132). A number of studies have demonstrated that transporter proteins, including OATs, can be sites of DDIs, and that transporter-mediated DDIs contributed to reported side effects (39, 77, 129). While some natural compounds are known substrates (*e.g.*, aristolochic acid, caffeic acid, dihydrocaffeic acid, dihydroferulic acid, and ferulic acid) or inhibitors (ellagic acid, stevioside, and caffeic acid) of OATs, the interaction of most natural products with OATs are virtually unknown (48, 50, 51). As a result, it is necessary to explore OAT-mediated natural product-drug interactions to improve herbal product safety and efficacy. This dissertation thus characterized the potential interaction of 22 selected natural

compounds as major organic acid components of herbal medicines/food and exhibiting significant systemic exposure.

Danshen (*Salvia miltiorrhiza*) is a commonly used Chinese herbal medicine for the treatment of cardiovascular diseases (100-102). In Chapters 3 and 4, the inhibitory effects of hydrophilic Danshen components on the function of mOat1 and mOat3 were assessed. At 1 mM, all of tested compounds, including LSA, RMA, SAA, SAB, and TSL, showed significant inhibition on mOat1 and mOat3. Kinetic analysis demonstrated a competitive mechanism of inhibition for LSA, RMA, SAA. K_i values were estimated as 14.9 ± 4.9 µM for LSA, 5.5 ± 2.2 µM for RMA, 4.9 ± 2.2 µM for SAA, 236 ± 90 µM for SAB, and 136 ± 17 µM for TSL on mOat1-mediated transport and as 31.1 ± 7.0 µM for LSA, 4.3 ± 0.2 µM for RMA, 21.3 ± 7.7 µM for SAA, 845 ± 287 µM for SAB, and 1940 ± 486 µM for TSL on mOat3-mediated transport. Further work was conducted to study the influence of five Danshen components (LSA, RMA, SAA, SAB, and TSL) on human OATs, including hOAT1, hOAT3, and hOAT4 (shown in Chapter 4). Similarly, these compounds exhibited competitive inhibition of hOAT1 and hOAT3. At clinical plasma concentrations, the calculated DDI indices were much greater than 0.1, indicating a strong interaction potential for LSA, RMA and TSL on both hOAT1 and hOAT3 and for LSA on hOAT3. In addition, notable species differences appeared to exist in terms of inhibitory potency among mouse and human. Generally, Danshen components showed preferential affinity (by 1-2 orders of magnitude) for human OATs compared with their murine orthologs.

Numerous studies have demonstrated that phenolic acids exert beneficial health effects such as anti-oxidant, anti-carcinogenic, and anti-inflammatory activities (140). In addition, people are exposed to these compounds from dietary sources, including common fruits, vegetables, and beverages (43). Some phenolic acids have been identified as the substrates or inhibitors of OATs

(50, 51). In Chapter 5, the potential interaction of nine dietary phenolic acids, including *p*-coumaric acid, ferulic acid, gallic acid, gentisic acid, 4-hydroxybenzoic acid, protocatechuic acid, sinapinic acid, syringic acid, and vanillic acid with hOAT1, hOAT3, and hOAT4 was investigated. At 100 µM, all compounds significantly inhibited hOAT3 transport, while ferulic, gallic, protocatechuic, sinapinic, and vanillic acid significantly blocked hOAT1 activity. Sinapinic acid was the only test compound exhibiting significant inhibition on hOAT4 (~35%). Estimated IC_{50} values ranged from 1.24 to 18.1 µM for hOAT1 and from 7.35 to 87.4 µM for hOAT3 for selected compounds exhibiting potent inhibition from the preliminary screening. Given the expected clinical unbound plasma concentrations, maximum DDI indices for gallic and gentisic acid are much greater than 0.1, indicating a very strong potential for DDIs on hOAT1 and/or hOAT3. Therefore, gallic acid from foods or herbal supplements, or gentisic acid from salicylate-based drug metabolism, may significantly alter the pharmacokinetics of concomitant drugs that are hOAT1 and/or hOAT3 substrates.

As shown in Chapter 6, the potential interaction of some natural dietary/herbal anionic compounds, including flavonoids (catechin and epicatechin), chlorogenic acids (1,3- and 1,5-dicaffeoylquinic acid), phenolic acids (ginkgolic acids (13:0), (15:1), and (17:1)), and other anionic compounds (ursolic acid and 18β-glycyrrhetinic acid), with hOAT1, hOAT3, and hOAT4 were also investigated. The most important finding of this part was that 1,3-dicaffeoylquinic acid and 18β-glycyrrhetinic acid exhibited high affinity with hOAT1, with IC_{50} values estimated as 1.2 ± 0.4 µM and 2.7 ± 0.2 µM, respectively. These data indicate that 1,3-dicaffeoylquinic acid and 18β-glycyrrhetinic acid have the potential to cause significant hOAT1-mediated DDIs *in vivo*, which should be considered during clinical use and in future drug development.

Among test phenolic acids, gallic acid and gentisic acid undergo renal elimination as their unchanged form (144, 163). As mentioned in Chapter 5, gallic acid and gentisic acid showed strong affinity with hOAT1 and hOAT3. Therefore, OATs might be involved in urinary excretion of these compounds. In Chapter 7, a new, rapid, and sensitive LC-MS/MS method was developed and validated for the simultaneous determination of gallic acid and gentisic acid in cell lysate, using Danshensu as the IS. Compared to previously reported LC-MS/MS-based methods, the established method increased speed, sensitivity and linear dynamic range. The total run time was 3 min and calibration curves were linear over the concentrations of 0.33–2400 ng/mL for both compounds (r^2>0.995). In addition, adverse matrix effects were investigated in samples with cell lysate-derived biological matrix. This assay was successfully applied in a cellular uptake study to determine the intracellular concentrations of gallic acid and gentisic acid in mOat1- and mOat3-expressing cells. Gallic acid was identified as a novel substrate of mOat1 using the method.

Most herbal medicines contain multiple components. Because of the marked similarity in their chemical structures, some, if not all, of these components may be involved in drug transporter-mediated DDI. As a result, investigations on a single component may underestimate the combined DDI potency for botanic products. In Chapter 4, five Danshen components (LSA, RMA, SAA, SAB, and TSL) showed significant inhibition on hOAT1 and hOAT3. In Chapter 8, the cumulative DDI index, defined as the sum of DDI indices for individual components, was calculated for Danshen injectables. Clearly, the cumulative DDI index was significantly higher as compared to individual component-related DDI indices for most Danshen pharmaceutical products. These results indicate that it is necessary to identify major components of herbal therapeutics, whether considered as active ingredients or not, and to investigate their DDI

potential. In addition, due to the variation in cultivation regions, extraction strategy, and manufacturing processes, quality control for herbal medicines is always difficult. In the present study, the cumulative DDI indices were highly variable among different manufacturers or batches. As a result, DDI potency could be different if patients take the same nominal dose of Danshen product, but from different sources. For herbal therapeutics like Danshen, standardized quality control criteria should be established.

These *in vitro* studies have essentially explored the potential inhibitory effects of natural anionic compounds on human and murine OATs. However, to the best of my knowledge, there have been no studies to demonstrate OAT-mediated natural product-drug interaction *in vivo*. Indeed, the findings in this work suggest further *in vivo* studies to confirm DDIs. To achieve this goal, species differences in transporter affinity need to be considered when choosing an appropriate animal model to demonstrate DDI. In Chapter 4, human OATs showed markedly higher affinity with Danshen components compared to murine orthologs. As a result, a clinically relevant concentration in mice would underestimate the clinical DDI magnitude. To solve this problem, a suitable animal model with minimal species differernce should be chosen. Otherwise, the dosing regimen for animal studies would need to be adjusted in order to balance the discrepancy between species. Additionally, DDI evaluations should be conducted with combination of multiple ingredients in addition to single components. With this information and *in vitro* results, the effects of the complete preparation or particular components can be specified from pharmacokinetic studies.

Previous studies demonstrated that typical substrates of OATs are small or medium molecules with negative charge(s) at physiological pH (3). However, it is not well defined what the influences of physicochemical properties are for interaction. In 2013, VanWert *et al.*

investigated the in-depth structure-activity relationship (SAR) of β-lactam antibiotics with respect to their inhibitory activity on mOat3 and hOAT3 (206). They found that a prohibitive hydrogen bond donor group in noninhibitors adjacent to a hydrophobic moiety was important for binding to Oat3 (206). In our study, SAR for phenolic acids with OATs was also performed through collaboration with scientists in the Medicinal Chemistry Department of our University. Unfortunately, there were no conclusive results, possibly due to an insufficient number of test compounds. In the future, as information on the interaction of natural anionic compounds and OATs becomes available, additionally SAR studies should be conducted to provide better understanding on OAT-substrate interaction and potentially indentify new strategy for target-delivered drug synthesis.

In Chapter 7, a sensitive, specific, and robust LC-MS/MS method was developed to determine the concentration of gallic acid and gentisic acid in cell lysate, and gallic acid was identified as a substrate of mOat1. However, the intracellular concentration of gallic acid in both mOat3-expressing and empty vector control cells were below the LLOQ, leaving open the possibility of gallic acid may be a substrate of mOat3. Similarly, whether gentisic acid is a substrate of mOat1 or mOat3 is still unclear. Future research requires modifications (*e.g.*, increased assay sensitivity, number of cells, incubation time, and subsrate concentrations) to accurately measure the cellular uptake of gallic acid and gentisic acid in these cell lines. In addition, it is necessary to determine cellular uptake of gallic acid and gentisic acid in hOAT1- and hOAT3-expressing cells. Unbound renal clearance of gallic acid is higher compared to GFR, indicating that gallic acid undergoes net renal tubular secretion (163). If marked cellular accumulation of gallic acid is observed in hOAT1- and hOAT3-expressing cells, these transporters might be involved in the active secretion of gallic acid. For gentisic acid, although a

significant portion is eliminated in the urine as the unchanged form, it is still necessary to determine unbound renal clearance in clinical studies in order to clarify the potential contrition of hOATs. Even if hOAT1 and hOAT3 transport gentisic acid, their actual contribution for renal elimination might be negligible if unbound renal clearance is not higher than GFR.

Overall, the results indicated a strong DDI potential on OATs for natural anionic components. Future studies need to elucidate such interactions in different populations. As indicated in Chapter 1, OAT-associated SNPs have been found in the human population. These OAT SNPs may lead to ultra, normal, reduced, or null transport activity. In addition, pathological conditions (*e.g.*, acute and chronic renal failure) influence OAT expression in the kidney. Other factors, including gender and age, also are known to have an impact on OAT expression and function. As a result, OAT-mediated DDI potential may be highly variable among these groups. Information on OAT expression and activity regulation would be helpful to predict OAT-mediated DDIs in patients with specific biological or pathological characters, moving towards personalized medicine. Another aspect for future study is to demonstrate potential interaction of other OATs (*e.g.*, OAT2, OAT7, and OAT10) with these test compounds. As OATs have a broad substrate/inhibitor specificity, it is highly possible that test compounds may interact with these transporters and affect organic anion solute flux in other organs such as liver. Furthermore, pharmaceutical industries which are developing herbal products need to refine standardization criteria for the manufacturing process. Finally, generation of humanized transgenic mice becomes increasingly important in an attempt to develop a model system that minimizes inter-species variation of drug transporter affinities. The combination of humanized transgenic mice with knockout mice might serve as suitable complementary preclinical animal models to demonstrate clinically relevant DDIs.

REFERENCES

1. **He L, Vasiliou K, and Nebert DW.** 2009. Analysis and update of the human solute carrier (SLC) gene superfamily. Hum Genomics **3:**195-206.

2. **Sweet DH.** 2005. Organic anion transporter (Slc22a) family members as mediators of toxicity. Toxicol Appl Pharmacol **204:**198-215.

3. **VanWert AL, Gionfriddo MR, and Sweet DH.** 2010. Organic anion transporters: discovery, pharmacology, regulation and roles in pathophysiology. Biopharm Drug Dispos **31:**1-71.

4. **Sweet DH.** 2010. Renal organic cation and anion transport: From physiology to genes. In: McQueen CA, editor. Comprehensive toxicology, 2nd ed., vol. 7. United Kingdom: Elsevier; 2010. p. 23-53.

5. **Tsuchida H, Anzai N, Shin HJ, Wempe MF, Jutabha P, Enomoto A, Cha SH, Satoh T, Ishida M, Sakurai H, and Endou H.** 2010. Identification of a novel organic anion transporter mediating carnitine transport in mouse liver and kidney. Cell Physiol Biochem **25:**511-22.

6. **Eraly SA, Hamilton BA, and Nigam SK.** 2003. Organic anion and cation transporters occur in pairs of similar and similarly expressed genes. Biochem Biophys Res Commun **300:**333-42.

7. **Li T, Walsh JR, Ghishan FK, and Bai L.** 2004. Molecular cloning and characterization of a human urate transporter (hURAT1) gene promoter. Biochim Biophys Acta **1681:**53-8.

8. **Ogasawara K, Terada T, Asaka J, Katsura T, and Inui K.** 2006. Human organic anion transporter 3 gene is regulated constitutively and inducibly via a cAMP-response element. J Pharmacol Exp Ther **319:**317-22.

9. **Wegner W, Burckhardt BC, Burckhardt G, and Henjakovic M.** 2012. Male-dominant activation of rat renal organic anion transporter 1 (Oat1) and 3 (Oat3) expression by transcription factor BCL6. PLoS One **7:**e35556.

10. **Blumenfeld M, Maury M, Chouard T, Yaniv M, and Condamine H.** 1991. Hepatic nuclear factor 1 (HNF1) shows a wider distribution than products of its known target genes in developing mouse. Development **113:**589-99.

11. **Mendel DB, and Crabtree GR.** 1991. HNF-1, a member of a novel class of dimerizing homeodomain proteins. J Biol Chem **266:**677-80.

12. **Lazzaro D, De Simone V, De Magistris L, Lehtonen E, and Cortese R.** 1992. LFB1 and LFB3 homeoproteins are sequentially expressed during kidney development. Development **114:**469-79.

13. **Maher JM, Slitt AL, Callaghan TN, Cheng X, Cheung C, Gonzalez FJ, and Klaassen CD.** 2006. Alterations in transporter expression in liver, kidney, and duodenum after targeted disruption of the transcription factor HNF1alpha. Biochem Pharmacol **72:**512-22.

14. **Kikuchi R, Kusuhara H, Hattori N, Kim I, Shiota K, Gonzalez FJ, and Sugiyama Y.** 2007. Regulation of tissue-specific expression of the human and mouse urate transporter 1 gene by hepatocyte nuclear factor 1 alpha/beta and DNA methylation. Mol Pharmacol **72:**1619-25.

15. **Saji T, Kikuchi R, Kusuhara H, Kim I, Gonzalez FJ, and Sugiyama Y.** 2008. Transcriptional regulation of human and mouse organic anion transporter 1 by hepatocyte nuclear factor 1 alpha/beta. J Pharmacol Exp Ther **324:**784-90.

16. **Kikuchi R, Kusuhara H, Hattori N, Shiota K, Kim I, Gonzalez FJ, and Sugiyama Y.** 2006. Regulation of the expression of human organic anion transporter 3 by hepatocyte nuclear factor 1alpha/beta and DNA methylation. Mol Pharmacol **70:**887-96.

17. **Klein K, Jungst C, Mwinyi J, Stieger B, Krempler F, Patsch W, Eloranta JJ, and Kullak-Ublick GA.** 2010. The human organic anion transporter genes OAT5 and OAT7 are transactivated by hepatocyte nuclear factor-1alpha (HNF-1alpha). Mol Pharmacol **78:**1079-87.

18. **Jin L, Kikuchi R, Saji T, Kusuhara H, and Sugiyama Y.** 2012. Regulation of tissue-specific expression of renal organic anion transporters by hepatocyte nuclear factor 1 alpha/beta and DNA methylation. J Pharmacol Exp Ther **340:**648-55.

19. **Ogasawara K, Terada T, Asaka J, Katsura T, and Inui K.** 2007. Hepatocyte nuclear factor-4{alpha} regulates the human organic anion transporter 1 gene in the kidney. Am J Physiol Renal Physiol **292:**F1819-26.

20. **Popowski K, Eloranta JJ, Saborowski M, Fried M, Meier PJ, and Kullak-Ublick GA.** 2005. The human organic anion transporter 2 gene is transactivated by hepatocyte nuclear factor-4 alpha and suppressed by bile acids. Mol Pharmacol **67:**1629-38.

21. **Ljubojevic M, Herak-Kramberger CM, Hagos Y, Bahn A, Endou H, Burckhardt G, and Sabolic I.** 2004. Rat renal cortical OAT1 and OAT3 exhibit gender differences determined by both androgen stimulation and estrogen inhibition. Am J Physiol Renal Physiol **287:**F124-38.

22. **Barros SA, Srimaroeng C, Perry JL, Walden R, Dembla-Rajpal N, Sweet DH, and Pritchard JB.** 2009. Activation of protein kinase Czeta increases OAT1 (SLC22A6)- and OAT3 (SLC22A8)-mediated transport. J Biol Chem **284:**2672-9.

23. **Li S, Duan P, and You G.** 2010. Regulation of human organic anion transporter 3 by peptide hormone bradykinin. J Pharmacol Exp Ther **333:**970-5.

24. **Duan P, Li S, and You G.** 2009. Angiotensin II inhibits activity of human organic anion transporter 3 through activation of protein kinase Calpha: accelerating endocytosis of the transporter. Eur J Pharmacol **627:**49-55.

25. **Zalups RK, and Ahmad S.** 2005. Handling of cysteine S-conjugates of methylmercury in MDCK cells expressing human OAT1. Kidney Int **68:**1684-99.

26. **Aslamkhan AG, Han YH, Yang XP, Zalups RK, and Pritchard JB.** 2003. Human renal organic anion transporter 1-dependent uptake and toxicity of mercuric-thiol conjugates in Madin-Darby canine kidney cells. Mol Pharmacol **63:**590-6.

27. **Torres AM, Dnyanmote AV, Bush KT, Wu W, and Nigam SK.** 2011. Deletion of multispecific organic anion transporter Oat1/Slc22a6 protects against mercury-induced kidney injury. J Biol Chem **286:**26391-5.

28. **Wojcikowski K, Johnson DW, and Gobe G.** 2004. Medicinal herbal extracts -- renal friend or foe? Part one: the toxicities of medicinal herbs. Nephrology (Carlton) **9:**313-8.

29. **Jha V, and Chugh KS.** 2003. Nephropathy associated with animal, plant, and chemical toxins in the tropics. Semin Nephrol **23:**49-65.

30. **Vanherweghem LJ.** 1998. Misuse of herbal remedies: the case of an outbreak of terminal renal failure in Belgium (Chinese herbs nephropathy). J Altern Complement Med **4:**9-13.

31. **Cosyns JP, Jadoul M, Squifflet JP, Wese FX, and van Ypersele de Strihou C.** 1999. Urothelial lesions in Chinese-herb nephropathy. Am J Kidney Dis **33:**1011-7.

32. **Reginster F, Jadoul M, and van Ypersele de Strihou C.** 1997. Chinese herbs nephropathy presentation, natural history and fate after transplantation. Nephrol Dial Transplant **12:**81-6.

33. **Debelle FD, Vanherweghem JL, and Nortier JL.** 2008. Aristolochic acid nephropathy: a worldwide problem. Kidney Int **74:**158-69.

34. **Lebeau C, Debelle FD, Arlt VM, Pozdzik A, De Prez EG, Phillips DH, Deschodt-Lanckman MM, Vanherweghem JL, and Nortier JL.** 2005. Early proximal tubule injury in experimental aristolochic acid nephropathy: functional and histological studies. Nephrol Dial Transplant **20:**2321-32.

35. **Pozdzik AA, Salmon IJ, Debelle FD, Decaestecker C, Van den Branden C, Verbeelen D, Deschodt-Lanckman MM, Vanherweghem JL, and Nortier JL.** 2008. Aristolochic acid induces proximal tubule apoptosis and epithelial to mesenchymal transformation. Kidney Int **73:**595-607.

36. **Dickman KG, Sweet DH, Bonala R, Ray T, and Wu A.** 2011. Physiological and molecular characterization of aristolochic acid transport by the kidney. J Pharmacol Exp Ther **338:**588-97.

37. **Sato N, Takahashi D, Chen SM, Tsuchiya R, Mukoyama T, Yamagata S, Ogawa M, Yoshida M, Kondo S, Satoh N, and Ueda S.** 2004. Acute nephrotoxicity of aristolochic acids in mice. J Pharm Pharmacol **56:**221-9.

38. **Shibutani S, Dong H, Suzuki N, Ueda S, Miller F, and Grollman AP.** 2007. Selective toxicity of aristolochic acids I and II. Drug Metab Dispos **35:**1217-22.

39. **Bakhiya N, Arlt VM, Bahn A, Burckhardt G, Phillips DH, and Glatt H.** 2009. Molecular evidence for an involvement of organic anion transporters (OATs) in aristolochic acid nephropathy. Toxicology **264:**74-9.

40. **Babu E, Takeda M, Nishida R, Noshiro-Kofuji R, Yoshida M, Ueda S, Fukutomi T, Anzai N, and Endou H.** 2010. Interactions of human organic anion transporters with aristolochic acids. J Pharmacol Sci **113:**192-6.

41. **Xue X, Gong LK, Maeda K, Luan Y, Qi XM, Sugiyama Y, and Ren J.** 2011. Critical role of organic anion transporters 1 and 3 in kidney accumulation and toxicity of aristolochic acid I. Mol Pharm **8:**2183-92.

42. **Lou Y, Li J, Lu Y, Wang X, Jiao R, Wang S, and Kong L.** 2011. Aristolochic acid-induced destruction of organic ion transporters and fatty acid metabolic disorder in the kidney of rats. Toxicol Lett **201:**72-9.

43. **Russell W, and Duthie G.** 2011. Plant secondary metabolites and gut health: the case for phenolic acids. Proc Nutr Soc **70:**389-96.

44. **Fleschhut J, Kratzer F, Rechkemmer G, and Kulling SE.** 2006. Stability and biotransformation of various dietary anthocyanins in vitro. Eur J Nutr **45:**7-18.

45. **Rababah TM, Ereifej KI, Esoh RB, Al-u'datt MH, Alrababah MA, and Yang W.** 2011. Antioxidant activities, total phenolics and HPLC analyses of the phenolic compounds of extracts from common Mediterranean plants. Nat Prod Res **25:**596-605.

46. **Maggi-Capeyron MF, Ceballos P, Cristol JP, Delbosc S, Le Doucen C, Pons M, Leger CL, and Descomps B.** 2001. Wine phenolic antioxidants inhibit AP-1 transcriptional activity. J Agric Food Chem **49:**5646-52.

47. **Kampa M, Alexaki VI, Notas G, Nifli AP, Nistikaki A, Hatzoglou A, Bakogeorgou E, Kouimtzoglou E, Blekas G, Boskou D, Gravanis A, and Castanas E.** 2004. Antiproliferative and apoptotic effects of selective phenolic acids on T47D human breast cancer cells: potential mechanisms of action. Breast Cancer Res **6:**R63-74.

48. **Whitley AC, Sweet DH, and Walle T.** 2005. The dietary polyphenol ellagic acid is a potent inhibitor of hOAT1. Drug Metab Dispos **33:**1097-100.

49. **Wang L, and Sweet DH.** Active hydrophilic components of the *medicinal herb salvia miltiorrhiza* (Danshen) potently inhibit organic anion transporters 1 (Slc22a6) and 3 (Slc22a8). Evid Based Complement Alternat Med vol. **2012**, Article ID 872458, 8 pages, 2012. .

50. **Wong CC, Barron D, Orfila C, Dionisi F, Krajcsi P, and Williamson G.** 2011. Interaction of hydroxycinnamic acids and their conjugates with organic anion transporters and ATP-binding cassette transporters. Mol Nutr Food Res **55:**979-88.

51. **Uwai Y, Ozeki Y, Isaka T, Honjo H, and Iwamoto K.** 2011. Inhibitory effect of caffeic acid on human organic anion transporters hOAT1 and hOAT3: a novel candidate for food-drug interaction. Drug Metab Pharmacokinet **26:**486-93.

52. **Wang L, and Sweet DH.** 2012. Potential for food-drug interactions by dietary phenolic acids on human organic anion transporters 1 (SLC22A6), 3 (SLC22A8), and 4 (SLC22A11). Biochem Pharmacol **84**:1088-96.

53. **Saito H.** 2009. Pathophysiological regulation of renal SLC22A organic ion transporters in acute kidney injury: pharmacological and toxicological implications. Pharmacol Ther **125:**79-91.

54. **Sun H, Frassetto L, and Benet LZ.** 2006. Effects of renal failure on drug transport and metabolism. Pharmacol Ther **109:**1-11.

55. **Enomoto A, and Endou H.** 2005. Roles of organic anion transporters (OATs) and a urate transporter (URAT1) in the pathophysiology of human disease. Clin Exp Nephrol **9:**195-205.

56. **Shobeiri N, Adams MA, and Holden RM.** 2010. Vascular calcification in animal models of CKD: A review. Am J Nephrol **31:**471-81.

57. **Ji L, Masuda S, Saito H, and Inui K.** 2002. Down-regulation of rat organic cation transporter rOCT2 by 5/6 nephrectomy. Kidney Int **62:**514-24.

58. **Naud J, Michaud J, Beauchemin S, Hebert MJ, Roger M, Lefrancois S, Leblond FA, and Pichette V.** 2011. Effects of chronic renal failure on kidney drug transporters and cytochrome P450 in rats. Drug Metab Dispos **39:**1363-9.

59. **Monica Torres A, Mac Laughlin M, Muller A, Brandoni A, Anzai N, and Endou H.** 2005. Altered renal elimination of organic anions in rats with chronic renal failure. Biochim Biophys Acta **1740:**29-37.

60. **Cihlar T, Lin DC, Pritchard JB, Fuller MD, Mendel DB, and Sweet DH.** 1999. The antiviral nucleotide analogs cidofovir and adefovir are novel substrates for human and rat renal organic anion transporter 1. Mol Pharmacol **56:**570-80.

61. **Uchino S, Kellum JA, Bellomo R, Doig GS, Morimatsu H, Morgera S, Schetz M, Tan I, Bouman C, Macedo E, Gibney N, Tolwani A, and Ronco C.** 2005. Acute renal failure in critically ill patients: a multinational, multicenter study. JAMA **294:**813-8.

62. **Corrigan G, Ramaswamy D, Kwon O, Sommer FG, Alfrey EJ, Dafoe DC, Olshen RA, Scandling JD, and Myers BD.** 1999. PAH extraction and estimation of plasma flow in human postischemic acute renal failure. Am J Physiol **277:**F312-8.

63. **Kwon O, Hong SM, and Blouch K.** 2007. Alteration in renal organic anion transporter 1 after ischemia/reperfusion in cadaveric renal allografts. J Histochem Cytochem **55:**575-84.

64. **Kwon O, Wang WW, and Miller S.** 2008. Renal organic anion transporter 1 is maldistributed and diminishes in proximal tubule cells but increases in vasculature after ischemia and reperfusion. Am J Physiol Renal Physiol **295:**F1807-16.

65. **Schneider R, Sauvant C, Betz B, Otremba M, Fischer D, Holzinger H, Wanner C, Galle J, and Gekle M.** 2007. Downregulation of organic anion transporters OAT1 and OAT3 correlates with impaired secretion of para-aminohippurate after ischemic acute renal failure in rats. Am J Physiol Renal Physiol **292:**F1599-605.

66. **Matsuzaki T, Watanabe H, Yoshitome K, Morisaki T, Hamada A, Nonoguchi H, Kohda Y, Tomita K, Inui K, and Saito H.** 2007. Downregulation of organic anion transporters in rat kidney under ischemia/reperfusion-induced acute renal failure. Kidney Int **71:**539-47.

67. **Di Giusto G, Anzai N, Endou H, and Torres AM.** 2009. Oat5 and NaDC1 protein abundance in kidney and urine after renal ischemic reperfusion injury. J Histochem Cytochem **57:**17-27.

68. **Kunin M, Holtzman EJ, Melnikov S, and Dinour D.** 2012. Urinary organic anion transporter protein profiles in AKI. Nephrol Dial Transplant **27:**1387-95.

69. **Sauvant C, Holzinger H, and Gekle M.** 2006. Prostaglandin E2 inhibits its own renal transport by downregulation of organic anion transporters rOAT1 and rOAT3. J Am Soc Nephrol **17:**46-53.

70. **Myers SI, Wang L, Liu F, and Bartula LL.** 2005. Suprarenal aortic clamping and reperfusion decreases medullary and cortical blood flow by decreased endogenous renal nitric oxide and PGE2 synthesis. J Vasc Surg **42:**524-31.

71. **Tokuyama H, Hayashi K, Matsuda H, Kubota E, Honda M, Okubo K, Ozawa Y, and Saruta T.** 2002. Stenosis-dependent role of nitric oxide and prostaglandins in chronic renal ischemia. Am J Physiol Renal Physiol **282:**F859-65.

72. **Feitoza CQ, Sanders H, Cenedeze M, Camara NO, and Pacheco-Silva A.** 2002. Pretreatment with indomethacin protects from acute renal failure following ischemia-reperfusion injury. Transplant Proc **34:**2979-80.

73. **Schneider R, Meusel M, Renker S, Bauer C, Holzinger H, Roeder M, Wanner C, Gekle M, and Sauvant C.** 2009. Low-dose indomethacin after ischemic acute kidney injury prevents downregulation of Oat1/3 and improves renal outcome. Am J Physiol Renal Physiol **297:**F1614-21.

74. **Hocherl K, Schmidt C, and Bucher M.** 2009. COX-2 inhibition attenuates endotoxin-induced downregulation of organic anion transporters in the rat renal cortex. Kidney Int **75:**373-80.

75. **Welling PG, Dean S, Selen A, Kendall MJ, and Wise R.** 1979. Probenecid: an unexplained effect on cephalosporin pharmacology. Br J Clin Pharmacol **8:**491-5.

76. **Bourke RS, Chheda G, Bremer A, Watanabe O, and Tower DB.** 1975. Inhibition of renal tubular transport of methotrexate by probenecid. Cancer Res **35:**110-6.

77. **Jaehde U, Sorgel F, Reiter A, Sigl G, Naber KG, and Schunack W.** 1995. Effect of probenecid on the distribution and elimination of ciprofloxacin in humans. Clin Pharmacol Ther **58:**532-41.

78. **Honari J, Blair AD, and Cutler RE.** 1977. Effects of probenecid on furosemide kinetics and natriuresis in man. Clin Pharmacol Ther **22:**395-401.

79. **Vallon V, Rieg T, Ahn SY, Wu W, Eraly SA, and Nigam SK.** 2008. Overlapping in vitro and in vivo specificities of the organic anion transporters OAT1 and OAT3 for loop and thiazide diuretics. Am J Physiol Renal Physiol **294:**F867-73.

80. **VanWert AL, and Sweet DH.** 2008. Impaired clearance of methotrexate in organic anion transporter 3 (Slc22a8) knockout mice: a gender specific impact of reduced folates. Pharm Res **25:**453-62.

81. **Vanwert AL, Bailey RM, and Sweet DH.** 2007. Organic anion transporter 3 (Oat3/Slc22a8) knockout mice exhibit altered clearance and distribution of penicillin G. Am J Physiol Renal Physiol **293:**F1332-41.

82. **Vanwert AL, Srimaroeng C, and Sweet DH.** 2008. Organic anion transporter 3 (Oat3/Slc22a8) interacts with carboxyfluoroquinolones, and deletion increases systemic exposure to ciprofloxacin. Mol Pharmacol **74:**122-31.

83. **Mulgaonkar A, Venitz J, and Sweet DH.** 2012. Fluoroquinolone disposition: identification of the contribution of renal secretory and reabsorptive drug transporters. Expert Opin Drug Metab Toxicol **8:**553-69.

84. **Takeda M, Babu E, Narikawa S, and Endou H.** 2002. Interaction of human organic anion transporters with various cephalosporin antibiotics. Eur J Pharmacol **438:**137-42.

85. **Eraly SA, Vallon V, Vaughn DA, Gangoiti JA, Richter K, Nagle M, Monte JC, Rieg T, Truong DM, Long JM, Barshop BA, Kaler G, and Nigam SK.** 2006. Decreased renal organic anion secretion and plasma accumulation of endogenous organic anions in OAT1 knock-out mice. J Biol Chem **281:**5072-83.

86. **Cutler MJ, Urquhart BL, Velenosi TJ, Meyer Zu Schwabedissen HE, Dresser GK, Leake BF, Tirona RG, Kim RB, and Freeman DJ.** 2012. In vitro and in vivo assessment of renal drug transporters in the disposition of mesna and dimesna. J Clin Pharmacol **52:**530-42.

87. **Kyrklund C, Backman JT, Neuvonen M, and Neuvonen PJ.** 2003. Gemfibrozil increases plasma pravastatin concentrations and reduces pravastatin renal clearance. Clin Pharmacol Ther **73:**538-44.

88. **Nakagomi-Hagihara R, Nakai D, and Tokui T.** 2007. Inhibition of human organic anion transporter 3 mediated pravastatin transport by gemfibrozil and the metabolites in humans. Xenobiotica **37:**416-26.

89. **Yuan H, Feng B, Yu Y, Chupka J, Zheng JY, Heath TG, and Bond BR.** 2009. Renal organic anion transporter-mediated drug-drug interaction between gemcabene and quinapril. J Pharmacol Exp Ther **330:**191-7.

90. **Giacomini KM, Huang SM, and Tweedie DJ.** 2010. Membrane transporters in drug development. Nat Rev Drug Discov **9:**215-36.

91. **Bhatnagar V, Xu G, Hamilton BA, Truong DM, Eraly SA, Wu W, and Nigam SK.** 2006. Analyses of 5' regulatory region polymorphisms in human SLC22A6 (OAT1) and SLC22A8 (OAT3). J Hum Genet **51:**575-80.

92. **Xu G, Bhatnagar V, Wen G, Hamilton BA, Eraly SA, and Nigam SK.** 2005. Analyses of coding region polymorphisms in apical and basolateral human organic anion

transporter (OAT) genes [OAT1 (NKT), OAT2, OAT3, OAT4, URAT (RST)]. Kidney Int **68:**1491-9.

93. **Bleasby K, Hall LA, Perry JL, Mohrenweiser HW, and Pritchard JB.** 2005. Functional consequences of single nucleotide polymorphisms in the human organic anion transporter hOAT1 (SLC22A6). J Pharmacol Exp Ther **314:**923-31.

94. **Fujita T, Brown C, Carlson EJ, Taylor T, de la Cruz M, Johns SJ, Stryke D, Kawamoto M, Fujita K, Castro R, Chen CW, Lin ET, Brett CM, Burchard EG, Ferrin TE, Huang CC, Leabman MK, and Giacomini KM.** 2005. Functional analysis of polymorphisms in the organic anion transporter, SLC22A6 (OAT1). Pharmacogenet Genomics **15:**201-9.

95. **Shima JE, Komori T, Taylor TR, Stryke D, Kawamoto M, Johns SJ, Carlson EJ, Ferrin TE, and Giacomini KM.** 2010. Genetic variants of human organic anion transporter 4 demonstrate altered transport of endogenous substrates. Am J Physiol Renal Physiol **299:**F767-75.

96. **Zhou F, Zhu L, Cui PH, Church WB, and Murray M.** 2010. Functional characterization of nonsynonymous single nucleotide polymorphisms in the human organic anion transporter 4 (hOAT4). Br J Pharmacol **159:**419-27.

97. **Han YF, Fan XH, Wang XJ, Sun K, Xue H, Li WJ, Wang YB, Chen JZ, Zhen YS, Zhang WL, Zhou X, and Hui R.** 2011. Association of intergenic polymorphism of organic anion transporter 1 and 3 genes with hypertension and blood pressure response to hydrochlorothiazide. Am J Hypertens **24:**340-6.

98. **Sakurai Y, Motohashi H, Ueo H, Masuda S, Saito H, Okuda M, Mori N, Matsuura M, Doi T, Fukatsu A, Ogawa O, and Inui K.** 2004. Expression levels of renal organic anion transporters (OATs) and their correlation with anionic drug excretion in patients with renal diseases. Pharm Res **21:**61-7.

99. **Sweet DH, Eraly SA, Vaughn DA, Bush KT, and Nigam SK.** 2006. Organic anion and cation transporter expression and function during embryonic kidney development and in organ culture models. Kidney Int **69:**837-45.

100. **Zhou L, Zuo Z, and Chow MS.** 2005. Danshen: an overview of its chemistry, pharmacology, pharmacokinetics, and clinical use. J Clin Pharmacol **45:**1345-59.

101. **Cheng TO.** 2007. Cardiovascular effects of Danshen. Int J Cardiol **121:**9-22.

102. **Jiang RW, Lau KM, Hon PM, Mak TC, Woo KS, and Fung KP.** 2005. Chemistry and biological activities of caffeic acid derivatives from Salvia miltiorrhiza. Curr Med Chem **12:**237-46.

103. **Yuan D, Pan YN, Fu WW, Makino T, and Kano Y.** 2005. Quantitative analysis of the marker compounds in *Salvia miltiorrihiza* root and its phytomedicinal preparations. Chem Pharm Bull (Tokyo) **53:**508-14.

104. **Li X, Yu C, Cai Y, Liu G, Jia J, and Wang Y.** 2005. Simultaneous determination of six phenolic constituents of danshen in human serum using liquid chromatography/tandem mass spectrometry. J Chromatogr B Analyt Technol Biomed Life Sci **820:**41-7.

105. **Zhang JL, Cui M, He Y, Yu HL, and Guo DA.** 2005. Chemical fingerprint and metabolic fingerprint analysis of Danshen injection by HPLC-UV and HPLC-MS methods. J Pharm Biomed Anal **36:**1029-35.

106. **Sweet DH, Bush KT, and Nigam SK.** 2001. The organic anion transporter family: from physiology to ontogeny and the clinic. Am J Physiol Renal Physiol **281:**F197-205.

107. **Sweet DH, Wolff NA, and Pritchard JB.** 1997. Expression cloning and characterization of ROAT1. The basolateral organic anion transporter in rat kidney. J Biol Chem **272:**30088-95.

108. **Sweet DH, Chan LM, Walden R, Yang XP, Miller DS, and Pritchard JB.** 2003. Organic anion transporter 3 (Slc22a8) is a dicarboxylate exchanger indirectly coupled to the Na+ gradient. Am J Physiol Renal Physiol **284:**F763-9.

109. **Schnabolk GW, Gupta B, Mulgaonkar A, Kulkarni M, and Sweet DH.** 2010. Organic anion transporter 6 (Slc22a20) specificity and Sertoli cell-specific expression provide new insight on potential endogenous roles. J Pharmacol Exp Ther **334:**927-35.

110. **Copeland R.** 2000. Enzymes: A practical introduction to structure, mechanism, and data analysis. Wiley-VCH Press Chapter 8.

111. **Cheng Y, and Prusoff WH.** 1973. Relationship between the inhibition constant (K1) and the concentration of inhibitor which causes 50 per cent inhibition (I50) of an enzymatic reaction. Biochem Pharmacol **22:**3099-108.

112. **Bent S.** 2008. Herbal medicine in the United States: review of efficacy, safety, and regulation: grand rounds at University of California, San Francisco Medical Center. J Gen Intern Med **23:**854-9.

113. **Dickman K, Bonala R, Ray T, Wu A, and Sweet DH.** 2008. Presented at the 41st Annual Meeting of the American Society of Nephrology, Philadelphia, PA, Nov. 4-9.

114. **Kaler G, Truong DM, Khandelwal A, Nagle M, Eraly SA, Swaan PW, and Nigam SK.** 2007. Structural variation governs substrate specificity for organic anion transporter (OAT) homologs. Potential remote sensing by OAT family members. J Biol Chem **282:**23841-53.

115. **Eraly SA.** 2008. Organic anion transporter 3 inhibitors as potential novel antihypertensives. Pharmacol Res **58:**257-61.

116. **Lu T, Yang J, Gao X, Chen P, Du F, Sun Y, Wang F, Xu F, Shang H, Huang Y, Wang Y, Wan R, Liu C, Zhang B, and Li C.** 2008. Plasma and urinary tanshinol from Salvia miltiorrhiza (Danshen) can be used as pharmacokinetic markers for cardiotonic pills, a cardiovascular herbal medicine. Drug Metab Dispos **36:**1578-86.

117. **Chang BB, Zhang L, Cao WW, Cao Y, Yang WL, Wang Y, Chen YC, and Liu XQ.** 2010. Pharmacokinetic interactions induced by content variation of major water-soluble components of Danshen preparation in rats. Acta Pharmacol Sin **31:**638-46.

118. **U. S. Department of Health and Human Services and Food and Drug Administration.** Guidance for Industry: Drug Interaction Studies-Study Design, Data Analysis, Implications for Dosing, and Labeling Recommendations 2012. http://www.fda.gov/downloads/Drugs/GuidanceComplianceRegulatoryInformation/Guidances/UCM292362.pdf

119. **Wong CC, Botting NP, Orfila C, Al-Maharik N, and Williamson G.** 2011. Flavonoid conjugates interact with organic anion transporters (OATs) and attenuate cytotoxicity of adefovir mediated by organic anion transporter 1 (OAT1/SLC22A6). Biochem Pharmacol **81:**942-9.

120. **Baba S, Osakabe N, Natsume M, Yasuda A, Muto Y, Hiyoshi K, Takano H, Yoshikawa T, and Terao J.** 2005. Absorption, metabolism, degradation and urinary excretion of rosmarinic acid after intake of Perilla frutescens extract in humans. Eur J Nutr **44:**1-9.

121. **Nakazawa T, and Ohsawa K.** 1998. Metabolism of rosmarinic acid in rats. J Nat Prod **61:**993-6.

122. **Shen Y, Wang X, Xu L, Liu X, and Chao R.** 2009. Characterization of metabolites in rat plasma after intravenous administration of salvianolic acid A by liquid chromatography/time-of-flight mass spectrometry and liquid chromatography/ion trap mass spectrometry. Rapid Commun Mass Spectrom **23:**1810-6.

123. **Zhao D, Gao ZD, Han DE, Li N, Zhang YJ, Lu Y, Li TT, and Chen XJ.** 2012. Influence of rifampicin on the pharmacokinetics of salvianolic acid B may involve inhibition of organic anion transporting polypeptide (Oatp) mediated influx. Phytother Res **26:**118-21.

124. **Takahashi K, Ouyang X, Komatsu K, Nakamura N, Hattori M, Baba A, and Azuma J.** 2002. Sodium tanshinone IIA sulfonate derived from Danshen (*Salvia miltiorrhiza*) attenuates hypertrophy induced by angiotensin II in cultured neonatal rat cardiac cells. Biochem Pharmacol **64:**745-9.

125. **Tang MK, Ren DC, Zhang JT, and Du GH.** 2002. Effect of salvianolic acids from *Radix Salviae miltiorrhizae* on regional cerebral blood flow and platelet aggregation in rats. Phytomedicine **9:**405-9.

126. **Liu CL, Xie LX, Li M, Durairajan SS, Goto S, and Huang JD.** 2007. Salvianolic acid B inhibits hydrogen peroxide-induced endothelial cell apoptosis through regulating PI3K/Akt signaling. PLoS One **2:**e1321.

127. **Zhao GR, Zhang HM, Ye TX, Xiang ZJ, Yuan YJ, Guo ZX, and Zhao LB.** 2008. Characterization of the radical scavenging and antioxidant activities of danshensu and salvianolic acid B. Food Chem Toxicol **46:**73-81.

128. **Li YG, Song L, Liu M, Hu ZB, and Wang ZT.** 2009. Advancement in analysis of Salviae miltiorrhizae Radix et Rhizoma (Danshen). J Chromatogr A **1216:**1941-53.

129. **Burnell JM, and Kirby WM.** 1951. Effectiveness of a new compound, benemid, in elevating serum penicillin concentrations. J Clin Invest **30:**697-700.

130. **Ho ES, Lin DC, Mendel DB, and Cihlar T.** 2000. Cytotoxicity of antiviral nucleotides adefovir and cidofovir is induced by the expression of human renal organic anion transporter 1. J Am Soc Nephrol **11:**383-93.

131. **Hu Z, Yang X, Ho PC, Chan SY, Heng PW, Chan E, Duan W, Koh HL, and Zhou S.** 2005. Herb-drug interactions: a literature review. Drugs **65:**1239-82.

132. **Fugh-Berman A.** 2000. Herb-drug interactions. Lancet **355:**134-8.

133. **Srimaroeng C, Chatsudthipong V, Aslamkhan AG, and Pritchard JB.** 2005. Transport of the natural sweetener stevioside and its aglycone steviol by human organic anion transporter (hOAT1; SLC22A6) and hOAT3 (SLC22A8). J Pharmacol Exp Ther **313:**621-8.

134. **Ueo H, Motohashi H, Katsura T, and Inui K.** 2005. Human organic anion transporter hOAT3 is a potent transporter of cephalosporin antibiotics, in comparison with hOAT1. Biochem Pharmacol **70:**1104-13.

135. **Hasegawa M, Kusuhara H, Endou H, and Sugiyama Y.** 2003. Contribution of organic anion transporters to the renal uptake of anionic compounds and nucleoside derivatives in rat. J Pharmacol Exp Ther **305:**1087-97.

136. **Giacomini KM, Huang SM, Tweedie DJ, Benet LZ, Brouwer KL, Chu X, Dahlin A, Evers R, Fischer V, Hillgren KM, Hoffmaster KA, Ishikawa T, Keppler D, Kim RB, Lee CA, Niemi M, Polli JW, Sugiyama Y, Swaan PW, Ware JA, Wright SH, Yee SW, Zamek-Gliszczynski MJ, and Zhang L.** 2010. Membrane transporters in drug development. Nat Rev Drug Discov **9:**215-36.

137. **Yang X, Wang Y, Liu Y, and Tang X.** 2007. Effects of *Panax quinquefolium* protopanaxadiol saponins on the animal and human plasma protein binding of salvianolic acids *in vitro*. *Asian Journal of Pharmaceutical Sciences* **2:**10.

138. **Xu JZ, Shen J, Cheng YY, and Qu HB.** 2008. Simultaneous detection of seven phenolic acids in Danshen injection using HPLC with ultraviolet detector. J Zhejiang Univ Sci B **9:**728-33.

139. **Kurlbaum M, and Hogger P.** 2011. Plasma protein binding of polyphenols from maritime pine bark extract (USP). J Pharm Biomed Anal **54:**127-32.

140. **Croft KD.** 1998. The chemistry and biological effects of flavonoids and phenolic acids. Ann N Y Acad Sci **854:**435-42.

141. **Karakaya S.** 2004. Bioavailability of phenolic compounds. Crit Rev Food Sci Nutr **44:**453-64.

142. **Manach C, Williamson G, Morand C, Scalbert A, and Remesy C.** 2005. Bioavailability and bioefficacy of polyphenols in humans. I. Review of 97 bioavailability studies. Am J Clin Nutr **81:**230S-242S.

143. **Hutt AJ, Caldwell J, and Smith RL.** 1986. The metabolism of aspirin in man: a population study. Xenobiotica **16:**239-49.

144. **Bochner F, Graham GG, Cham BE, Imhoff DM, and Haavisto TM.** 1981. Salicylate metabolite kinetics after several salicylates. Clin Pharmacol Ther **30:**266-75.

145. **Rechner AR, Spencer JP, Kuhnle G, Hahn U, and Rice-Evans CA.** 2001. Novel biomarkers of the metabolism of caffeic acid derivatives in vivo. Free Radic Biol Med **30:**1213-22.

146. **Kay CD, Kroon PA, and Cassidy A.** 2009. The bioactivity of dietary anthocyanins is likely to be mediated by their degradation products. Mol Nutr Food Res **53 Suppl 1:**S92-101.

147. **Aura AM, Martin-Lopez P, O'Leary KA, Williamson G, Oksman-Caldentey KM, Poutanen K, and Santos-Buelga C.** 2005. In vitro metabolism of anthocyanins by human gut microflora. Eur J Nutr **44:**133-42.

148. **Vitaglione P, Donnarumma G, Napolitano A, Galvano F, Gallo A, Scalfi L, and Fogliano V.** 2007. Protocatechuic acid is the major human metabolite of cyanidin-glucosides. J Nutr **137:**2043-8.

149. **Li X, Yu C, Lu Y, Gu Y, Lu J, Xu W, Xuan L, and Wang Y.** 2007. Pharmacokinetics, tissue distribution, metabolism, and excretion of depside salts from Salvia miltiorrhiza in rats. Drug Metab Dispos **35:**234-9.

150. **Zhou F, Xu W, Hong M, Pan Z, Sinko PJ, Ma J, and You G.** 2005. The role of N-linked glycosylation in protein folding, membrane targeting, and substrate binding of human organic anion transporter hOAT4. Mol Pharmacol **67:**868-76.

151. **Duan P, and You G.** 2009. Novobiocin is a potent inhibitor for human organic anion transporters. Drug Metab Dispos **37:**1203-10.

152. **Grimm T, Skrabala R, Chovanova Z, Muchova J, Sumegova K, Liptakova A, Durackova Z, and Hogger P.** 2006. Single and multiple dose pharmacokinetics of maritime pine bark extract (pycnogenol) after oral administration to healthy volunteers. BMC Clin Pharmacol **6:**4.

153. **Qiu XJ, Huang X, Chen ZQ, Ren P, Huang W, Qin F, Hu SH, Huang J, He J, Liu ZQ, and Zhou HH.** 2011. Pharmacokinetic study of the prokinetic compounds meranzin hydrate and ferulic acid following oral administration of Chaihu-Shugan-San to patients with functional dyspepsia. J Ethnopharmacol **137:**205-13.

154. **Kurlbaum M, and Hogger P.** 2010. Plasma protein binding of polyphenols from maritime pine bark extract (USP). J Pharm Biomed Anal **54:**127-32.

155. **Roberts AT, Martin CK, Liu Z, Amen RJ, Woltering EA, Rood JC, Caruso MK, Yu Y, Xie H, and Greenway FL.** 2007. The safety and efficacy of a dietary herbal supplement and gallic acid for weight loss. J Med Food **10:**184-8.

156. **Russell WR, Scobbie L, Labat A, and Duthie GG.** 2009. Selective bio-availability of phenolic acids from Scottish strawberries. Mol Nutr Food Res **53 Suppl 1:**S85-91.

157. **Lares-Asseff I, Flores-Perez J, Juarez-Olguin H, Ramirez-Lacayo M, Loredo-Abdala A, and Carbajal-Rodriguez L.** 1999. Influence of nutritional status on the pharmacokinetics of acetylsalicylic acid and its metabolites in children with autoimmune disease. Am J Clin Nutr **69:**318-24.

158. **Liu JH, and Smith PC.** 1996. Direct analysis of salicylic acid, salicyl acyl glucuronide, salicyluric acid and gentisic acid in human plasma and urine by high-performance liquid chromatography. J Chromatogr B Biomed Appl **675:**61-70.

159. **Juarez Olguin H, Flores Perez J, Lares Asseff I, Loredo Abdala A, and Carbajal Rodriguez L.** 2004. Comparative pharmacokinetics of acetyl salicylic acid and its metabolites in children suffering from autoimmune diseases. Biopharm Drug Dispos **25:**1-7.

160. **Azzini E, Vitaglione P, Intorre F, Napolitano A, Durazzo A, Foddai MS, Fumagalli A, Catasta G, Rossi L, Venneria E, Raguzzini A, Palomba L, Fogliano V, and Maiani G.** 2010. Bioavailability of strawberry antioxidants in human subjects. Br J Nutr **104:**1165-73.

161. **Koli R, Erlund I, Jula A, Marniemi J, Mattila P, and Alfthan G.** 2010. Bioavailability of various polyphenols from a diet containing moderate amounts of berries. J Agric Food Chem **58:**3927-32.

162. **Shahrzad S, and Bitsch I.** 1998. Determination of gallic acid and its metabolites in human plasma and urine by high-performance liquid chromatography. J Chromatogr B Biomed Sci Appl **705:**87-95.

163. **Shahrzad S, Aoyagi K, Winter A, Koyama A, and Bitsch I.** 2001. Pharmacokinetics of gallic acid and its relative bioavailability from tea in healthy humans. J Nutr **131:**1207-10.

164. **Needs CJ, and Brooks PM.** 1985. Clinical pharmacokinetics of the salicylates. Clin Pharmacokinet **10:**164-77.

165. **Nozaki Y, Kusuhara H, Endou H, and Sugiyama Y.** 2004. Quantitative evaluation of the drug-drug interactions between methotrexate and nonsteroidal anti-inflammatory drugs in the renal uptake process based on the contribution of organic anion transporters and reduced folate carrier. J Pharmacol Exp Ther **309:**226-34.

166. **Liegler DG, Henderson ES, Hahn MA, and Oliverio VT.** 1969. The effect of organic acids on renal clearance of methotrexate in man. Clin Pharmacol Ther **10:**849-57.

167. **Takeda M, Khamdang S, Narikawa S, Kimura H, Hosoyamada M, Cha SH, Sekine T, and Endou H.** 2002. Characterization of methotrexate transport and its drug interactions with human organic anion transporters. J Pharmacol Exp Ther **302:**666-71.

168. **Maeda A, Tsuruoka S, Kanai Y, Endou H, Saito K, Miyamoto E, and Fujimura A.** 2008. Evaluation of the interaction between nonsteroidal anti-inflammatory drugs and methotrexate using human organic anion transporter 3-transfected cells. Eur J Pharmacol **596:**166-72.

169. **Kindla J, Muller F, Mieth M, Fromm MF, and Konig J.** 2011. Influence of non-steroidal anti-inflammatory drugs on organic anion transporting polypeptide (OATP) 1B1- and OATP1B3-mediated drug transport. Drug Metab Dispos **39:**1047-53.

170. **Pedersen JM, Matsson P, Bergstrom CA, Norinder U, Hoogstraate J, and Artursson P.** 2008. Prediction and identification of drug interactions with the human ATP-binding cassette transporter multidrug-resistance associated protein 2 (MRP2; ABCC2). J Med Chem **51:**3275-87.

171. **Lien EJ, Lien LL, Wang R, and Wang J.** 2011. Phytochemical analysis of medicinal plants with kidney protective activities. Chin J Integr Med **18**:790-800.

172. **Rice-Evans CA, Miller NJ, and Paganga G.** 1996. Structure-antioxidant activity relationships of flavonoids and phenolic acids. Free Radic Biol Med **20:**933-56.

173. **Karamac M, Kosinska A, and Pegg RB.** 2005. Comparison of radical-scavenging activities for selected phenolic acids. Pol. J. Food Nutr. Sci. **14:**6.

174. **Perazella MA.** 2003. Drug-induced renal failure: update on new medications and unique mechanisms of nephrotoxicity. Am J Med Sci **325:**349-62.

175. **Tune BM.** 1997. Nephrotoxicity of beta-lactam antibiotics: mechanisms and strategies for prevention. Pediatr Nephrol **11:**768-72.

176. **Mulato AS, Ho ES, and Cihlar T.** 2000. Nonsteroidal anti-inflammatory drugs efficiently reduce the transport and cytotoxicity of adefovir mediated by the human renal organic anion transporter 1. J Pharmacol Exp Ther **295:**10-5.

177. **Wang L, and Sweet DH.** 2013. Renal Organic Anion Transporters (SLC22 Family): Expression, Regulation, Roles in Toxicity, and Impact on Injury and Disease. AAPS J **15**:53-69.

178. **Renouf M, Redeuil K, Longet K, Marmet C, Dionisi F, Kussmann M, Williamson G, and Nagy K.** 2011. Plasma pharmacokinetics of catechin metabolite 4'-O-Me-EGC in healthy humans. Eur J Nutr **50:**575-80.

179. **Chow HH, and Hakim IA.** 2011. Pharmacokinetic and chemoprevention studies on tea in humans. Pharmacol Res **64:**105-12.

180. **Schram K, Miketova P, Slanina J, Humpa O, and Taborska E.** 2004. Mass spectrometry of 1,3- and 1,5-dicaffeoylquinic acids. J Mass Spectrom **39:**384-95.

181. **King PJ, Ma G, Miao W, Jia Q, McDougall BR, Reinecke MG, Cornell C, Kuan J, Kim TR, and Robinson WE, Jr.** 1999. Structure-activity relationships: analogues of the dicaffeoylquinic and dicaffeoyltartaric acids as potent inhibitors of human immunodeficiency virus type 1 integrase and replication. J Med Chem **42:**497-509.

182. **Mahadevan S, and Park Y.** 2008. Multifaceted therapeutic benefits of Ginkgo biloba L.: chemistry, efficacy, safety, and uses. J Food Sci **73:**R14-9.

183. **Zou Q, Wei P, Li J, Ge ZX, and Ouyang P.** 2009. Simultaneous determination of 18alpha- and 18beta-glycyrrhetic acid in human plasma by LC-ESI-MS and its application to pharmacokinetics. Biomed Chromatogr **23:**54-62.

184. **Xia Y, Wei G, Si D, and Liu C.** 2011. Quantitation of ursolic acid in human plasma by ultra performance liquid chromatography tandem mass spectrometry and its pharmacokinetic study. J Chromatogr B Analyt Technol Biomed Life Sci **879:**219-24.

185. **Gu R, Dou G, Wang J, Dong J, and Meng Z.** 2007. Simultaneous determination of 1,5-dicaffeoylquinic acid and its active metabolites in human plasma by liquid

chromatography-tandem mass spectrometry for pharmacokinetic studies. J Chromatogr B Analyt Technol Biomed Life Sci **852:**85-91.

186. **Ploeger B, Mensinga T, Sips A, Seinen W, Meulenbelt J, and DeJongh J.** 2001. The pharmacokinetics of glycyrrhizic acid evaluated by physiologically based pharmacokinetic modeling. Drug Metab Rev **33:**125-47.

187. **Ploeger B, Mensinga T, Sips A, Deerenberg C, Meulenbelt J, and DeJongh J.** 2001. A population physiologically based pharmacokinetic/pharmacodynamic model for the inhibition of 11-beta-hydroxysteroid dehydrogenase activity by glycyrrhetic acid. Toxicol Appl Pharmacol **170:**46-55.

188. **Bakhiya N, Monien B, Frank H, Seidel A, and Glatt H.** 2009. Renal organic anion transporters OAT1 and OAT3 mediate the cellular accumulation of 5-sulfooxymethylfurfural, a reactive, nephrotoxic metabolite of the Maillard product 5-hydroxymethylfurfural. Biochem Pharmacol **78:**414-9.

189. **Jung KY, Takeda M, Kim DK, Tojo A, Narikawa S, Yoo BS, Hosoyamada M, Cha SH, Sekine T, and Endou H.** 2001. Characterization of ochratoxin A transport by human organic anion transporters. Life Sci **69:**2123-35.

190. **Wang L, and Sweet DH.** 2013. Competitive inhibition of human organic anion transporters 1 (SLC22A6), 3 (SLC22A8) and 4 (SLC22A11) by major components of the medicinal herb Salvia miltiorrhiza (Danshen). Drug Metab Pharmacokinet **28**:220-8.

191. **Koenen A, Kock K, Keiser M, Siegmund W, Kroemer HK, and Grube M.** 2012. Steroid hormones specifically modify the activity of organic anion transporting polypeptides. Eur J Pharm Sci **47:**774-80.

192. **Zhu X, Zhang H, and Lo R.** 2004. Phenolic compounds from the leaf extract of artichoke (Cynara scolymus L.) and their antimicrobial activities. J Agric Food Chem **52:**7272-8.

193. **Dong GC, Chuang PH, Chang KC, Jan PS, Hwang PI, Wu HB, Yi M, Zhou HX, and Chen HM.** 2009. Blocking effect of an immuno-suppressive agent, cynarin, on CD28 of T-cell receptor. Pharm Res **26:**375-81.

194. **Pellati F, Benvenuti S, Magro L, Melegari M, and Soragni F.** 2004. Analysis of phenolic compounds and radical scavenging activity of Echinacea spp. J Pharm Biomed Anal **35:**289-301.

195. **Gao S, Zhan Q, Li J, Yang Q, Li X, Chen W, and Sun L.** 2010. LC-MS/MS method for the simultaneous determination of ethyl gallate and its major metabolite in rat plasma. Biomed Chromatogr **24:**472-8.

196. **Pirker R, Huck CW, Popp M, and Bonn GK.** 2004. Simultaneous determination of gentisic, salicyluric and salicylic acid in human plasma using solid-phase extraction, liquid chromatography and electrospray ionization mass spectrometry. J Chromatogr B Analyt Technol Biomed Life Sci **809:**257-64.

197. **Wang L, Sun Y, Du F, Niu W, Lu T, Kan J, Xu F, Yuan K, Qin T, Liu C, and Li C.** 2007. 'LC-electrolyte effects' improve the bioanalytical performance of liquid chromatography/tandem mass spectrometric assays in supporting pharmacokinetic study for drug discovery. Rapid Commun Mass Spectrom **21:**2573-84.

198. **Liu AH, Li L, Xu M, Lin YH, Guo HZ, and Guo DA.** 2006. Simultaneous quantification of six major phenolic acids in the roots of Salvia miltiorrhiza and four related traditional Chinese medicinal preparations by HPLC-DAD method. J Pharm Biomed Anal **41:**48-56.

199. **Zhou L, Chow M, and Zuo Z.** 2006. Improved quality control method for Danshen products--consideration of both hydrophilic and lipophilic active components. J Pharm Biomed Anal **41:**744-50.

200. **Li G, Shi Z, Yang H, and Du J.** 2009. Comparative analysis on the major constituents in Radix Salviae Miltiorrhizae injectable preparations. China Pharmacy **20:**3.

201. **Han HK.** 2011. Role of transporters in drug interactions. Arch Pharm Res **34:**1865-77.

202. **Gurley BJ, Fifer EK, and Gardner Z.** 2012. Pharmacokinetic herb-drug interactions (part 2): drug interactions involving popular botanical dietary supplements and their clinical relevance. Planta Med **78:**1490-514.

203. **Shi S, and Klotz U.** 2012. Drug interactions with herbal medicines. Clin Pharmacokinet **51:**77-104.

204. **Pei WJ, Zhao XF, Zhu ZM, Lin CZ, Zhao WM, and Zheng XH.** 2004. Study of the determination and pharmacokinetics of Compound Danshen Dripping Pills in human serum by column switching liquid chromatography electrospray ion trap mass spectrometry. J Chromatogr B Analyt Technol Biomed Life Sci **809:**237-42.

205. **Chauhan B, Kumar G, Kalam N, and Ansari SH.** 2013. Current concepts and prospects of herbal nutraceutical: A review. J Adv Pharm Technol Res **4:**4-8.

206. **Wolman AT, Gionfriddo MR, Heindel GA, Mukhija P, Witkowski S, Bommareddy A, and Vanwert AL.** 2013. Organic anion transporter 3 interacts selectively with lipophilic beta-lactam antibiotics. Drug Metab Dispos **41:**791-800.

207. **Astorga B, Wunz TM, Morales M, Wright SH, and Pelis RM.** 2011. Differences in the substrate binding regions of renal organic anion transporters 1 (OAT1) and 3 (OAT3). Am J Physiol Renal Physiol **301:**F378-86.

208. **Rodiger M, Zhang X, Ugele B, Gersdorff N, Wright SH, Burckhardt G, and Bahn A.** 2010. Organic anion transporter 3 (OAT3) and renal transport of the metal chelator 2,3-dimercapto-1-propanesulfonic acid (DMPS). Can J Physiol Pharmacol **88:**141-6.

209. **Makino T, Okajima K, Uebayashi R, Ohtake N, Inoue K, and Mizukami H.** 2012. 3-Monoglucuronyl-glycyrrhretinic acid is a substrate of organic anion transporters expressed in tubular epithelial cells and plays important roles in licorice-induced pseudoaldosteronism by inhibiting 11beta-hydroxysteroid dehydrogenase 2. J Pharmacol Exp Ther **342:**297-304.

210. **Uwai Y, and Iwamoto K.** 2010. Transport of aminopterin by human organic anion transporters hOAT1 and hOAT3: Comparison with methotrexate. Drug Metab Pharmacokinet **25:**163-9.

211. **Chiba S, Ikawa T, Takeshita H, Ichiba K, Sagi M, Mukai T, and Anzai N.** 2011. Interactions of human organic anion transporter 1 (hOAT1) with substances associated with forensic toxicology. Leg Med (Tokyo) **13:**180-5.

212. **Ahn SY, Jamshidi N, Mo ML, Wu W, Eraly SA, Dnyanmote A, Bush KT, Gallegos TF, Sweet DH, Palsson BO, and Nigam SK.** 2011. Linkage of organic anion transporter-1 to metabolic pathways through integrated "omics"-driven network and functional analysis. J Biol Chem **286:**31522-31.

213. **Zeng Y, Zhang R, Wu J, Liu M, Peng W, Yu X, and Yang X.** 2011. Organic anion transporter 1 (OAT1) involved in renal cell transport of aristolochic acid I. Hum Exp Toxicol.

214. **Zhu Y, Meng Q, Wang C, Liu Q, Sun H, Kaku T, and Liu K.** 2012. Organic anion transporters involved in the excretion of bestatin in the kidney. Peptides **33:**265-71.

215. **Zhang J, Wang C, Liu Q, Meng Q, Cang J, Sun H, Gao Y, Kaku T, and Liu K.** 2010. Pharmacokinetic interaction between JBP485 and cephalexin in rats. Drug Metab Dispos **38:**930-8.

216. **Larsen M, Holm R, Jensen KG, Sveigaard C, Brodin B, and Nielsen CU.** 2010. 5-Hydroxy-L-tryptophan alters gaboxadol pharmacokinetics in rats: involvement of PAT1 and rOat1 in gaboxadol absorption and elimination. Eur J Pharm Sci **39:**68-75.

217. **Wikoff WR, Nagle MA, Kouznetsova VL, Tsigelny IF, and Nigam SK.** 2011. Untargeted metabolomics identifies enterobiome metabolites and putative uremic toxins as substrates of organic anion transporter 1 (Oat1). J Proteome Res **10:**2842-51.

218. **Uwai Y, Honjo H, and Iwamoto K.** 2010. Inhibitory effect of selective cyclooxygenase-2 inhibitor lumiracoxib on human organic anion transporters hOAT1 and hOAT3. Drug Metab Pharmacokinet **25:**450-5.

219. **Choi MK, Jin QR, Choi YL, Ahn SH, Bae MA, and Song IS.** 2011. Inhibitory effects of ketoconazole and rifampin on OAT1 and OATP1B1 transport activities: considerations on drug-drug interactions. Biopharm Drug Dispos **32:**175-84.

220. **Elsby R, Fox L, Stresser D, Layton M, Butters C, Sharma P, Smith V, and Surry D.** 2011. In vitro risk assessment of AZD9056 perpetrating a transporter-mediated drug-drug interaction with methotrexate. Eur J Pharm Sci **43:**41-9.

221. **Fork C, Bauer T, Golz S, Geerts A, Weiland J, Del Turco D, Schomig E, and Grundemann D.** 2011. OAT2 catalyses efflux of glutamate and uptake of orotic acid. Biochem J **436:**305-12.

222. **Sato M, Mamada H, Anzai N, Shirasaka Y, Nakanishi T, and Tamai I.** 2010. Renal secretion of uric acid by organic anion transporter 2 (OAT2/SLC22A7) in human. Biol Pharm Bull **33:**498-503.

223. **Lai Y, Sampson KE, Balogh LM, Brayman TG, Cox SR, Adams WJ, Kumar V, and Stevens JC.** 2010. Preclinical and clinical evidence for the collaborative transport and renal secretion of an oxazolidinone antibiotic by organic anion transporter 3 (OAT3/SLC22A8) and multidrug and toxin extrusion protein 1 (MATE1/SLC47A1). J Pharmacol Exp Ther **334:**936-44.

224. **Maeda A, Tsuruoka S, Ushijima K, Kanai Y, Endou H, Saito K, Miyamoto E, and Fujimura A.** 2010. Drug interaction between celecoxib and methotrexate in organic anion transporter 3-transfected renal cells and in rats in vivo. Eur J Pharmacol **640:**168-71.

225. **Miyajima M, Kusuhara H, Fujishima M, Adachi Y, and Sugiyama Y.** 2011. Organic anion transporter 3 mediates the efflux transport of an amphipathic organic anion, dehydroepiandrosterone sulfate, across the blood-brain barrier in mice. Drug Metab Dispos **39:**814-9.

226. **Yang CH, Glover KP, and Han X.** 2010. Characterization of cellular uptake of perfluorooctanoate via organic anion-transporting polypeptide 1A2, organic anion transporter 4, and urate transporter 1 for their potential roles in mediating human renal reabsorption of perfluorocarboxylates. Toxicol Sci **117:**294-302.

227. **Shin HJ, Takeda M, Enomoto A, Fujimura M, Miyazaki H, Anzai N, and Endou H.** 2011. Interactions of urate transporter URAT1 in human kidney with uricosuric drugs. Nephrology (Carlton) **16:**156-62.

228. **Uetake D, Ohno I, Ichida K, Yamaguchi Y, Saikawa H, Endou H, and Hosoya T.** 2010. Effect of fenofibrate on uric acid metabolism and urate transporter 1. Intern Med **49:**89-94.

229. **Nakamura M, Anzai N, Jutabha P, Sato H, Sakurai H, and Ichida K.** 2010. Concentration-dependent inhibitory effect of irbesartan on renal uric acid transporters. J Pharmacol Sci **114:**115-8.

230. **Miura D, Anzai N, Jutabha P, Chanluang S, He X, Fukutomi T, and Endou H.** 2011. Human urate transporter 1 (hURAT1) mediates the transport of orotate. J Physiol Sci **61:**253-7.

231. **Wempe MF, Jutabha P, Quade B, Iwen TJ, Frick MM, Ross IR, Rice PJ, Anzai N, and Endou H.** 2011. Developing potent human uric acid transporter 1 (hURAT1) inhibitors. J Med Chem **54:**2701-13.

APPENDIX I

ORGANIC ANION TRANSPORTER SUBSTRATES AND INHIBITORS (REPORTED FROM 2010 TO 2012)

Compound	Transporter[a]	Interaction[b]	System[c]	Kinetics (μM)			Reference
				K_m	K_i	IC_{50}[d]	
1-butanesulfonic acid	hOAT1 mOat1 rbOat1	I	CHO			514±72.1 (0.25 PAH) 313±26.9 (0.25 PAH) 421±89.4 (0.25 PAH)	(207)
1-propanesulfonic acid	hOAT1 mOat1 rbOat1	I	CHO			2036±28.3 (0.25 PAH) 4156±1079 (0.25 PAH)	(207)
2,3-dimercapto-1-propanesulfonic acid	hOAT1	I	CHO			83±3 (0.25 PAH)	(207)
			HEK293			104.6±13.1 (5 CF) 85.1±8.8 (5 CF)	(208)[e]
	mOat1		CHO			55±4.9 (0.25 PAH)	(207)
	rbOat1		CHO			72±9.9 (0.25 PAH)	(207)
			HEK293			237.4±23 (5 CF) 123±14 (5 CF)	(208)[e]
3-mercapto-1-propanesulfonic acid	hOAT1 mOat1 rbOat1	I	CHO			204±54.2 (0.25 PAH) 151±19.8 (0.25 PAH) 204±34.9 (0.25 PAH)	(207)
3-monoglucuronyl-glycyrrhetinic acid	hOAT1	S	HEK293	49.0±18.3			(209)
Aminopterin	hOAT1	I	*X.laevis*			160±58 (0.221 PAH)	(210)
Amitriptyline	hOAT1	I	S2		573.9	354 (5 PAH)	(211)

Appendix I Continued

Compound	Transporter[a]	Interaction[b]	System[c]	Kinetics (μM)			Reference
				K_m	K_i	IC_{50}[d]	
Arginine	mOat1	I	CHO			1600±300 (5 CF)	(212)
	hOAT1	I	HEK293		0.5		(39)
	hOAT1	I	S2		0.80±0.15	0.44±0.08 (5 PAH)	(40)
Aristolochic acid I	hOAT1	S	HEK293				(41)
	mOat1	S	CHO	0.79±0.01			(36)
	rOat1	S	HEK293				(213)
Aristolochic acid II	hOAT1	I	S2			1.06±0.09 (5 PAH)	(40)
	mOat1	S	CHO	1.50±0.37			(36)
Bestatin	hOAT1	S	HEK293	679±7			(214)
Caffeic acid	hOAT1	S/I	HEK293	28.6±3.7		5.22 (25 PAH)	(50)
	hOAT1	I	*X.laevis*			16.6±3.7 (0.221 PAH)	(51)
Caffeic acid-3-O-glucuronide	hOAT1	S/I	HEK293				(50)
Caffeic acid-4-O-glucuronide	hOAT1	S	HEK293				(50)
Caffeic acid-3-O-sulfate	hOAT1	S	HEK293	38.9±3.3			(50)
Caffeic acid-4-O-sulfate	hOAT1	S	HEK293				(50)
Cephalexin	hOAT1	S	HEK293				(215)
Chlorpyrifosmethyl	hOAT1	I	S2		324.6	191.5 (5 PAH)	(211)
Cyclo-*trans*-4-L-hydroxyprolyl-L-serine	hOAT1	S	HEK293				(215)
Daidzein-7-O-glucuronide	hOAT1	I	HEK293				(119)
Daidzein-7,4'-O-disulfate	hOAT1	I	HEK293				(119)
Diazepam	hOAT1	I	S2		83.5	133.3 (5 PAH)	(211)
Dihydrocaffeic acid	hOAT1	S/I	HEK293	21.4±4.2			(50)
Dihydroferulic acid	hOAT1	S/I	HEK293				(50)
Dihydrocaffeic acid-3-O-glucuronide	hOAT1	S	HEK293				(50)
Dihydrocaffeic acid-4-O-glucuronide	hOAT1	S	HEK293				(50)
Dihydrocaffeic acid-3-O-sulfate	hOAT1	S/I	HEK293	76.7±16.3			(50)
Dihydrocaffeic acid-4-O-sulfate	hOAT1	S/I	HEK293	115±31			(50)
Dihydroferulic acid-4-O-sulfate	hOAT1	S/I	HEK293				(50)
Ferulic acid-4-O-sulfate	hOAT1	S	HEK293	54.2±3.6			(50)

Appendix I Continued

Compound	Transporter[a]	Interaction[b]	System[c]	Kinetics (μM)			Reference
				K_m	K_i	IC_{50}[d]	
Fenitrothion	hOAT1	I	S2		51.2	26.6 (5 PAH)	(211)
Ferulic acid	hOAT1	S/I	HEK293			9.01 (25 PAH)	(50)
		I	CHO				(52)
Gaboxadol	rOat1	S	*X. laevis*	151±58			(216)
Gallic acid	hOAT1	I	CHO			1.24±0.36 (1 PAH)	(52)
Genistein-4'-O-sulfate	hOAT1	S/I	HEK293	5.07±1.81			(119)
Genistein-7-O-glucuronide	hOAT1	I	HEK293				(119)
Glycitein-7-O-glucuronide	hOAT1	I	HEK293				(119)
Indoxyl sulfate	mOat1	I	*X. laevis*			18 (30 CF)	(217)
Isoferulic acid	hOAT1	I	HEK293				(50)
Isoferulic acid-3-O-glucuronide	hOAT1	S	HEK293				(50)
Isoferulic acid-3-O-sulfate	hOAT1	S/I	HEK293	32.7±5.3			(50)
Lithospermic acid	mOat1	I	CHO		14.9±4.9		(49)
Lumiracoxib	hOAT1	I	*X. laevis*			3.3±1.1 (0.221 PAH)	(218)
Ketoconazole	hOAT1	I	*X. laevis*			319 (1 PAH)	(219)
α-Ketoglutarate	mOat1	I	*X. laevis*			40±3 (30 CF)	(212)
Malathion	hOAT1	I	S2		134.0	114.2 (5 PAH)	(211)
Mianserin	hOAT1	I	S2		99.0	312.6 (5 PAH)	(211)
Probenecid	hOAT1	I	*X. laevis*			17 (3 PAH); 14 (10 MTX)	(220)
Protocatechuic acid	hOAT1	I	CHO			18.08±2.59 (1 PAH)	(52)
	mOat1	I					(49)
Pyruvate	mOat1	I	CHO			4300±600 (5 CF)	(212)
Quercetin-3-O-glucuronide	hOAT1	S/I	HEK293				(119)
Quercetin-3'-O-glucuronide	hOAT1	I	HEK293				(119)
Quercetin-3'-O-sulfate	hOAT1	S/I	HEK293	1.73±0.38		1.22 (25 PAH)	(119)
Quercetin-7-O-glucuronide	hOAT1	S/I	HEK293				(119)
Rifampin	hOAT1	I	*X. laevis*		62.2	79.1 (1 PAH)	(219)
Rosmarinic acid	mOat1	I	CHO		5.5±2.2		(49)
Salvianolic acid A	mOat1	I	CHO		4.9±2.2		(49)

Appendix I Continued

Compound	Transporter[a]	Interaction[b]	System[c]	Kinetics (μM)			Reference
				K_m	K_i	IC_{50}[d]	
Salvianolic acid B	mOat1	I	CHO				(49)
Sinapinic acid	hOAT1	I	CHO			11.02±1.55 (1 PAH)	(52)
Spermidine	mOat1	I	*X. laevis*			2000±700 (30 CF)	(212)
Spermine	mOat1	I	*X. laevis*			1600±600 (30 CF)	(212)
Sulfasalazine	hOAT1	I	*X. laevis*			4.6 (10 MTX)	(220)
Tanshinol	mOat1	I	CHO				(49)
Triazolam	hOAT1	I	S2		86.0	185.2 (5 PAH)	(211)
Vanillic acid	hOAT1	I	CHO			7.65±2.92 (1 PAH)	(52)
Aristolochic acid I	mOat2	S	CHO	0.36±0.05			(36)
Aristolochic acid II	mOat2	S	CHO	0.67±0.19			(36)
Orotic acid	hOAT2 rOAT2	S	HEK293				(221)
Uric acid	hOAT2	S	HEK293	1168±335			(222)
N-({(5*S*)-3-[4-(1,1-dioxidothiomorpholin-4-yl)-3,5-difluorophenyl]-2-oxo-1,3-oxazolidin-5-yl}methyl)acetamide	hOAT3	S	HEK293	44±5			(223)
1-butanesulfonic acid	hOAT3 mOat3 rbOat3	I	CHO			5098±184.3 (0.015 ES) 10975±2647 (0.015 ES) 5640±715.9 (0.015 ES)	(207)
1-propanesulfonic acid	rbOat3	I	CHO				(207)
	hOAT3		CHO			40±7.4 (0.015 ES)	(207)
			HEK293			31.6±6.6 (5 CF) 172±36 (5 CF)	(208)[e]
2,3-dimercapto-1-propanesulfonic acid	mOat3	I	CHO			85±16.9 (0.015 ES)	(207)
	rbOat3		CHO			18±2.5 (0.015 ES)	(207)
			HEK293			52.4±7.6 (5 CF) 172±22 (5 CF)	(208)[e]

Appendix I Continued

Compound	Transporter[a]	Interaction[b]	System[c]	Kinetics (μM)			Reference
				K_m	K_i	IC_{50}[d]	
2,4-dichlorophenoxyacetate	mOat3	I	CHO		2.0±0.4		(109)
2,4-dihydroxyphenylacetic acid	mOat3	I	CHO		347±98		(109)
	hOAT3					2139±289 (0.015 ES)	
3-mercapto-1-propanesulfonic acid	mOat3	I	CHO			2325±268 (0.015 ES)	(207)
	rbOat3					2320 ±785 (0.015 ES)	
3-monoglucuronyl-glycyrrhetinic acid	hOAT3	S	HEK293	30.1±2.9			(209)
4-hydroxybenzoic acid	hOAT3	I	HEK293				(52)
5-hydroxyindoleacetic acid	mOat3	I	CHO		67.8±7.2		(109)
Aminopterin	hOAT3	I	*X. laevis*			59.2±14.9 (0.0184 ES)	(210)
	hOAT3	I	HEK293		0.4		(39)
	hOAT3	I	S2		0.84±0.10	0.65±0.08 (0.05 ES)	(40)
Aristolochic acid I	hOAT3	S	HEK293				(41)
	mOat3	S	CHO	0.51±0.06			(36)
	hOAT3	I	S2			1.28 ± 0.18 (0.05 ES)	(40)
Aristolochic acid II	mOat3	S	CHO	1.05±0.36			(36)
Bestatin	hOAT3	S	HEK293	632±14			(214)
Bumetanide	hOAT3	I	*X. laevis*			7.8 (2 ES); 5.4 (10 MTX)	(220)
	hOAT3	S/I	HEK293			30.8 (100 CF)	(50)
Caffeic acid	hOAT3	I	*X.laevis*			5.4±1.3 (0.0175 ES)	(51)
Caffeic acid-3-O-glucuronide	hOAT3	S	HEK293				(50)
Caffeic acid-4-O-glucuronide	hOAT3	S	HEK293				(50)
Caffeic acid-3-O-sulfate	hOAT3	S	HEK293				(50)
Caffeic acid-4-O-sulfate	hOAT3	S	HEK293				(50)
Celecoxib	hOAT3	I	S2		35.3		(224)
Cephalexin	hOAT3	S	HEK293				(215)
p-Coumaric acid	hOAT3	I	HEK293				(52)
Cyclo-*trans*-4-L-hydroxyprolyl-L-serine	hOAT3	S	HEK293				(215)
Daidzein-7-O-glucuronide	hOAT3	S/I	HEK293	19.1±1.9			(119)
Daidzein-7,4'-O-disulfate	hOAT3	S/I	HEK293				(119)

Appendix I Continued

Compound	Transporter[a]	Interaction[b]	System[c]	Kinetics (μM)			Reference
				K_m	K_i	IC_{50}[d]	
Dehydroepiandrosterone sulfate	mOat3	I	CHO		3.8±1.1		(109)
		S	*X. laevis*				(109, 225)
Dihydrocaffeic acid	hOAT3	S/I	HEK293	21.4±4.2		14.2 (100 CF)	(50)
Dihydrocaffeic acid-3-O-glucuronide	hOAT3	S	HEK293				(50)
Dihydrocaffeic acid-4-O-glucuronide	hOAT3	S	HEK293				(50)
Dihydrocaffeic acid-3-O-sulfate	hOAT3	S	HEK293				(50)
Dihydrocaffeic acid-4-O-sulfate	hOAT3	S	HEK293				(50)
Dihydroferulic acid-4-O-glucuronide	hOAT3	S	HEK293				(50)
Dihydroferulic acid-4-O-sulfate	hOAT3	S	HEK293				(50)
Ferulic acid	hOAT3	I	HEK293			7.35±3.73 (1 ES)	(52)
Ferulic acid-4-O-glucuronide	hOAT3	S	HEK293				(50)
Ferulic acid-4-O-sulfate	hOAT3	S	HEK293				(50)
Gallic acid	hOAT3	I	HEK293			9.02±3.24 (1 ES)	(52)
Genistein-4'-O-glucuronide	hOAT3	S/I	HEK293				(119)
Genistein-7-O-glucuronide	hOAT3	S/I	HEK293	7.94±1.42			(119)
Gentisic acid	hOAT3	I	HEK293			86.81±21.78 (1 ES)	(52)
Glycitein-7-O-glucuronide	hOAT3	S/I	HEK293	17.6±3.9			(119)
Hippuric acid	mOat3	I	CHO		79.3±4.0		(109)
Homovanillic acid	mOat3	I	CHO		135±27		(109)
Isoferulic acid-3-O-glucuronide	hOAT3	S	HEK293				(50)
Isoferulic acid-3-O-sulfate	hOAT3	S	HEK293				(50)
Lithospermic acid	mOat3	I	CHO		31.1±7.0		(49)
Lumiracoxib	hOAT3	I	*X. laevis*			1.9±0.4 (0.0184 ES)	(218)
Penicillin G	mOat3	I	CHO		60.7±5.9		(109)
Probenecid	mOat3	I	CHO		0.8±0.2		(109)
Protocatechuic acid	hOAT3	I	CHO			87.36±28.57 (1 ES)	(52)
	mOat3	I	CHO				(49)
Quercetin-3-O-glucuronide	hOAT3	S/I	HEK293			0.43 (100 CF)	(119)
Quercetin-3'-O-glucuronide	hOAT3	S/I	HEK293	5.25±0.86		1.31 (100 CF)	(119)
Quercetin-3'-O-sulfate	hOAT3	S/I	HEK293			0.75 (100 CF)	(119)

Appendix I Continued

Compound	Transporter[a]	Interaction[b]	System[c]	Kinetics (μM)			Reference
				K_m	K_i	IC_{50}[d]	
Quercetin-7-O-glucuronide	hOAT3	S/I	HEK293				(119)
Rosmarinic acid	mOat3	I	CHO		4.3±0.2		(49)
Salicylate	mOat3	I	CHO		343±93		(109)
Salvianolic acid A	mOat3	I	CHO		21.3±7.7		(49)
Salvianolic acid B	mOat3	I	CHO				(49)
Sinapinic acid	hOAT3	I	HEK293			25.74±1.56 (1 ES)	(52)
Sulfasalazine	hOAT3	I	*X. laevis*			3.0 (10 MTX)	(220)
Syringic acid	hOAT3	I	HEK293				(52)
Tanshinol	mOat3	I	CHO				(49)
Vanillic acid	hOAT3	I	HEK293				(52)
Aristolochic acid I	hOAT4	I	HEK293		22.4		(39)
	hOAT4	I	S2			61.3±8.35 (0.05 ES)	(40)
Aristolochic acid II	hOAT4	I	S2			72.0±9.32 (0.05 ES)	(40)
Caffeic acid-3-O-sulfate	hOAT4	S	HEK293				(50)
Caffeic acid-4-O-sulfate	hOAT4	S	HEK293				(50)
Ferulic acid-4-O-sulfate	hOAT4	S	HEK293				(50)
Isoferulic acid-3-O-sulfate	hOAT3	S	HEK293				(50)
Perfluorooctanoate	hOAT4	S	CHO	172±46 (pH6); 310± 30 (pH7.4)			(226)
Sinapinic acid	hOAT4	I	CHO				(52)
6-Hydroxybenzbromarone	hURAT1	I	MDCK			0.23±0.05 (100 U)	(227)
Benzarone	hURAT1	I	MDCK			0.12±0.03 (100 U)	(227)
Benzbromarone	hURAT1	I	MDCK			0.05±0.02 (100 U)	(227)
Captopril	hURAT1	I	MDCK			>5000 (100 U)	(227)
Enalapril	hURAT1	I	MDCK			648±77 (100 U)	(227)
Fenofibric acid	hURAT1	I	HEK293			35.7±3.9 (20 U)	(228)
Fenofibric acid (reduced)	hURAT1	I	HEK293			570±25 (20 U)	(228)
Indomethacin	hURAT1	I	MDCK			40.7±2.20 (100 U)	(227)

Appendix I Continued

Compound	Transporter[a]	Interaction[b]	System[c]	Kinetics (µM)			Reference
				K_m	K_i	IC_{50}[d]	
Irbesartan	hURAT1	I	*X. laevis*			121.7 (20 U)	(229)
Losartan	hURAT1	I	HEK293			571±28 (20 U)	(228)
			X. laevis				(229)
Orotate	hURAT1	S	HEK293	5.2±0.4			(230)
Perfluorooctanoate	hURAT1	S	HEK293	64.1±30.5			(226)
Phenylbutazone	hURAT1	I	MDCK			197±48.5 (100 U)	(227)
Probenecid	hURAT1	I	MDCK			86.39±0.07 (10 U)	(231)
						41.7±3.70 (100 U)	(227)
Sulfinpyrazone	hURAT1	I	MDCK			716±34.3 (100 U)	(227)
Telmisartan	hURAT1	I	*X. laevis*				(229)
Valsartan	hURAT1	I	*X. laevis*				(229)
2,4-dichlorophenoxyacetate	mOat6	I	CHO		15.7±2.0		(109)
2,4-dihydroxyphenylacetic acid	mOat6	I	CHO		61.4±7.1		(109)
5-hydroxyindoleacetic acid	mOat6	I	CHO		48.9±10.3		(109)
Dehydroepiandrosterone sulfate	mOat6	I	CHO		38.8±3.1		(109)
Hippuric acid	mOat6	I	CHO		59.9±4.9		(109)
Homovanillic acid	mOat6	I	CHO		3.0±0.5		(109)
Penicillin G	mOat6	I	CHO		1450±480		(109)
Probenecid	mOat6	I	CHO		8.3±2.5		(109)
Salicylate	mOat6	I	CHO		49.0±4.4		(109)

[a]Transporter species: h, human; m, mouse; r, rat; rb, rabbit; [b]Interaction: I, inhibitor; S, substrate; [c]Expression system: CHO, Chinese hamster ovary cells; HEK293, human embryonic kidney cell line; MDCK, Madin Darby canine kidney cell line; S2, cell line derived from second segment of proximal tubule; *X. laevis*, *Xenopus laevis* oocytes; [d]IC_{50}: concentration of inhibited substrate is shown in parentheses (in µM), substrate abbreviations: CF, carboxyfluorescein; ES, estrone sulfate; MTX, methotrexate; PAH, para-aminohippurate; U, Urate; [e]This reference reported values for both the oxidized and reduced forms of this substrate, respectively.

VITA

Li Wang was born on January 4, 1981 in Zhangjiakou, China and is a Chinese citizen.

He received his Bachelor of Science in Biology from Xiamen University, Xiamen, China in 2004 and a Master of Science in Pharmacology from Shanghai Institute of Materia Medica, Chinese Academy of Sciences, Shanghai, China in 2007. He worked as a Research Associate Scientist in Hutchison MediPharma Ltd for one year. Then he went to Singapore working as Research Assistant in Department of Pharmacy, National University of Singapore.

He joined the Drug Transporter Research Group at Department of Pharmaceutics, Virginia Commonwealth University (VCU) in 2009. During his PhD graduate education, Li has published five manuscripts and three abstracts. He has presented his research at Annual Meetings of the American Association of Pharmaceutical Scientists (AAPS) in 2011 and 2012, and AAPS Workshop on Drug Transporters in ADME: From the Bench to the Bedside in 2013, in addition to the poster presentation within School of Pharmacy.

He received an AAPS-Pharmacokinetics, Pharmacodynamics, and Drug Metabolism (PPDM) Section Travelship Award in 2012. Additionally, he has also received VCU School of Pharmacy Jyotsna and Mavji Thacker Award for academic excellence in Department of Pharmaceutics in 2010.

PUBLICATIONS

1. Li Wang and Douglas H. Sweet. Active hydrophilic components of the medicinal herb salvia miltiorrhiza (Danshen) potently inhibit organic anion transporters 1 (Slc22a6) and 3 (Slc22a8). Evid Based Complement Alternat Med 2012; Article ID 872458, 8 pages.
2. Li Wang and Douglas H. Sweet. Potential for food-drug interactions by dietary phenolic acids on human organic anion transporters 1 (SLC22A6), 3 (SLC22A8), and 4 (SLC22A11). Biochem Pharmacol 2012; 84:1088-95.
3. Li Wang and Douglas H. Sweet. Competitive inhibition of human organic anion transporters 1 (SLC22A6), 3 (SLC22A8) and 4 (SLC22A11) by major components of the medicinal herb Salvia miltiorrhiza (Danshen). Drug Metabolism and Pharmacokinetics 2013; 28:220-8
4. Li Wang and Douglas H. Sweet. Interaction of natural dietary and herbal anionic compounds and flavonoids with human organic anion transporters 1 (SLC22A6), 3 (SLC22A8), and 4 (SLC22A11). Evid Based Complement Alternat Med. 2013; Article ID 612527, 7 pages.
5. Li Wang and Douglas H. Sweet. Renal organic anion transporters (SLC22 family): expression, regulation, roles in toxicity, and impact on injury and disease. AAPS J. 2013; 15: 53-69.
6. Xiaolei Pan, Li Wang, Dirk Gründeman, and Douglas H. Sweet. Interaction of ethambutol with human organic cation transporters (SLC22 Family) indicates potential for drug-drug

interactions during antituberculosis therapy. Antimicrobial Agents and Chemotherapy 2013 (accepted).

ABSTRACTS

1. Li Wang and Dougals H. Sweet. Inhibitory Effects of Active Hydrophilic Components of *Salvia Miltiorrhiza* (Danshen) on Transport Activity of Organic Anion Transporter3 Indicate Potential Herb-drug Interaction AAPS Annual Meeting and Exposition, Washington DC, October 2011.
2. Li Wang and Dougals H. Sweet.Evaluation of Organic Anion Transporter-based Drug-drug Interaction Potency of Danshen (*Salvia miltiorrhiza*) Pharmaceutical Preparations. AAPS Annual Meeting and Exposition, Chicago, IL, October 2012.
3. Li Wang and Dougals H. Sweet. Potential for Food-Drug Interactions by Dietary Phenolic Acids on Human Organic Anion Transporters 1 (SLC22A6), 3 (SLC22A8), and 4 (SLC22A11). AAPS Workshop on Drug Transporters in ADME: From the Bench to the Bedside in 2013. Bethesda, MD, March 2013.